Three Dimensional Printing: Solenoid Valve-Jet for Continuous High-Speed Application

by

Phay Kiat Tan

B.S., Mechanical Engineering
University of Illinois at Urbana-Champaign, 1998

Submitted to the Department of Mechanical Engineering
in Partial Fulfillment of the Requirements for the Degree of

MASTERS OF SCIENCE IN MECHANICAL ENGINEERING

at the

Massachusetts Institute of Technology

February, 2000

Signature of Author_____
Department of Mechanical Engineering
Dec 17, 1999

Certified by_____
Emanuel M. Sachs
Professor of Mechanical Engineering
Thesis Supervisor

Accepted by_____
A. Sonin
Chairman, Graduate Committee

Three Dimensional Printing:
Solenoid Valve-Jet for Continuous High-Speed Applications

by

Phay Kiat Tan

Submitted to the Department of Mechanical Engineering
in partial fulfillment of the requirements for the degree of
Masters of Science in Mechanical Engineering
Dec 17, 1999

ABSTRACT

3D Printing is the rapid prototyping of parts by the deposition of a binder material in successive layers onto specific regions of a powder substrate. The current challenge in 3DP^{TM} is the demand for larger built-volume in a shorter time with a high level operational reliability. The solenoid valve-jet printhead possesses key characteristics, which can be used in the design of a scaled-up 3DP^{TM} machine.

An experimental study was conducted on the performance of the solenoid valve-jet under variable pressure and operational frequency. A flow-rate of 5cm^3/min is obtainable at a pressure of 10psi. A linear relationship is observed between pressure and fluid flow-rate, with an upper operational limit of 25psi. An individual valve-jet evaluated is capable of producing fluid stream with a variability of ± 0.01mm on the front edge and ± 0.1 mm on the trailing edge. A build time of 4.5 hours, with a single valve-jet printing water into PVA load stainless steel powder as the material system, is required for a volume of 150x300x30 mm with the bulk of time taken by the drying process. Continuous 5 days run of a valve-jet indicate very little deterioration in performance with a flow-rate variance of ±0.2cm^3/min over the test duration. A printhead made up of two valve-jets printing bi-directionally was able to produce geometrical parts but with stepped edges caused the performance variability between different valve-jets. Each solenoid valve-jet needs to be calibrated offline and those with similar capabilities can be put together onto a single printhead.

These experimental results indicate that an array of solenoid valve-jet can be assembled into the printhead of a larger scaled-up 3DP^{TM} machine to fabricate larger and accurate parts with minimal maintenance and low risks of failure.

Thesis Supervisor: Dr. Emanuel M. Sachs
Title: Professor of Mechanical Engineering

DEDICATION

To my parents and my brother, for all their love and encouragement. And to Yingyuan, who has stood by me and put up with my solenoid valve-jet the past year.

ACKNOWLEDGEMENTS

I would like to express his sincere gratitude to the following people:

Ely Sachs – For the opportunity to work with him over the last one and a half years. He has showed me a great deal about problem solving from different perspectives. Also for the opportunity to present my work at the consortium meetings, which I thought were really helpful to building self-confidence and presentation skills.

Dave Brancazio – For providing many valuable insights that really gets to the heart of the problem. I am especially grateful for all his help in the electronics aspects and Alpha machine modifications that made the majority of my work possible.

Jim Serdy – For helping with the fluid supply system, and always ready to give a helping hand and some friendly encouragement.

To the rest of the ME 3DP™ contingent (Adam, David Guo, Ram) - It has been a pleasure working and sharing the lab with you. Wish you all the best of luck with 3DP™ and beyond.

A special word of thanks also goes to Mark and Gerry from the machine shop for providing valuable guidance and experience in machining.

The staff from Therics Inc. including Chris Gaylo, James Fayerweather and Tom Brad for their many valuable insights and experience on using the solenoid valve-jet.

Last but not least, I would like to thank the support of my sponsor organization, the Sembawang Corporation Industries group of companies of Singapore. Without their support, this work would not have been possible.

1. INTRODUCTION

1.1 Overview of the 3DP™ process

Three Dimensional Printing (3DP™) is a rapid prototyping process that makes parts directly from CAD models [Sachs, Cima, et al. November 1992]. Like many other solid freeform, rapid prototyping processes, it is an additive process where parts are built based on a layer-by-layer architecture. Rapid prototyping processes are useful for flexible manufacturing by reducing time in the product development cycle and purging the need for product-specific tooling. Time and cost savings in manufacturing prototype parts will allow for numerous design iterations without risking any competitive edge.

3DP™ process begins by creating a CAD model of the part. The model is sliced into thin layers by a computer algorithm. Each layer represents a detailed 2-D cross-section of the original model. These layers are then printed sequentially to produce the final part.

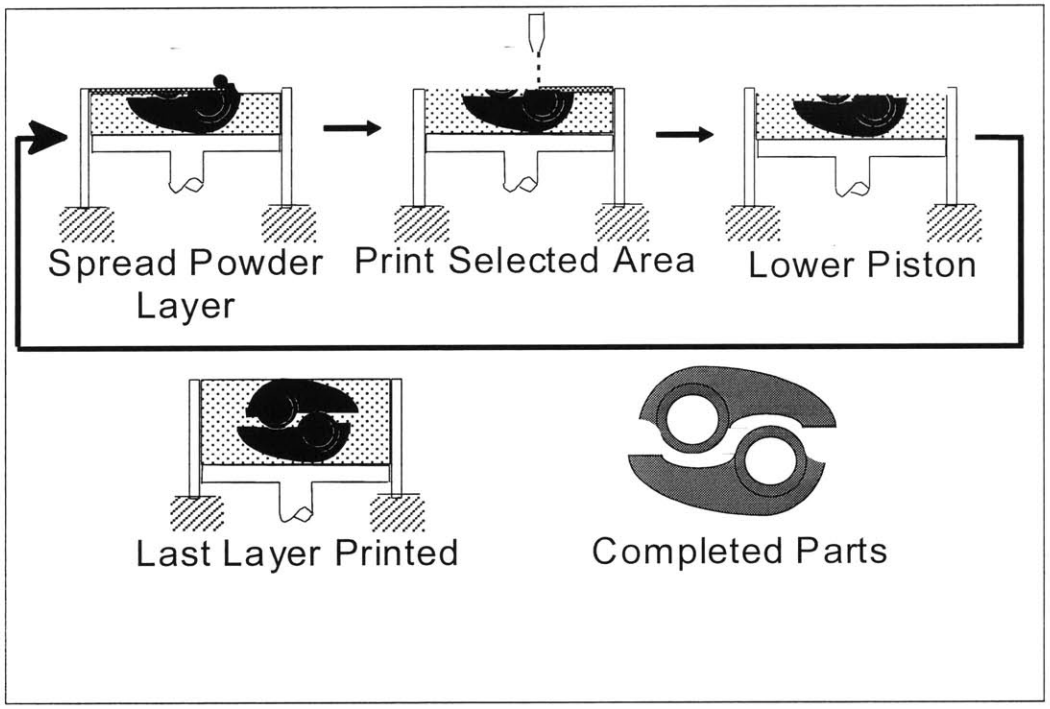

Figure 1.1: 3DP™ Process

Figure 1.1 illustrates the 3DP™ process. A thin layer of powder is first spread across a rectangular cylinder by a counter rotating spreader bar. A printhead, similar to that used in ink-jet printing, then travels across the powder bed depositing the binder material to glue the powder particles together. Information from the part file limits binder deposition to the areas of the powder-bed where the part is to be formed. After the printhead has finished creating the layer, the powder piston is lowered by one layer thickness, additional powder is deposited at one end of the powder-bed, and the spreader bar spreads it evenly over the entire powder-bed. These steps are repeated until the entire part is built. The unbound powder is removed leaving the green part with the desired geometry. Post-processing operations such as firing, sintering and infiltration with another material is performed to achieve full density and improve on part strength and material properties.

3DP™ offer several key features, which defines its competitive advantage. Being an additive manufacturing process, it is able to create complex geometries and shapes such as the detailed internal passages of conformal cooling channels in metal tooling that cannot be done with other manufacturing techniques. The loose powder supports overhangs, undercuts, and internal cavities so that very complex parts can be printed without generating additional support structures. Additional flexibility is provided in the kind of materials that can be used for production. It can be used to print 3DP™ parts, as long as the material (including ceramics, metals, polymers and composites) can be obtained in powder form and a viable binder is available to be dispensed from the printhead. Furthermore, because different materials can be dispensed either via different nozzles on the same printhead, 3DP™ can control the local material composition. This capability would allow designers to vary the material properties within a single part. The proper placement of the binder droplets can be used to create surfaces of controlled texture and to control the final internal microstructure of the printed prototype.

Possible applications of 3DP™ include printing of direct metal parts and tools, structural ceramics, injection molding tooling, appearance models and functionally gradient parts. Prototype parts can be manufactured from using any geometry, any

material, and any composition. This is what 3DP™ can offer that puts it at the forefront of all the available Rapid Prototyping manufacturing processes.

1.2 Printer Architecture

The most fundamental component of a 3DP™ machine is the printhead. As such, the major effort in the area of research is in printhead development. The printing architecture of a 3DP™ machine can be broken down into two main categories: Jetting style and Scanning Style.

1.2.1 Jetting Style

There are two types of binder-jetting mechanisms used in 3DP™, one being a continuous jet (CJ) stream printhead and the other is a drop-on-demand (DOD) stream printhead.

In the CJ system, the liquid binder material emerges continuously from each jet nozzle under high pressure. Further downstream, the jet will disintegrate into a train of droplets. This droplet break-off will tend to occur at a characteristic frequency known as the Rayleigh frequency. A device such as a piezo-electric transducer can be used to energize the stream at a frequency near the Rayleigh frequency, causing it to break up into uniformly spaced droplets at the drive frequency. The Rayleigh frequency is controlled by the jet's orifice size and flow rate. The smaller the orifice and the higher the flow rate, the higher the Rayleigh frequency required. The CJ can operate over a very broad range of frequency with magnitude varying from a hundred to thousands of Hertz (Hz). However, a single jet cannot operate over the entire range. For 3DP™, typical values of the jet are an orifice diameter of 50μm and a flow rate in the range of 1.0cc/min to 1.5cc/min. This produces jet velocities from 10m/s to 15m/s and Rayleigh frequencies ranging from 45kHz to 65kHz, producing droplets 90 microns in diameter.

Drop-on-demand systems create only 1 droplet each time. Droplets are individually forced out of a fluid chamber through a small orifice by a pressure wave of either mechanical or thermal origin. After the droplet has been expelled, a meniscus of

the printed fluid reforms at the orifice and the jet is ready to be fired again. This process is limited to comparatively lower frequencies due to the physics of meniscus formation. The meniscus must be allowed a finite time to form before the next droplet can be produced. The upper limit on DOD is about 10 kHz. It has the advantage that the frequency of the jet may be continuously varied from 0 Hz to some higher limit, determined by the jet construction.

1.2.2 Scanning Style

Scanning style refers to the manner the printhead moves over the powder bed as binder material is deposited into each layer. There are three possible methods of scanning: raster, vector, and vector edge tracing with raster fill as shown in **Figure 1.2** below. The three print styles are illustrated schematically below.

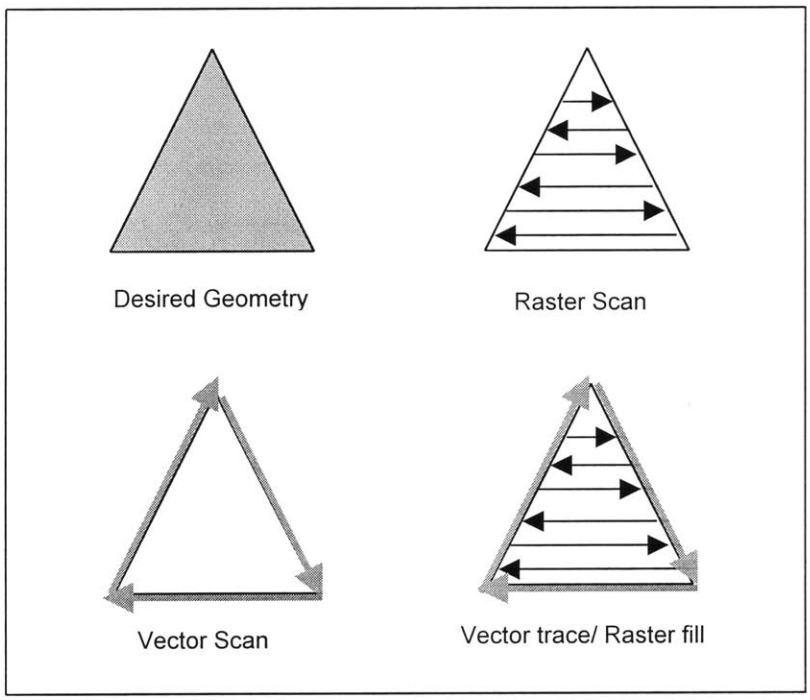

Figure 1.2: Scanning Styles for 3DP™

1.2.2.1 Raster

Raster scanning is the style used on the Alpha 3DP™ machine. The printhead moves back and forth over the powder bed in a linear fashion. After finishing one pass,

the printhead steps forward a distance equivalent to one line spacing, perpendicular to the scanning direction. Printing can be performed uni-directionally or bi-directionally. This technique is most suitable for printing parts that have a small surface area to volume ratio because the printhead will be actively dispensing binder during a major portion of the scanning process. In raster printing, the printhead moves over the entire footprint of the layer as it prints. If there is little material to actually be printed, this results in a large amount of "wasted" time where the printhead is moving but no value is being added to the part.

1.2.2.2 Vector

Vector printing involves the printhead tracing over the parts of the powder-bed where the part is to have volume. The most important advantage of this kind of motion is that proportional deflection is not required to get high quality definition of the edges of the layer. Instead of many lines defining an edge, (as in raster printing), each edge of a vector print is now defined by a single line, and hence "knitting" problems between each line is not encountered.

However, the major disadvantage for vector motion is in printhead speed. In continuous jet printing, the printhead must move at a constant velocity because the droplet frequency is not easily varied. A vector CJ machine would need to be able to achieve very high accelerations to trace around small radii in the part. DOD has the advantage that the frequency can be easily varied. This eliminates the need for constant printhead speed. However, the low frequencies associated with DOD would limit the printhead speed. The scaling of a pure vector machine is also limited. It would not be feasible to have more than one jet per part. In a multi-jet vector machine, each jet would create an identical part in the powderbed. The size of the powderbed must increase with the number of jets. This will limit the number of parts that such a machine could be designed to manufacture. Therefore, the most likely application for a pure vector machine would be for DOD printing of relatively small parts.

1.2.2.3 Vector Trace with raster fill

This is the combination of the two basic scanning styles mentioned earlier. The hybrid of scanning style will drastically increase the rate at which a layer may be printed. Instead of each part being printed by a single jet, each part is printed by a single printhead. A DOD printhead for this scanning architecture would be very similar to that which is used in ink-jet desktop printers, typically with 50 jets per printhead. A single jet would be used to vector trace all of the part edges and all of the jets would be used to fill in the part where it is to have volume.

1.3 Motivation

One of the major challenges facing 3DP™ is the demand for larger parts in a shorter time. Scaling-up the 3DP™ printing process necessarily involves two steps: 1) increase build-volume and 2) decrease build-time. Increasing the build-volume allows us to print bigger parts while decreasing the build-time will reduce the lead-time needed to print a part.

In the current tooling technology embodied in the MIT alpha 3DP™ machine, the creation of a layer involves three steps: i) spreading the layer, ii) printing the binder, and iii) drying the binder. The current build volume for the 3DP™ machine at MIT is 150 x 300 x 300 mm. If the required scaled-up size of the print bed is 800 x 380 x 250 mm, and the machine should be capable of printing the full volume in a run of 8 hour duration, then each layer must take, on average, 23 seconds to create (assuming a layer thickness of 200 microns for acceptable resolution and surface finish. With the currently technology applied to the larger print volume, the following layer time budget results:

Spreading:	8	seconds
Printing:	270	seconds
Drying:	20	seconds
Total:	298	seconds

To achieve the target of 23 seconds/layer, the layer creation budget must be reduced to:

Spreading:	4	seconds

Printing:	12	seconds
Drying:	7	seconds
Total:	23	seconds

All the three steps have to be improved upon when attempting to scale-up the 3DP™ process, with a special emphasis on printhead development because this represents the main bulk of our build time reduction objective. Equally important in a scaled-up machine are issues such as greater machine reliability and modularity for ease of maintenance and fault-finding. Component parts of the new machine, and especially the printhead, should be designed for easy disassembly and offline repair and servicing.

The solenoid valve-jet has been identified as one of the potential choices for further investigation because it offers us three key potential advantages: 1) the possibility of a faster print rate and 2) high operational reliability in a modular, integrated package and 3) easy scalability to a larger 3DP™ machine. Current CJ and DOD printhead constructions generate droplets, which are deposited onto the substrate material. If the binder material could instead, be dispensed in one continuous stream, significantly higher flow-rates (hence faster printing speeds), can potentially be achieved. By operating the solenoid valve as a DOD printhead, and varying the duration of the signal pulse applied on the solenoid, we can either actuate a stream of droplets (with short signal pulses) or a continuous hose of binder material, which is turned on at one transition of the part and off at the back end of the printed part. Wide ranges of printed dimensions are readily obtained by simply varying the duration for which the valve-jet is open.

The compact and integral architecture of the pre-manufactured solenoid valve offers an extremely elegant method of efficiently delivering binder material onto the substrate material with easy maintenance and replacement when damage occurs. Its compact and modular construction allows us to envision assembling an array of these solenoid valves into a single printhead, shown in **Figure 1.3**, for use in a large-scale and high-speed 3DP™ machine.

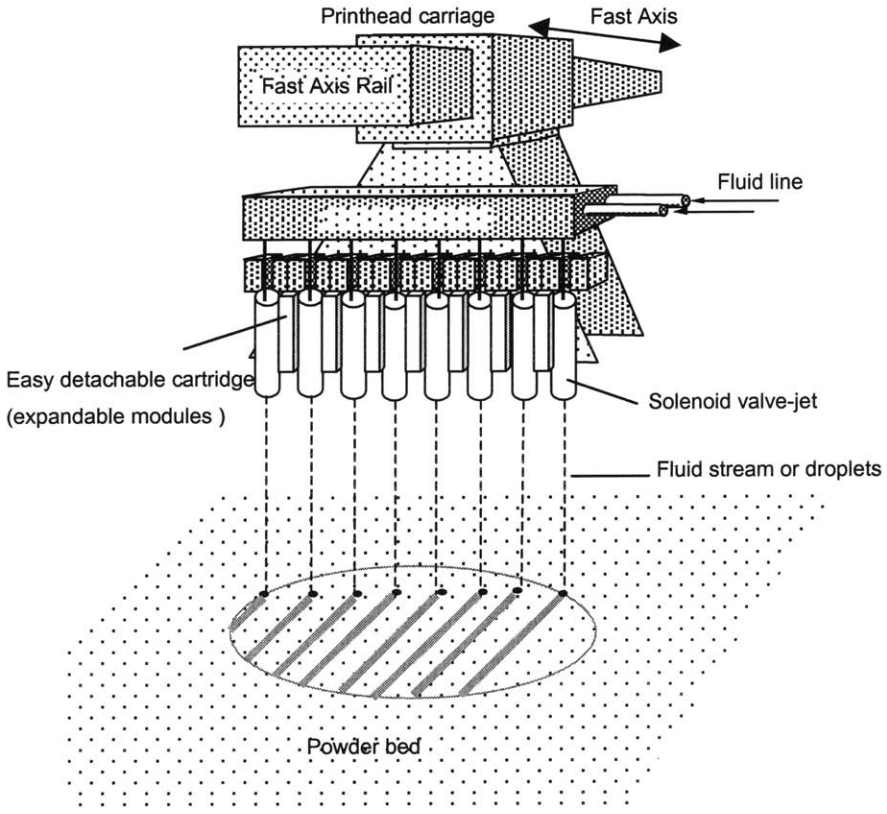

Figure 1.3: Envisioned solenoid valve-jet printhead

1.4 Approach

The primary objective of this work is to investigate the feasibility of using a solenoid-actuated valve-jet in a DOD mode of operation for high-speed and large-scale printing operations. The basic idea is to actuate a continuous hose of binder fluid by turning it on at the front edge of the part and off at the back end and depositing this onto the powder material in a layer-by-layer fashion to create the 3-D part. The printing process is analogous to the present technology where a stream of droplets are deflected by piezo-electricity into the required print areas but with two major differences: 1) a continuous jet-stream impacts the powder bed instead of a stream of droplets 2) the stream deflection using piezo-electricity is replaced by a turn-on and turn-on operation of the valve-jet.

The investigation will first begin by gaining an understanding of the physical and electrical characteristics of the solenoid valve on a test-stand setup. A suitable electrical driver circuit will have to be constructed to generate an input signal to actuate the valve to produce a continuous hose of binder fluid with a variable duration and length. This test-stand setup is then used to determine various valve properties and limitations such as flow-rate, response time, reproducibility of turn-on and turn-off transitions, dimensions of jet-stream released by the valve and the amount of variability between different valves. With an understanding of the solenoid valve's capabilities and limitations, we can then proceed to perform preliminary printing of single powder layers using a rudimentary rotary 3DP™ machine. The final step for this effort is to incorporate one or an array of solenoid valves onto the Alpha Machine to print geometrical test parts and evaluate the dimensional accuracy and surface finish quality of these printed parts.

1.5 Content and organization

The work described in this thesis focuses on understanding the capabilities as well as limitations of the solenoid valve-jet for suitability in 3DP™ operations. Each chapter will begin by providing the goals and objective of the work, followed by a description of the experimental setup and procedure used, and finally concludes with the empirical results obtained.

Chapter 2 provides a detailed description of the physical and electrical characteristics of the solenoid valve-jet. Chapter 3 covers the electronics aspects of two different driver circuits that can be used to actuate the valve. Chapter 4 describes the experimental setup and results of various tests conducted to determine the characteristics of the fluid-stream produced by the valve-jet as well as the of a rudimentary rotary 3DP™ machine setup to print primitive lines on paper and single layer metal powder. Chapter 5 discusses the requirements for integration of the solenoid valve-jet onto the Alpha 3DP™ machine and the printing of a few 3-D geometry test geometries. Chapter 6 covers printing of 3-D parts to determine the valve-jet's

capabilities and limitations. Finally, Chapter 7 provides a summary of the progress made and also points to the direction for future work.

2. PHYSICAL CHARACTERISTICS AND PROPERTIES OF SOLENOID VALVE-JET

The solenoid valve-jet is designed with a very simple and modular architecture. Its modularity gives us a great advantage of easily assembling a series of these valve-jets into a complete printhead module, which is ready for print applications with the addition of a few minor modifications. The complexity of the mechanical and electrical requirements for producing a jet-stream has been designed for and integrated together into a self-contained, capsule-like device which is ready for use.

The solenoid valve-jet mode of operation is fundamentally different from that of the continuous jet (CJ) printhead developed at MIT. The printhead on the Alpha 3DP™ machine produces single droplets, which are generated by a piezo-induced pressure wave. This causes the fluid stream to break off into droplets at the piezo-frequency. Charging each droplet with a certain voltage between the high-voltage charging cells enable deflection of the droplets between the deflection plates. The electrostatic force of this field deflects each droplet to its predetermined position. As droplets are continuously generated, deflecting a droplet into a catcher will cause that droplet not to be printed.

The solenoid valve-jet however, operates by turning on and releasing the binder fluid under pressure onto the areas where there is to be volume and turning off when there is nothing to be printed. It has a plunger mechanism to do this. When an electric current passes through the solenoid coil, a magnetic field is instantaneously created which exerts a force on the metallic plunger, causing it to jump into its "turn on" position. When the current is cutoff, the electric field collapses and the plunger is returned to its "off" position, under the forces exerted by the spring and the fluid back-pressure. In the "off" position, the plunger rests on the nozzle seat, covering the entrance to the ruby orifice; while in the "on" position, a gap of approximately 120 microns wide is created between the plunger and the nozzle seat.

There are two models of the INKX solenoid valve-jet manufactured by The Lee Fluidic Co.: 1) INKX0505950A and 2) INKX0503850A. Both are designed specifically for

ink-jet printing applications. The INKX0505950A model has an integrated ruby orifice, and is more suitable to work with in a testing situation. The INKX0503850A valve-jet does not have the integrated ruby but is more suitable if an array of valve-jets within a system is required. However, these valves require tubing and an orifice downstream of the valve-jet. Both models are in current production by The Lee Fluidic Co. and are readily available in stock. The INKX0503850A will be the primary model of valve-jet studied in this investigation because it offers the advantage of a built-in ruby orifice which allows it to be used almost readily in actual printing operations without the additional step of having to incorporate a separate orifice, as in the case of the INKX0503850A valve-jet. The INKX0503850A is mentioned to emphasize that a variety of solenoid valve-jets are available which could potentially be more suitable in different printing requirements and conditions.

This chapter discusses the physical and structural characteristics, as well as the recommended operational specifications of the INKX0505950A and INKX0503850A solenoid valve-jets. This provides a thorough knowledge of the basic characteristics of the valve-jets, which are extremely important and useful for further investigative efforts.

2.1 The INKX0505950A solenoid valve-jet

2.1.1. Physical and structural characteristics

The INKX0505950A solenoid valve-jet is illustrated in **Figure 2.1** below. Each of these devices is cylindrically shaped with approximate dimensions of 21.1 mm in length by 5.7 mm in diameter. On the upper face is a pair of solenoid pins for attachment of the electrical leads and a barbed port where the fluid inflow tubing is connected. On the bottom face is a 130 μm diameter ruby orifice from which binder fluid-stream is dispensed.

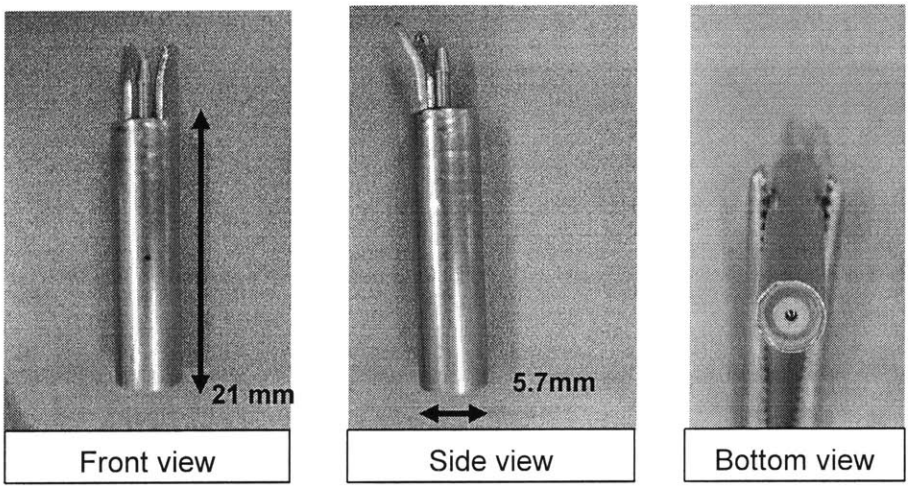

Figure 2.1: External full view picture of INKX0505950A valve-jet

The valve-jet's simple exterior belies its complex internal structure. The heart of the solenoid valve-jet consists of a piston-shaped plunger made of a magnetic material (430F stainless steel), resting in contact on a ruby orifice in the closed position. Separated by a gap approximately 120$_{\mu}$m wide further upstream of the plunger is a cylindrical metallic core of magnetic 430F stainless steel. When an electric current is passed through the copper solenoid coil, a magnetic field is generated which magnetizes both the plunger and metallic core, causing them to be attracted to each other. This closes the gap between the plunger and metallic core but also simultaneously creates a small separation of 128$_{\mu}$m between the plunger base and the plastic seat. Fluid is hence forced out of the valve-jet under pressure for the duration for which the plunger is in the open position. **Figure 2.2** shows a schematic of the internal layout of the valve-jet to illustrate the internal components in a generic Lee valve-jet.

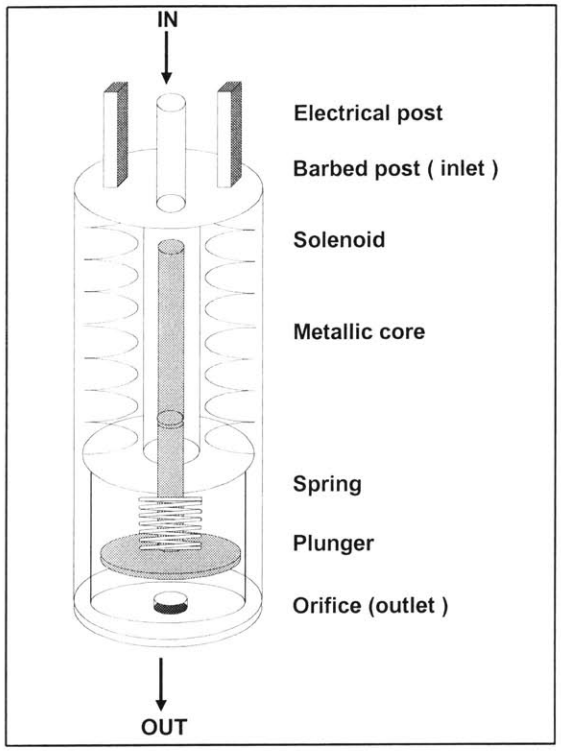

Figure 2.2: Internal schematic layout of solenoid valve-jet

A damaged valve-jet was dissected to verify the internal architecture of the valve-jet. This has to be performed without disturbing or damaging any of the internal component parts because the purpose is to study the internal structure of the valve-jet in their original placement. A two-step procedure was used: first immersing the valve-jet in an epoxy resin under vacuum to remove all air bubbles in the interior, and subsequently hardening the resin at an elevated temperature. The resin treated valve-jet was then polished, allowing us to observe the internal structure at different depths.

Figure 2.3 is the polished-away view through the mid-section of the INKX0505950 solenoid valve-jet. The valve-jet has an outer casing and inlet port made of 316 grade stainless steel. Fluid material entering through the inlet port is channeled to a plastic tube skeleton made of a PEEK (polyetheretherketone). A metallic core and plunger resides in the mid-plane of the plastic tube with a clearance of approximately 10 μm around its circumference with the inner face of the plastic tube skeleton. Surrounding

the plastic tube is a coil of copper wires, which creates a magnetic field to actuate the valve when electric current flows through it. There is an air cavity between the stainless steel outer casing and the solenoid coils, presumably for heat transfer to the external environment. A coil spring provides the spring-back force to return the plunger to the closed position. The plunger is coated with rubber EDPM, which lies in direct contact with the orifice to provide a tight seal to prevent fluid from leaking out when the valve-jet is in the closed position.

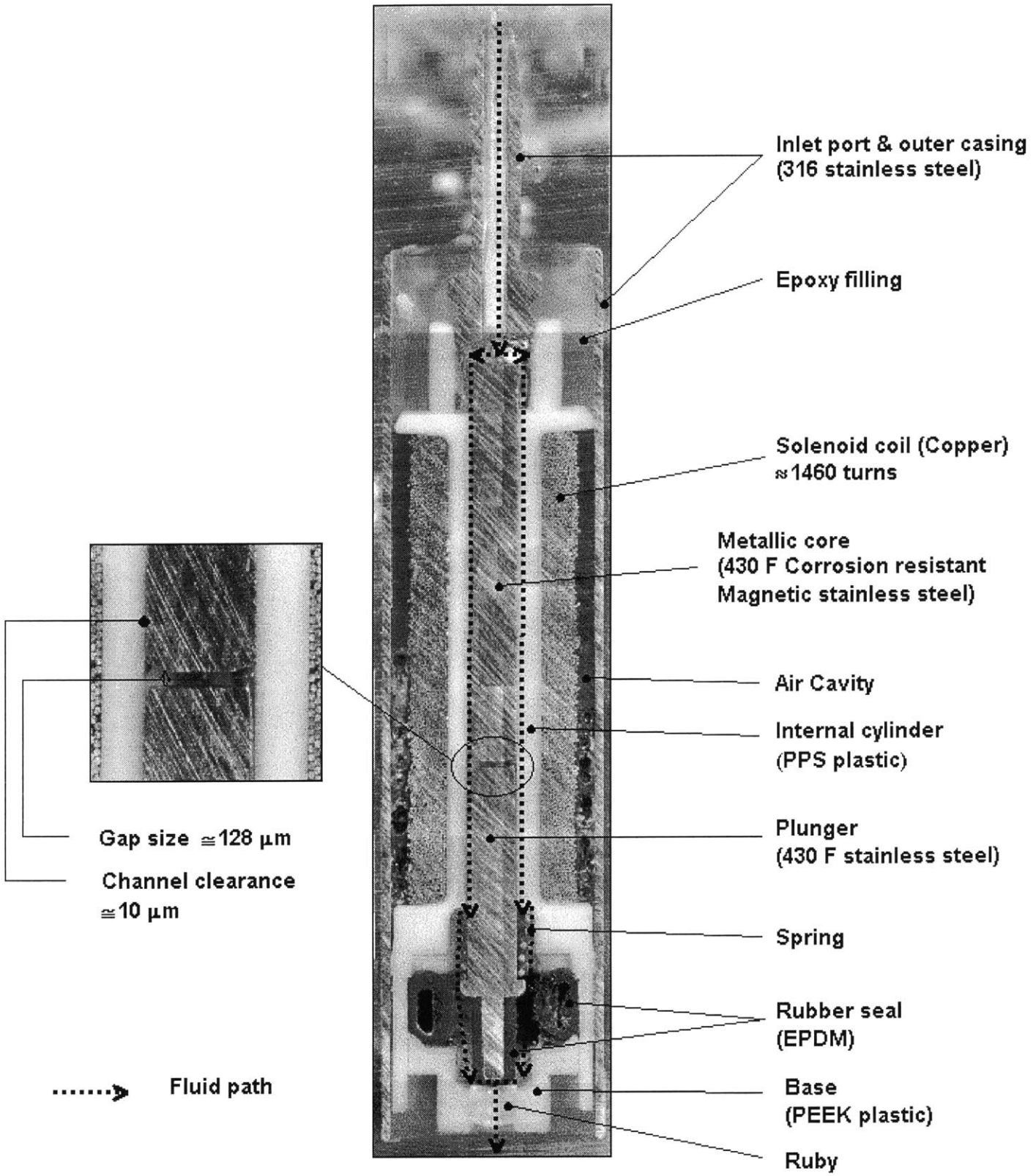

Figure 2.3: Polished cross-sectional view of INKX0505950A valve

The ruby orifice on the INKX0505950 valve-jet is available separately in stand-alone units. **Figure 2.4** contains various views of one of these ruby orifices. Each ruby orifice is approximately 1.20 mm in diameter with a 0.13 mm hole drilled through its center. Depending on the operation requirements and type of prototype parts to be printed, it is possible to design a solenoid valve-jet with different performance characteristics by simply changing orifice size of the ruby used. Pressure loss and flow-rate experiments using the stand-alone ruby orifice are discussed in section 4.2.

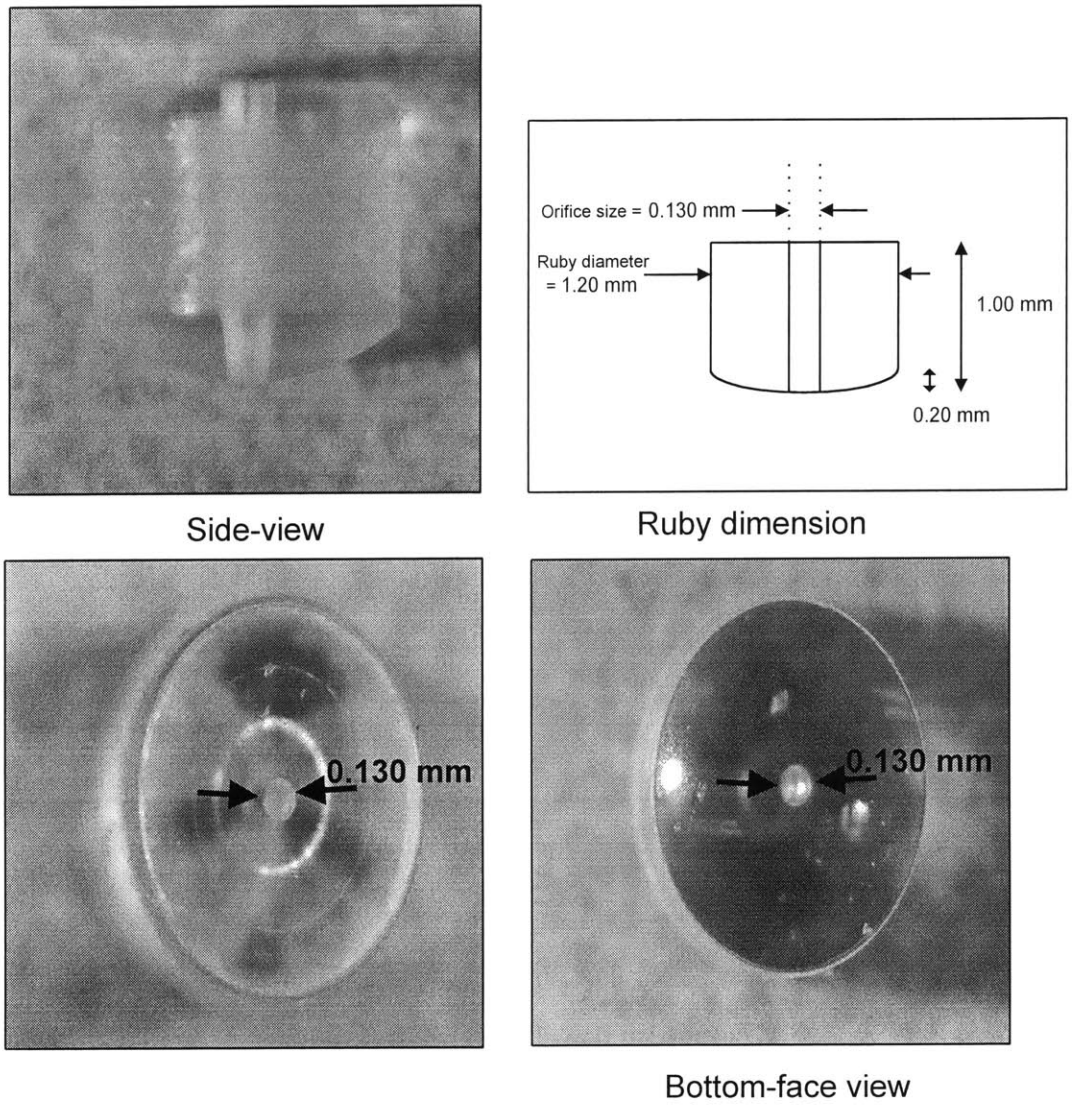

Figure 2.4: Ruby orifice from INKX0505950A valve-jet

2.1.2. Operational specifications

Table 2.1 summarizes the recommended maximum frequency, voltage and fluid pressure for operating the INKX0505950A solenoid valve, as recommended by The Lee Fluidic Co. [Electro-fluidic systems technical handbook 6th edition, The Lee Co.]. The specification drawing for the INKX0505950A valve-jet is attached in Appendix A.1. It is the Lee's company intention that when the stock of INKX0505950A runs out, the product number will be obsolete and it will be replaced by INKA2457210H model shown in Appendix A.2. Both valves are otherwise identical.

Parameter	Recommended condition
Maximum operating frequency	1000 Hz at 24 V_{DC} pulse
Operating voltage	24 V_{DC} pulse
Operating pressure	0-10 psi
Coil resistance	110 Ohms nominal
Coil inductance	26.7 mH
Wetted material	• 430F corrosion resistant magnetic stainless steel • 316 stainless steel • PPS (polyphosphine sulfide) • PEEK (polyetheretherketone) • EPDM (propylene) • Epoxy • Sapphire/Ruby

Table 2.1: INKX0505950A solenoid valve-jet specifications

There are two variable parameters in the INKX0505950A valve-jet, which influence its performance: 1) operation frequency 2) fluid pressure. The recommended maximum operating frequency of 1000Hz stipulates that the valve-jet can be opened and closed 1000 repetitions per second with a voltage of 24 V_{DC}. This control signal is a square-wave function which instantaneously rises from 0 V_{DC} to 24 V_{DC}. The actual drive signal used is a spike-and-hold signal, which rises instantaneously to 24 V_{DC} for a very

short duration and is very quickly dropped to 3 V_{DC} to maintain the plunger in the open position. The spike-and-hold drive signal is discussed in section 3.4.

A pressure of approximately 10 psi has to be maintained in the fluid supply line to push the fluid through and out of the valve-jet during operation. We may possibly get superior valve-jet performance by operating at higher pressures and this is discussed in section 4.3.

The valve-jet has to be designed with robust, durable and inert materials that are resistant to chemicals and high temperatures. This was achieved by a careful selection of the materials used in manufacturing the valve-jet components. The internal cylinder containing the plunger needs to be resistant to a wide range of fluids that may be used with the valve-jet and also needs to be manufactured within a very tight tolerance limit to accommodate the plunger precisely. Although the material information for the components were not provided in the specification drawings, it is easy to deduce this information and understand the material properties, especially the various plastics used in making the valve-jet components.

PPS (PolyPhenylene Sulfide) was probably the material used for the internal cylinder because it offers the broadest resistance to chemicals of any advanced engineering plastic. There are no known solvents below 200°C and it is inert to steam, strong bases, fuels and acids. Minimal moisture absorption and a very low coefficient of linear thermal expansion, combined with stress-relieving manufacturing, make PPS ideally suited for precise tolerance machined components. It is the ideal material for structural applications in corrosive environments. PEEK (PolyEtherEther-Ketone) is a high-performance engineering thermoplastic, which offers very good chemical and water resistance. It inherently has good wear and abrasion resistance with very low moisture absorption and is unaffected by continuous exposure to hot water or steam. Hence PEEK is an ideal material for the base plastic into which the ruby orifice is fitted because it will not be affected by shrinkage or wear when used with various demanding types of fluid under extreme conditions. EPDM is a ter-polymer of ethylene and propylene. It has a saturated polymer backbone, which gives it excellent resistance to ozone, polar

solvents (i.e. esters and ketones), acids and caustics as well as to denting. These physical and chemical properties make it ideal in this particular application, which require continued deformation and compression of the rubber material during the open and closing operations.

2.2 The INKX0503850A solenoid valve-jet

2.2.1. Physical and structural characteristics

The INKX0503850A solenoid valve-jet in **Figure 2.5** is identical to the INKX0505950A valve-jet except that it has a Teflon tube instead of a ruby orifice at the outlet port. An orifice has to be fitted on at the outlet before it can be used in printing operations. This design may advantageous because it allows the flexibility of switching between orifice sizes for different print applications, unlike the INKX0505950A valve-jet where we are limited to a single orifice size.

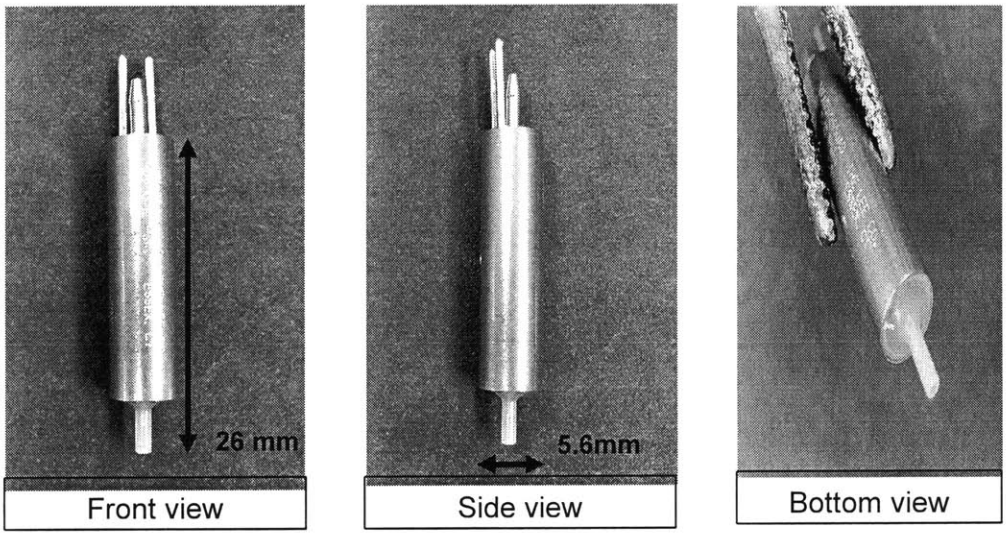

Figure 2.5: External full view picture of INKX0503850A valve

Figure 2.6 is a view through the mid-section of the INKX0503850A solenoid valve-jet. There are three differences from the INKX0505950A: 1) The plunger mechanism has a different geometry from that in the INKX0503850A valve-jet, separated by a smaller gap size of 60μm from the metallic core and circumferential

channel clearance of 20μm with the cylindrical container around it. 2) The air cavity between the stainless steel outer casing and the solenoid coil has been filled with epoxy to enhance heat transfer out of the valve-jet. 3) It does not have an integrated ruby orifice at the outlet port. The INKX0503850A is an older model of the solenoid valve-jet than the INKX0505950A, and hence it is conceivable that the difference in plunger geometry is a design improvement by the Lee Co. to produce valves with better performance capabilities. Another reason is that the integration of the ruby orifice requires a different design for the plunger interface.

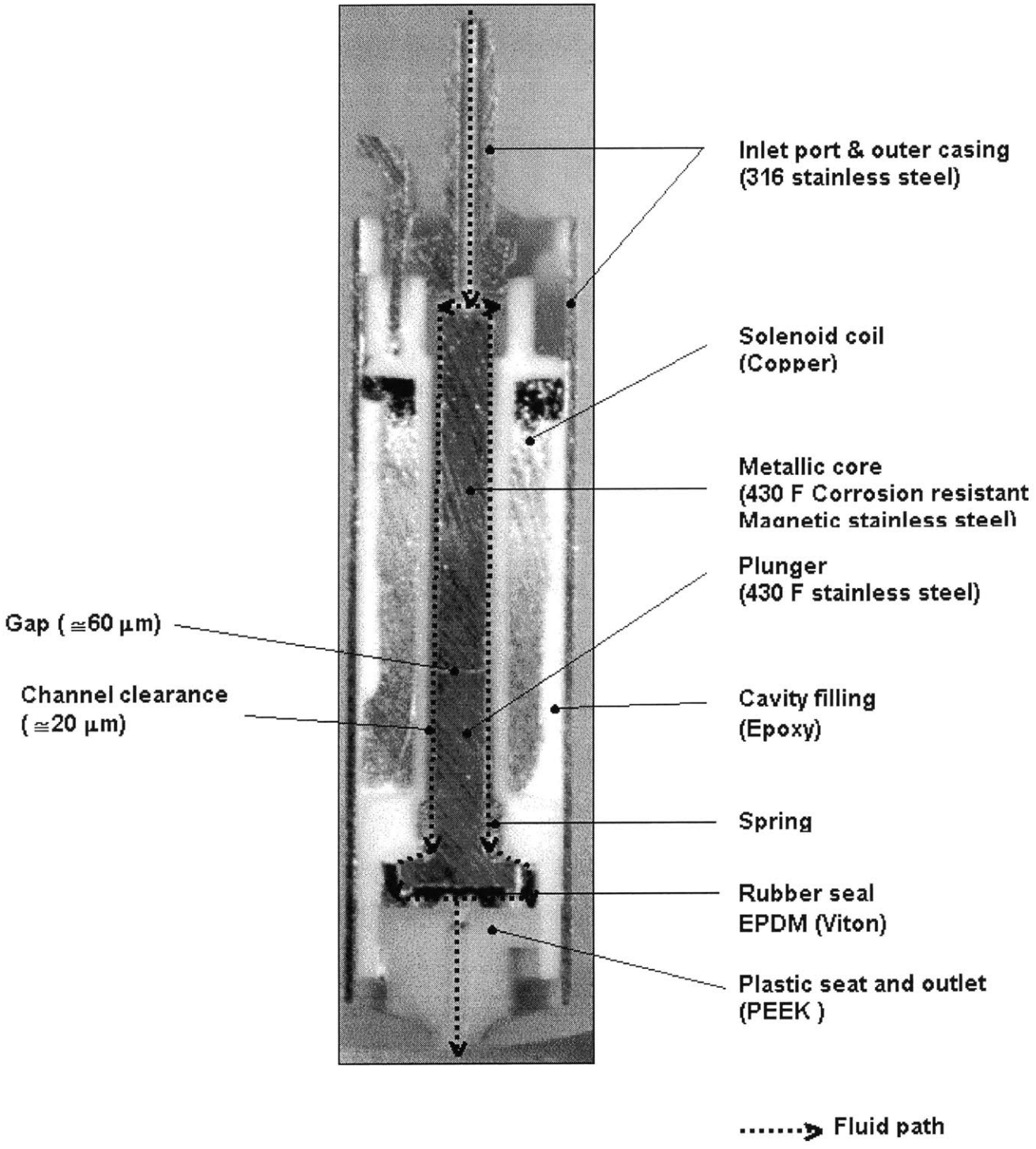

Figure 2.6: Polished cross-sectional view of INKX0503850A valve

2.2.2. Operational specifications

Table 2.2 summarizes the recommended maximum frequency, voltage and fluid pressure for the INKX0503850A solenoid valve, as recommended by The Lee Fluidic Co. [Electro-fluidic systems technical handbook 6th edition, The Lee Co.]. The specification drawing for the INKX0503850A valve-jet is attached in Appendix A.3.

Characteristic	Condition
Maximum operating frequency	1000 Hz at 12 VDC pulse
Operating voltage	12 VDC pulse
Operating pressure	0-10 psi
Coil resistance	10.7 Ohms nominal
Coil inductance	2.5 mH
Wetted material	• 430 corrosion resistant magnetic stainless steel • 316 or 302 stainless steel • PPS (Polyphosphine sulfide) • PEEK • EPDM (propylene) • Epoxy

Table 2.2: INKX0503850A solenoid valve-jet characteristics

The recommended maximum operating frequency is 1000Hz using a 12 V_{DC} spike-and 3 V_{DC} hold input signal. An operating pressure range of 0-10psi is recommended. Although the electrical inductance and resistance of the INKX0505950A and INKX0503850A valve-jets are significantly different, both have time constants of approximately 0.25 milliseconds. The time constant of valve-jet is discussed in section 3.1.1.

3. VALVE-JET ELECTRONICS DRIVE CIRCUIT

In the DC solenoid valve-jet, there is a magnetic coil that actuates the valve mechanism. The coil can be electrically modeled as an inductance and a resistance connected in series. It presents the drive circuit with a resistive and inductive load. The coil resistance and operating voltage will determine the steady state current and power consumption.

This chapter first presents the electrical properties of the solenoid valve-jet, after which the spike-and-hold input signal and the electrical circuit required to drive the valve-jet to produce a fluid stream with a variable duration is discussed.

3.1 Valve-jet electrical properties

3.1.1 Time constant of valve-jet

The copper solenoid coil in the valve-jet is an inductive load and therefore will produce an inductance effect on the electrical drive circuit. For a inductive load, the time constant, τ, (defined as the time required for the current in the valve coil to reach 63% of its steady state value when subjected to a step voltage input), is given by:

$$\boxed{\tau = \frac{L}{R}} \qquad (3.1)$$

For the INKX0505950A valve-jet, where the coil inductance, where L =26.7 mH and coil resistance R =110 Ω,

$$\tau = \frac{L}{R}$$
$$= \frac{26.7 \times 10^{-3}}{110}$$
$$= 0.242ms$$

This gives us a theoretical rise time of 0.242 milliseconds for the valve-jet. The coil inductance and the resistance will affect the valve's response time by opposing changes in the coil current. When the solenoid valve is turned off, the energy stored in the coil's magnetic field will have to be dissipated by some means, usually through a diode to keep the circuit operation within predictable, safe limits. The diodes act as a current clamp. They provide a dissipation loop when the valve drive potential is released to prevent damage to other circuit components. This concept of a diode clamp is an integral part of the solenoid valve-jet drive circuit is discussed in section 3.4.

3.1.2 Power dissipation in valve-jet

The total power dissipation is a useful measure of the solenoid drive level and also provides an estimation of the amount of heat transfer from the valve-jet during steady-state operation. The lumped electrical characteristics of the valve-jet provided by The Lee Co. are:

$$R = 110\Omega$$
$$L = 26.7mH$$
$$V_{drive} = 24V(\max)(\text{held no longer than 1 ms})$$
$$Power\ rating = 500\ mW$$

The average power generated by operating the valve-jet with a spike and hold signal at 30 Hz can be calculated using the following relationships:

$$Power_{average} = 30 \times \left\{ \left(\int_{0}^{0.25\times10^{-3}} I^2 R dt \right)_{spike} + \left(\int_{0.25\times10^{-3}}^{0.033} I^2 R dt \right)_{hold} \right\} \quad (3.2)$$

$$I(t)_{spike} = \frac{V}{R} \times \left(1 - e^{-\frac{R}{L}t} \right) \quad (3.3)$$

$$I(t)_{hold} = A \times \left(\frac{V}{R}\right) e^{-\frac{R}{L}t} + B \qquad (3.4)$$

where, A is the initial boundary condition on the current value at the end of the spike voltage and B is the steady state holding voltage (3V). Equation (3.2) integrates the total power dissipated during both the spike and hold durations of the L-R circuit. Equation (3.3) describes the exponential rise of the current during the spike and equation (3.4) describes the exponential fall of the current beginning at the falling edge of the spike signal to the steady hold voltage and finally the falling edge of the hold voltage, as a function of time. Because the circuit does not actually behave in the manner of a step function, it is more precise to use an expression of this form involving the time constant and rise time of a L-R circuit. Note that the duration of the spike used is 0.24 milliseconds while the hold duration is 33.1 milliseconds. The average power dissipation calculated using the above relationships when operating at 30 Hz is 0.088 watts, which is much lower than the 500 milli-watts stipulated in The Lee Co. technical specifications. This can be explained because Lee's calculations were based on a higher operating frequency of probably 1000 Hz as well as a much shorter holding period, although this was not explicitly stated in the documentation.

3.2 The spike-and-hold drive signal

A spike-and-hold signal waveform shown in **Figure 3.1** can be used to drive the INKX0505950 solenoid valve-jet. The signal spike has a magnitude of $24V_{DC}$ for duration of 0.24 milliseconds while the hold portion of the signal is dropped from $24V_{DC}$ to 3 V_{DC} and maintained at this level of a variable duration, depending on the amount of time for which the valve-jet is required to be held open. It was determined earlier that the valve-jet has a theoretical time constant of approximately 0.242 milliseconds. It can be deduced that the current will rise to only 63% of the steady state value within the 0.24 milliseconds of the initial signal spike.

The $24V_{DC}$ voltage spike sends a current through the copper coil which instantaneously builds a magnetic field to temporarily magnetize the metallic core and plunger so that plunger gets attracted very rapidly to the metallic core. This lifts the plunger off its resting position above the orifice, creating a gap between the plunger and ruby orifice through which fluid is forced out under pressure. This voltage impulse provides the energy required to overcome the spring force and fluid back-pressure which normally keeps the valve-jet closed. It can subsequently be dropped to $3V_{DC}$ for the holding phase, as only this level is necessary to maintain the plunger in the open position. Reducing the voltage level also helps to reduce the power consumption and any danger of valve damage caused by overheating.

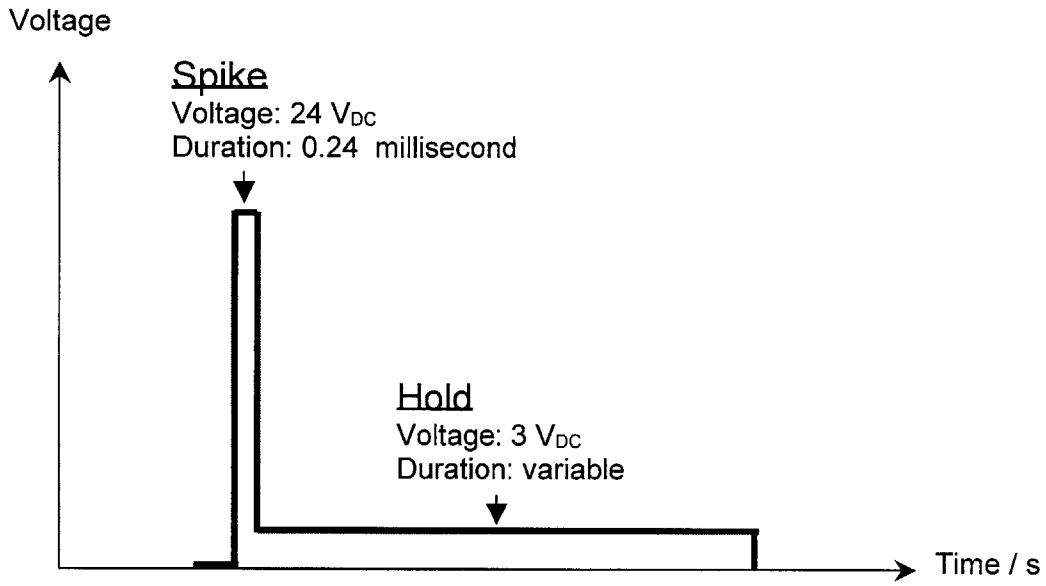

Figure 3.1: Spike-and-hold signal

3.3 Electrical drive circuit

Two different electrical circuits were investigated and both proved to be successful in providing the drive signal necessary to operate the valve-jet. They are:

i) The arbitrary signal function generator with power amplifier circuit.

ii) Spike-and-hold driver circuit by The Lee Co.

The first makes use of the arbitrary signal function generator to create a spike-and-hold signal and then amplifies this output before feeding this into the solenoid valve-jet. The driver circuit designed by The Lee Co. consists of a timer chip and a network of transistors to create a similar spike-and-hold signal. Although the two circuits appear different, both essentially perform a similar function: to generate a spike-and-hold input signal to operate the valve-jet. These two setups are discussed in greater details in following sections 3.3.1 and 3.3.2.

3.3.1. The arbitrary signal function generator with power amplifier circuit

The arbitrary signal function generator with power amplifier circuit is a very quick and simple setup which can be used to create the signal input required to drive the solenoid valve-jet, without constructing the complete drive circuit recommended by The Lee Co., especially in the preliminary stages of this investigation. This circuit makes use of the programmable arbitrary waveform function in the Hewlett-Packard HP33120A function generator. It offers us the flexibility of easily and quickly programming spike-and-hold waveforms with different frequencies and voltages for investigative purposes of the valve-jet characteristics.

Figure 3.2 is the electrical circuit diagram for this setup. The HP function generator is limited to a voltage output range of 0 - 5 V_{DC}. A power amplifier (Khronhite 2230 power amplifier) is therefore required to magnify this output to the required 24 V_{DC} input voltage (i.e. the 2.4 V_{DC} function generator output is magnified 10 times to 24 V_{DC} and then applied to the solenoid valve-jet). A combination of a 1N4005 diode and 1N4749A zener diode is added in parallel with the solenoid valve (modeled as a resistor and inductor in series). This acts as a diode clamp for the current loop through the coil, providing a dissipation loop when the valve drive potential is released. A 2N3904 transistor serves as a switch, which is in the closed position, drawing current through the valve-jet, during the rising edge of the spike-and-hold signal. It immediately reverses to the open position during at the falling edge of the control signal. This "immunizes" the function generator and power amplifier from the inductive "kick-back" created in the solenoid valve-jet during turn-off (hence avoiding damage to both equipment), and

leaves the current to be dissipated in the diode clamp loop. The 1 Ω resistor is included for the purpose of monitoring the current flowing through the circuit.

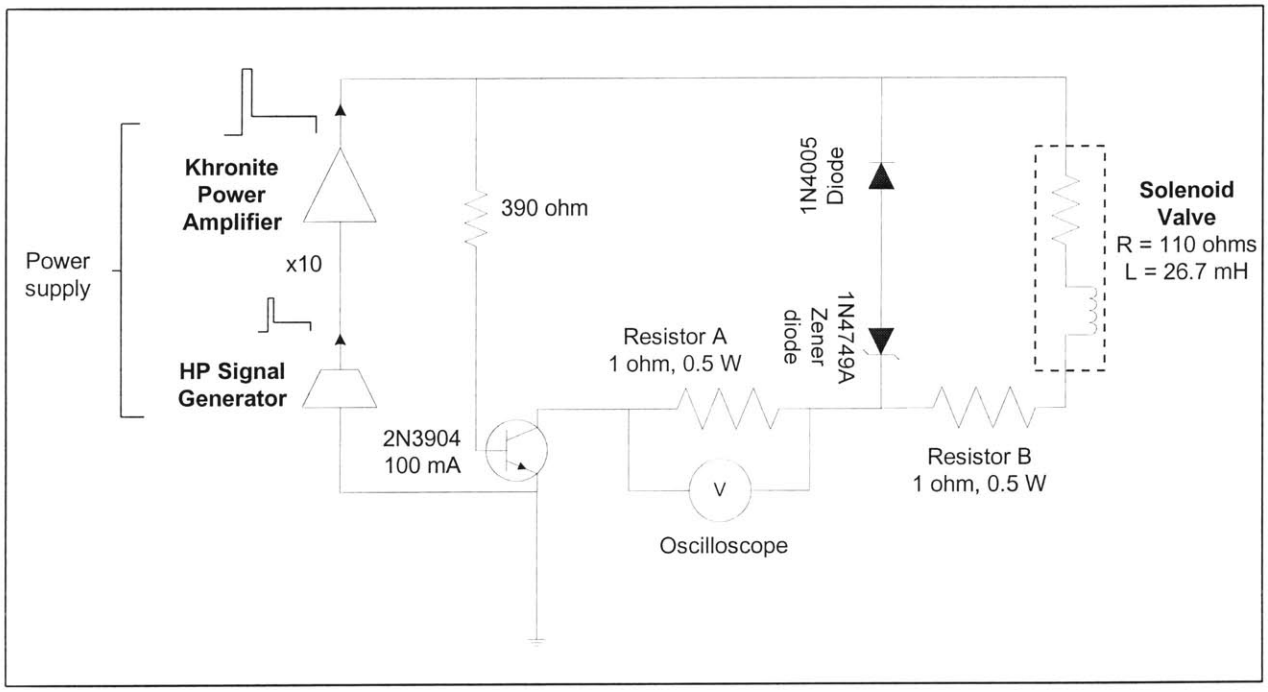

Figure 3.2: Arbitrary function generator with power amplifier driver circuit diagram

3.3.1.1 Limitation of the HP function generator

Although this setup allows us the flexibility of changing the frequency and voltage of the signal waveform very easily, it has the disadvantage of limiting us to signal duration up to a maximum of 3.6 seconds (i.e. the maximum time for which the valve can be opened is 3.6 seconds). This limitation is caused by these two reasons:

1) The HP function generator has sufficient memory to store up to a maximum of 15000 programmable data points.
2) A single data point represents a specific amount of time, which in our case is the duration of the spike duration lasting for 240 $x10^{-6}$ seconds.

Frequency limit calculation:

We are constrained in this case to use a smallest time unit of 240 x 10^{-6} s for the "spike". The time period 240 x 10^{-6} s will represent one basic data point. Therefore, the expression relating the number of data points used to the signal frequency is:

$$\text{number of data points} = \frac{\left(\frac{1}{\text{frequency}}\right)}{240 \times 10^{-6}}$$

or

$$(\text{number of data points}) \times (\text{frequency}) = 416 \qquad (3.5)$$

Since the maximum data points available on the HP function generator is 15000, we can deduce that the smallest frequency obtainable on this setup is approximately 0.2778 Hz, which is equivalent to a period of 3.6 seconds.

Note that after the spike-and-hold waveform has been programmed to accommodate a particular number of data points, we are then restricted to using the frequency that has been tailored for this waveform. Altering the frequency without re-programming the waveform to take a different number of data points will result in a data point that is not 240 x 10^{-6} seconds in duration. Information on the operation of the HP function generator can be obtained from [HP33120A Function Generator / Arbitrary Waveform Generator User Guide].

3.3.1.2 Diode clamp

The 2N3904 transistor behaves like an electrical switch, flipping between the close and open positions, which correspond to the rising and falling edge of the input signal. However, because inductors have the property:

$$V = L\frac{dI}{dt} \qquad (3.6)$$

it is impossible to turn off the current suddenly, since it would imply an infinite voltage across the inductor's terminals. Instead the voltage across the inductor suddenly rises until it forces current to flow; this will cause the electronics controlling the inductive loads to be easily damaged. The best solution is to put a diode across the inductor, as in **Figure 3.3.** When the switch is on, the diode is back-biased. At turn-off the diode goes into conduction, putting the switch terminal a diode drop above the positive supply voltage. The diode should be chosen to be able to handle the initial diode current, which equals the steady current of 0.218A flowing through the inductor. The 1N4005 diode with a rated maximum forward current of 1.1A is ideal for this purpose.

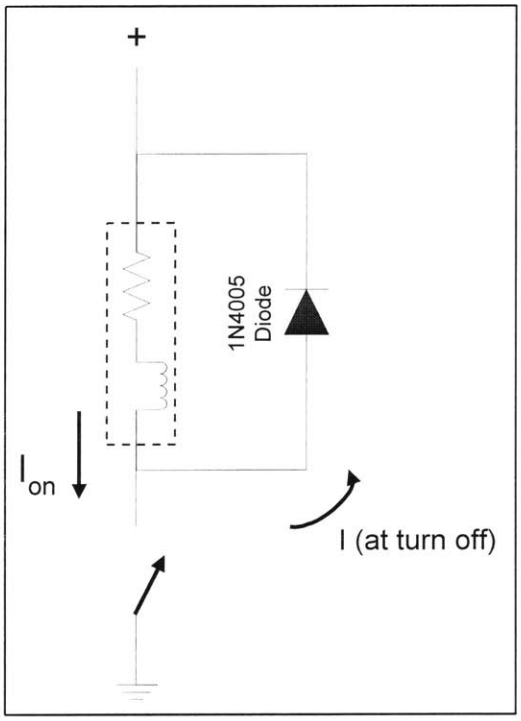

Figure 3.3: Blocking inductive kick during turn-off

However, this protection circuit has a disadvantage in lengthening the decay of current through the inductor, since the rate of change of inductor current is proportional to the voltage across it. Therefore, to achieve the fastest decay with a maximum voltage of 24V, a 1N4749A zener diode (rated 24V; 1W) is added in series with the diode as in **Figure 3.2**. This causes the voltage across the inductor to rise, and therefore increases the rate of decay of current through the circuit. This gives us a ramp-down of current

rather than an exponential decay. The waveform observed on the oscilloscope using with and without including the zener diode is shown in **Figure 3.4** below.

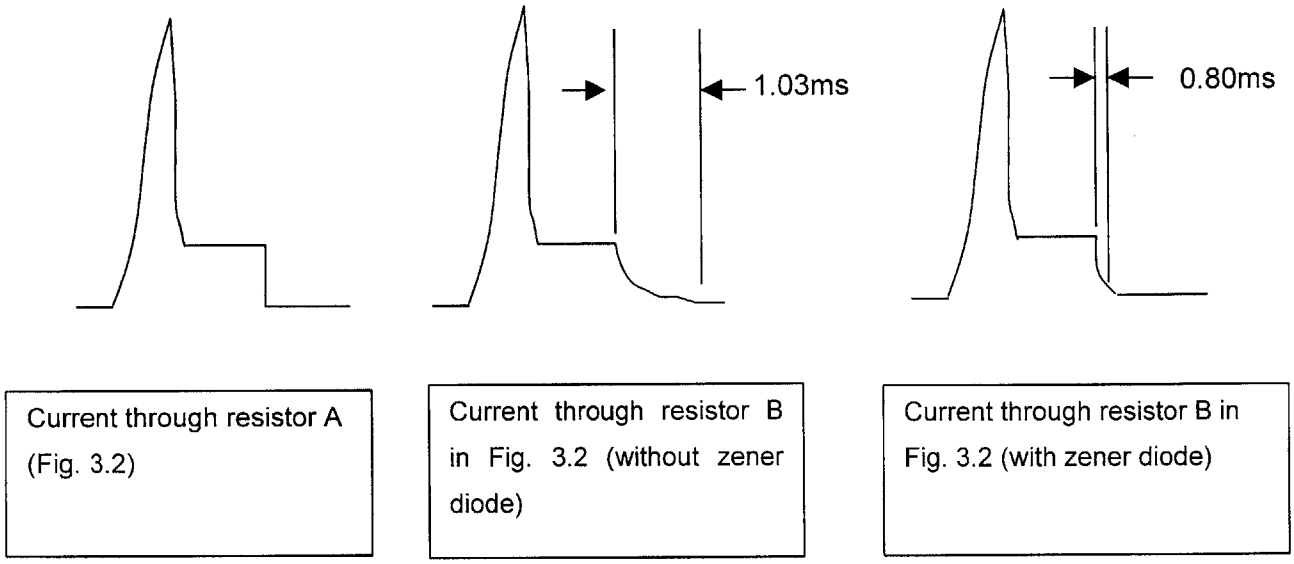

Figure 3.4: Effects of zener diode on decay time

3.3.2 The Lee "Spike and Hold" driver circuit

The Lee drive circuit generates a spike-and-hold signal waveform identical to that in the HP arbitrary waveform generator but using a network of discrete electronic components. Its main advantage is that there is no limitation on the hold duration of the signal (compared to the previous setup where the hold signal duration is limited to only 3.6 seconds). The Lee circuit diagram shown in **Figure 3.7** can be imagined as being made up of two sub-units: 1) Timer sub-unit and 2) Voltage supply and diode clamp sub-unit, each performing different functions.

3.3.2.1 Timer sub-unit

The NE555V integrated chip and the electrical components connected around it constitutes the timer sub-unit. The NE555V is an integrated timer chip, which controls the duration of the spike (denoted λ in **Figure 3.7**) through the combination of the R1 resistor and C1 capacitor given by the relationship:

$$\lambda \text{ pulse duration} = 1.1 \times R1 \times C1 (\text{seconds}) \qquad (3.7)$$

Values of R1 and C1 have to be adjusted as required to obtain the desired pulse duration. For the V1 spike duration of λ = 0.240 milliseconds, a feasible combination is to use R1 = 320 kohms and C1 = 680 pF. The control signal input in **Figure 3.7** takes the form of a square wave where its period determines the open time for the valve-jet. This control signal can be tapped out from either a HP function generator or the Alpha 3DP™ machine (discussed in section 6.1). The function of the pins on the NE555 chip is shown in **Figure 3.5** below.

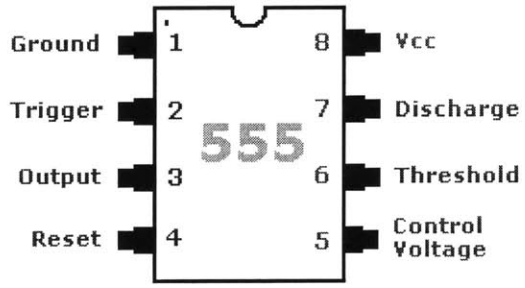

Figure 3.5: NE555 timer chip pin labeling

The ZN3053 transistor connected to pin 2 of the NE555 chip is usually in the non-conducting condition, but becomes conducting when the control input signal is applied. This creates a voltage drop of 0.6V between pin 2 and ground across the transistor and immediately triggers (on the rising edge) the NE555 chip to release signal of λ = 0.240 milliseconds duration. This signal is passed onwards to the MPSA42 transistor in the voltage supply and diode clamp sub-unit.

3.3.2.2 Voltage supply and diode clamp sub-unit

The spike signal (duration 0.240 milliseconds) created by the timer sub-unit is passed on to the next stage of the spike-and-hold circuit. The MPSA42 and SK3038

transistors are set up in a beta-boosting configuration as a Sziklai connection ("complementary Darlington") for high current gain. The arrival of the 0.240 milliseconds signal from the NE555 timer causes the MPSA42 transistor to switch to the closed position thus drawing current from the V1 source through the 10 kΩ resistor and the SK3038 transistor through the valve-jet. Throughout the 0.240 milliseconds duration, the 1N4005 diode connected to the 3 V supply is in reverse bias. The 24V voltage drop is seen by the valve-jet because it is connected in parallel and therefore it is kicked open by this spike voltage. The MPSA42 transistor flips to the open position on the falling edge of the signal from the timer chip and therefore the circuit stops drawing current from the 24 V source. Simultaneously, the 1N4005 diode becomes forward bias and starts drawing current from the V2 source. The V2 source provides the steady state holding voltage required to hold the valve-jet open. It is determined experimentally that although the V2 source is supposed to supply a 3 V holding voltage, the actual holding voltage across the valve-jet was about 2 V. The remaining 1V is lost to the voltage drop across the diode and wire resistance. Finally, the SK3440 transistor switches to the open position on the falling edge of the input control signal. The remaining current is allowed to dissipate through the diode clamp (1N4005 and 1N4749 transistor pair). A diode clamp in parallel with the valve-jet was used to provide a dissipation loop for the current during the switching off (discussed in section 3.5.2.1). The response time of the solenoid valve was reduced by operating the valve at higher than normal supply voltage in conjunction with the 1N4749 zener diode. The inclusion of the zener diode enhances the response of the valve, reducing the valve's response time. The creation of this spike-and-hold signal is illustrated in **Figure 3.6**.

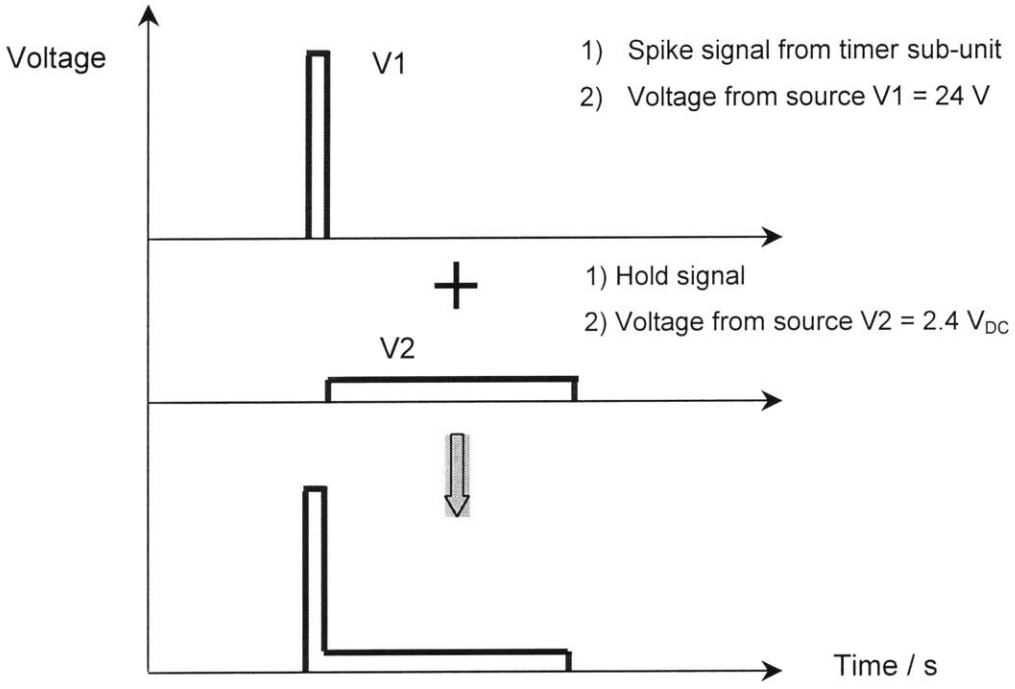

Figure 3.6: Super-position of spike-and-hold signal using Lee circuit

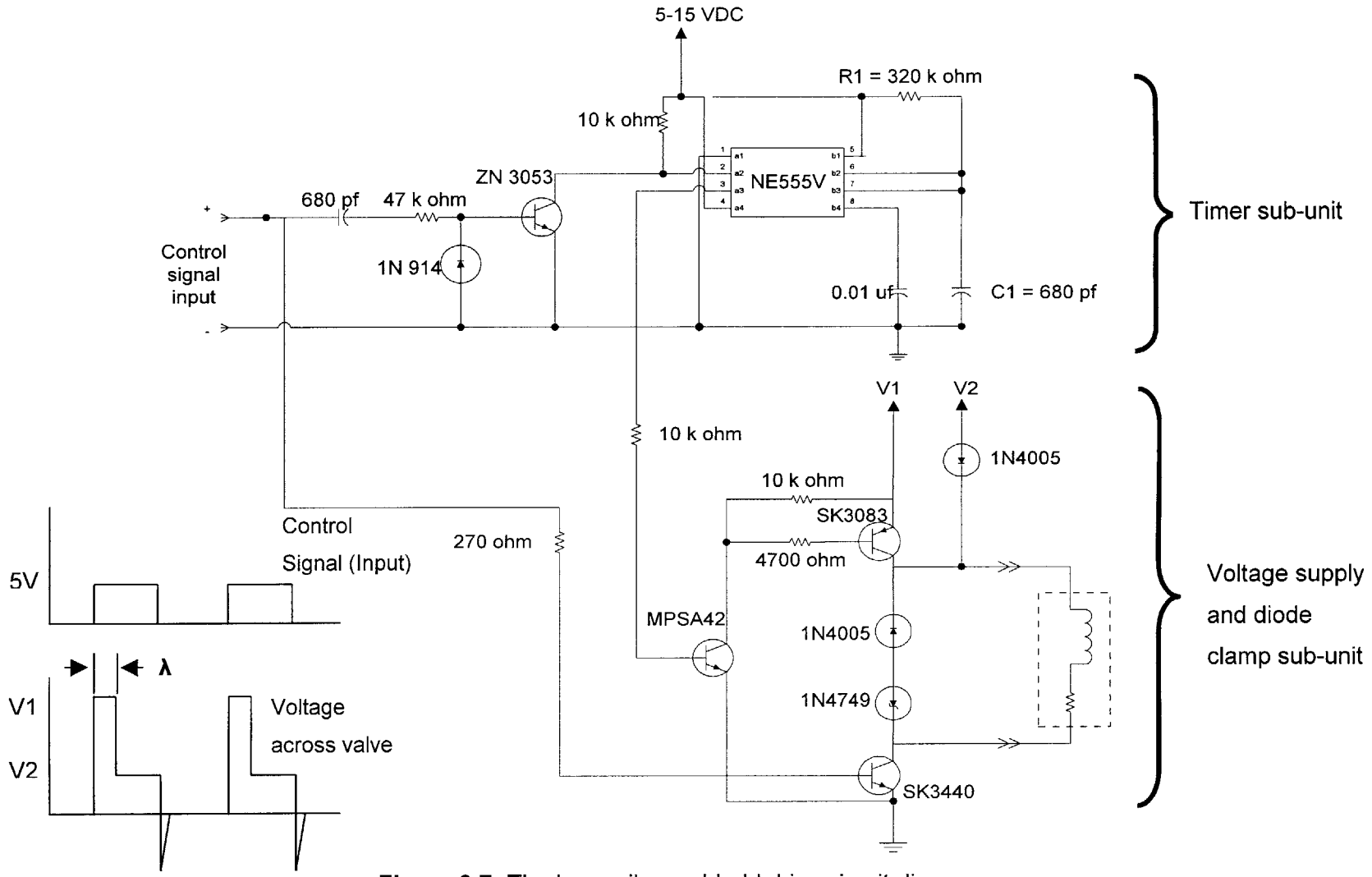

Figure 3.7: The Lee spike-and-hold drive circuit diagram

3.4 Minimum spike and hold voltage for valve-jet operation

For the INKX0505950A valve-jet rated at $24V_{DC}$, it was experimentally shown that the recommended "spike" voltage of 24 V_{DC} followed by a "hold" voltage of $3V_{DC}$ can successfully actuate the valve-jet.

However, an experiment using the arbitrary function generator and power amplifier setup showed that it is possible to go even below these recommended values for actuating the valve-jet. The minimum spike voltage to actuate the valve obtained experimentally is actually 21V (i.e. minimum "spike" voltage > 21V) instead of 24V. No fluid is released at 20V because the spike is not sufficiently high. The minimum "hold" voltage is 2V (i.e. minimum "hold" voltage >2V), below which the valve-jet cannot be kept open. The experiment was performed at 10 psi.

The purpose of dropping the spike voltage from 24V to a hold of 3V is to minimize the power consumption (and hence the problem of over-heating) in the valve-jet (especially when operating at high frequencies). The other advantage of using a low holding voltage may be that the decay time for the current during turn-off will be reduced and hence allow the valve-jet to close more rapidly. However, since the minimum spike and hold voltages that we have determined are not significantly different from the recommended values, there are no major advantages to be gained from operating the valve-jet at these absolute lower limits.

4. JET-STREAM CHARACTERISTICS

Having constructed the necessary electrical drive circuit and fluid supply system to operate the valve-jet, we are now ready to evaluate its performance under varying parameters such as operating frequency and pressure. The results from the tests will reveal the capabilities and operational limitations of the valve-jet, and will eventually be used in order to obtain the best part quality in subsequent printing operations.

This chapter presents several performance parameter including flow-rate, stream velocity, response time and time of flight of the stream under varying frequency and pressure conditions. The stream observation station to capture an image of a single fluid stream is also described together with the head and tail images.

4.1 Valve-jet flow-rate

Flow-rate is the most important variable characterizing valve performance. Defined as the volume of fluid dispensed by the valve-jet per unit time, the appropriate unit for flow-rate measurement is m^3/sec or cm^3/min. It influences the maximum traverse speed that can be used on the fast axis during printing, the saturation level of the printed green part and layer drying time after each pass.

Because the plunger has a clearance of approximate 130 microns maximum displacement during operation, while the channel clearance between the plunger and cylinder that holds it is 10 microns, we are faced with the limitation of using fluids with particulate sizes that are not larger than 10 microns to avoid any clogging occurrences. The best fluid to use in the evaluation tests of the valve-jet would be water.

4.1.1 Fluid supply system

A recycling pump and clam-shell pressure sensor shown in **Figure 4.1** was used as the fluid supply system into the solenoid valve-jet. This system allows us to recycle the fluid, and eliminates the hassle of having to refill the reservoir every time the fluid is depleted. The clam-shell is connected to a pressure sensor and a wall air pressure

outlet. It maintains in its interior a small reservoir of pressurized fluid, which is supplied to the valve-jet. As the fluid reservoir is depleted, the internal pressure of the clam-shell decreases. The sensor unit detects this, activates the feedback loop, which starts the motor-pump to pump more fluid into the clam-shell. A 5μm pore-size filter was added before the inlet to the clam-shell to remove any particulates that may clog up the valve-jet. To minimize shock wave propagation through the fluid supply line generated by the "water-hammer" effect when the plunger slams shut against the ruby orifice, a water capacitor was added to create an air-reservoir, which can absorb and dampen the shock wave propagation.

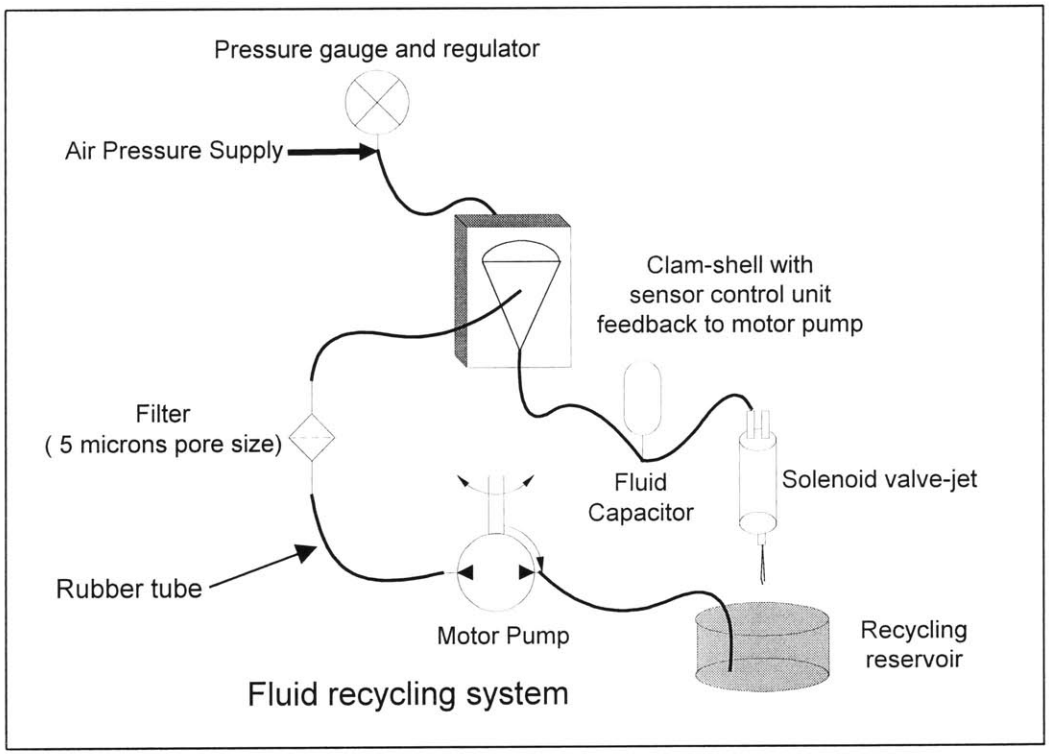

Figure 4.1: Fluid supply system: Recycling pump and clam-shell design

4.1.2 Flow-rate as a function of control signal duration

The Lee circuit setup discussed in section 3.5.2 was used together with the fluid recycling system in a test-stand setup to evaluate the valve-jet's flow-rate. The control signal was a square wave, whose duration was varied by simply changing the control

signal frequency. It should be noted that the square wave produced by the HP function generator is a "half-wave" with a ½ duty cycle, meaning that the valve-jet is open for only half of the entire period. The fluid was pressurized at 10psi. At 30Hz, the fluid dispensed from 100 cycles of these square waves were collected, while at higher frequencies of 200 Hz and above, the fluid had to be collected from 1000 cycles of signal inputs so that more fluid can be collected to reduce inaccuracies caused by the 3 decimal place restriction on the weighing scale.

The flow-rate vs. frequency plot is shown in **Figure 4.2** below. A half square wave was used as the control signal in all cases. The valve was open for half the time and closed for the remaining of the signal, representing a 50% duty cycle. Interestingly, the flow-rate remains relatively constant in the range of 5.5 – 6.0 cm^3/min for frequencies up to 500Hz, but increases very quickly to 10 cm^3/min at higher frequencies exceeding 500Hz. It is believed that the reason for this occurrence at high frequencies is that the valve-jet is oscillating so quickly that each signal pulse is not sufficiently long to allow the plunger to complete its entire stroke length. The valve-jet may also have different opening and closing times and one of them becomes the limiting factor to valve response time at high frequencies.

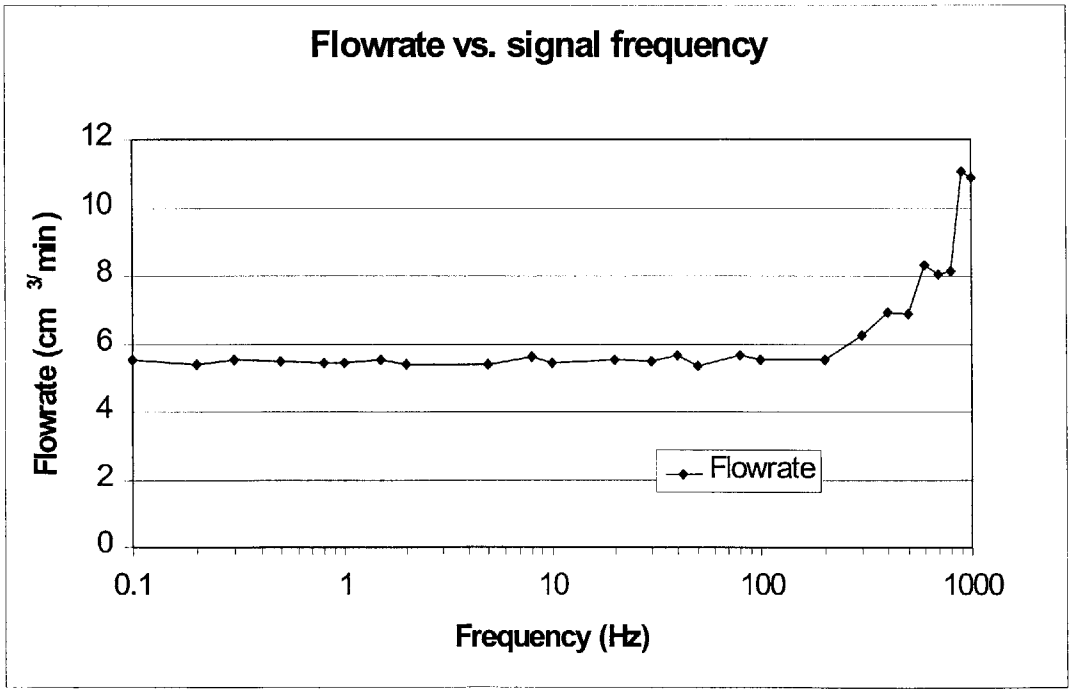

Figure 4.2: Pot of flow-rate vs. signal frequency (Water; pressure = 10psi)

The average jet-stream velocity is determined by dividing the flow-rate by the cross-sectional area of the valve-jet orifice. The average velocity vs. signal frequency plot is shown in **Figure 4.3**. Results indicate that the average stream speed is about 7 m/s using a fluid pressure of 10 psi. However, this velocity is true only when the valve-jet is used with water as the fluid medium. Different flow-rates and average velocities are expected if different fluids are run through the solenoid valve-jet.

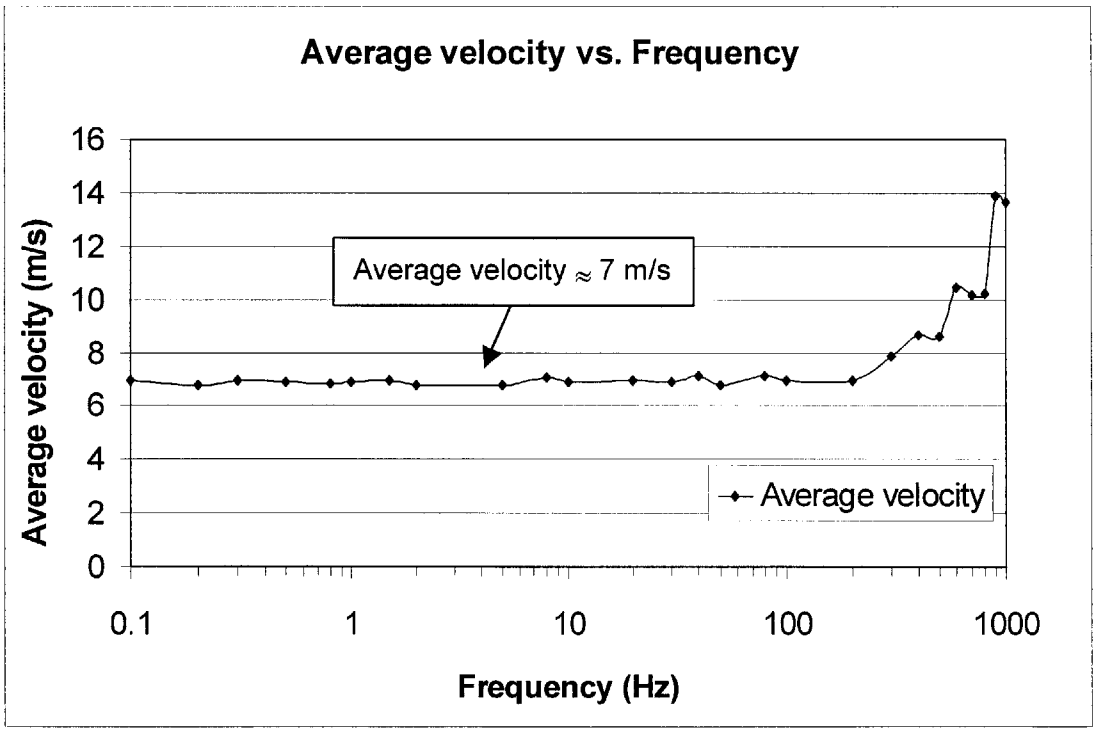

Figure 4.3: Plot of average stream velocity vs. signal frequency
(Water; Pressure = 10psi)

4.1.3 Flow-rate as a function of pressure

Fluid pressure is another important parameter influencing flow-rate of the valve-jet. Higher flow-rates are obtainable at higher working pressures. The recommended

operational pressure for the Lee valve-jet is 10 psi with a maximum working limit of 30 psi. To investigate the relationship between flow-rate and pressure, we have to hold the valve operating frequency constant at 30Hz, and allow the valve-jet to run for 100 cycles. This means that the total duration of each "burst" signal generated by the HP function generator is 3.33 seconds, but because the square wave used has only a duty cycle of ½, the valve-jet is only open for 1.67 seconds (when fluid is being collected) and closed for the remaining 1.67 seconds (no fluid collected). This was for flow-rates when the valve-jet was opening and closing dynamically. To determine the steady flow-rate, the valve-jet was held open for 1 minute at the different pressures and the fluid collected was measured. The results of the valve-jet in a dynamic and steady state operation are summarized into **Figure 4.4**. There is an approximately linear relationship between flow-rate and fluid pressure and the dynamic flow-rate (based on a 30Hz square wave with 50% duty cycle) is slightly larger than the steady state flow-rate.

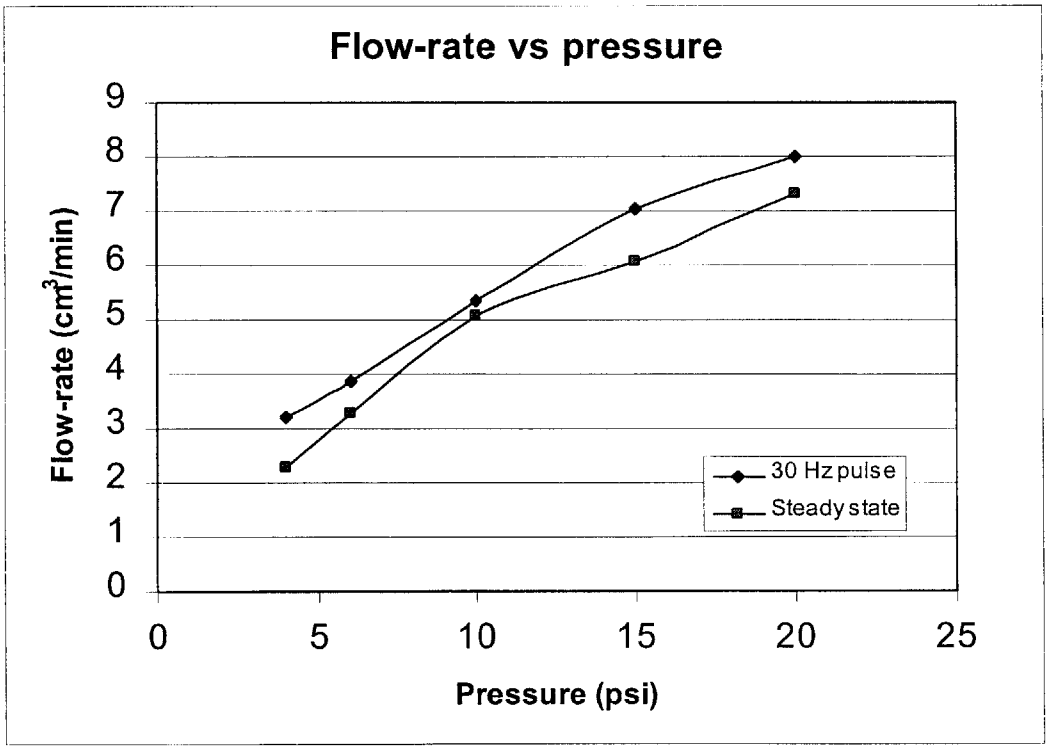

Figure 4.4: Plot of flow-rate vs. pressure

Because the operating pressure has a significant impact on valve-jet performance, it is important to have minimal pressure loss between the pressure-outlet in the wall and the fluid inlet port of valve-jet. Care must also be taken to ensure that no air bubbles or particulate debris are introduced and collected in the recycling clam-shell pump system. The air pressure gauge at the wall outlet was calibrated against a mercury manometer so that the required pressure is obtained at the inlet port to the valve-jet.

4.2 Pressure losses in valve-jet

4.2.1 Theoretical pressure losses

Fluid pressure losses in the valve-jet can be decomposed into two components: 1) pressure drop across ruby orifice, and 2) losses in valve-jet internal channels.

The pressure required to move a jet of fluid through the ruby orifice could be calculated in two components: 1) pressure to accelerate the fluid column and 2) viscous pressure drop. The kinetic pressure and viscous pressure drop required to accelerate a fluid column is given by:

$$\text{Kinetic Pressure} = \frac{\rho \times v^2}{2} \tag{4.1}$$

$$\text{Viscous Pressure} = \frac{32 \times v \times \mu \times l}{d^2} \tag{4.2}$$

where, ρ = density of fluid and v = fluid velocity, μ = fluid viscosity, l = length of orifice tube and d = diameter of orifice. Using fluid velocity v = 6.6 m/s, l = 1.0 mm, d = 0.13 mm (Section 2.1), the kinetic and viscous pressure are calculated to be 3.10 psi and 1.78 psi respectively; i.e. the total pressure loss in the ruby orifice is 4.88 psi. It can further be deduced that the pressure losses in the internal channels will be approximately 5.22 psi (assuming the total back pressure applied was 10 psi). Thus, approximately half of the

pressure is lost in the ruby orifice and the remaining half is lost as fluid flows through the internal structure of the valve-jet.

4.2.2 Experimental pressure losses

Actual pressure losses in the orifice and the internal structure of the valve-jet can be experimentally determined. A stand-alone ruby orifice fitted onto a plastic casing, shown in **Figure 4.6**, had fluid running through it subjected to different pressures for a fixed duration of 10 seconds. A clip attached to the rubber tube was used to stop the flow after every 10 seconds run. This procedure was performed at a range of pressures and the mass of fluid collected in each 10 seconds run was measured. An INKX0505950A solenoid valve-jet was then operated at the identical range of pressure for a 10 second period. The mass of fluid (water) collected was measured to obtain the equivalent flow-rate. These results are plotted together onto **Figure 4.5** below. Series 1 and Series 2 are the flow-rates obtained from a complete valve-jet and a stand-alone orifice respectively. We notice that the difference in flow-rate remains somewhat constant in the range of 0.60 cm^3/min at the range of pressures tested (neglecting the two readings at 6 and 8 psi). The flow-rate at 10 psi using a stand-alone ruby orifice is 6 cc/min, while the flow-rate from the valve-jet is about 5 cc/min. Since pressure loss is inversely proportional flow-rate (i.e. a larger pressure loss leads to lower flow-rate), it can be deduced that the major bulk of pressure losses (approximately 80%) occurs in the orifice, while only a small loss (20%) occurs through the internal structures of the valve-jet.

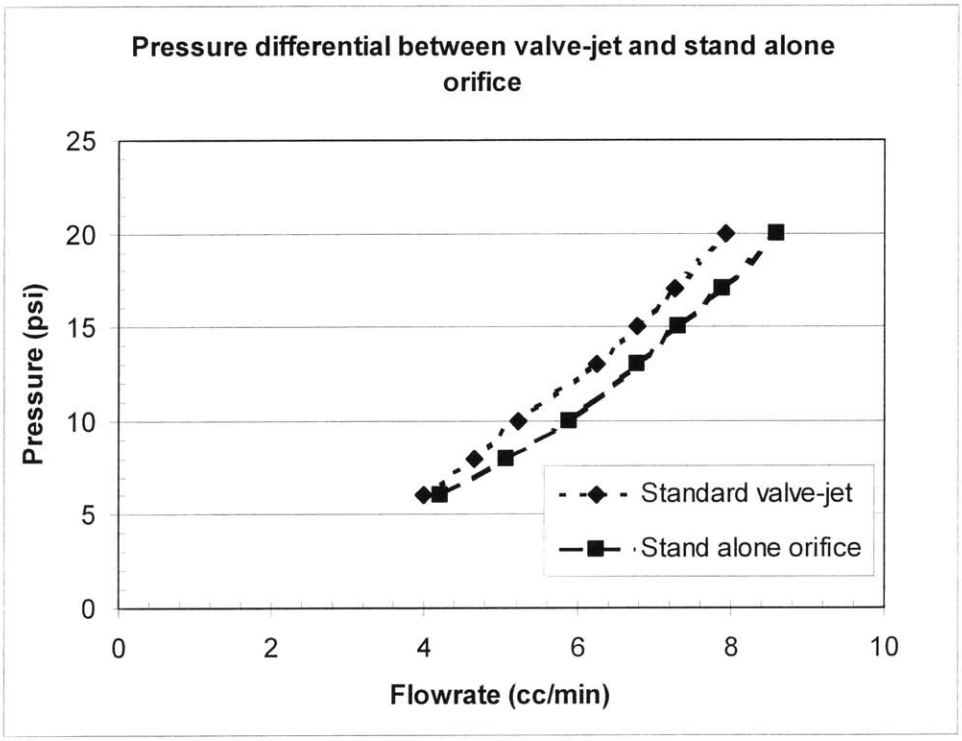

Figure 4.5: Pressure differential of INKX0505950A valve-jet vs. stand-alone ruby orifice

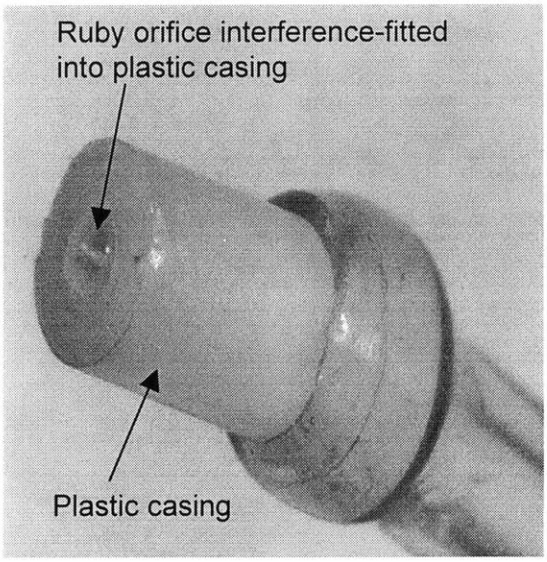

Figure 4.6: Ruby orifice interference-fitted in plastic casing

4.3 Shape and physical dimension

A single jet-stream is the basic fluid element producible by the solenoid valve-jet. Understanding its physical shape and dimension gives us an idea of the shape and smallest printable strand of powder material using the solenoid valve-jet.

It is extremely difficult to see the fluid stream with the naked eye because: 1) it is very small and 2) the frequency at which it is released is very high. The strobe helps to "freeze" the fluid stream as a stationary image by emitting light pulses at the same frequency at which the fluid is released. A CCD camera with a magnifying lenses linked to a television screen captures and magnifies the stationary image of the stream onto a display screen. The jet-stream image is magnified a total of 70x using this combination of the magnifying lenses and the television screen. Finally, video-capture software was used to download the screen image onto a computer for documentation purposes. The setup used is shown in **Figure 4.7** below. The Lee drive circuit was used to actuate the valve-jet, while the recycling pump system supplies the pressurized fluid to the inlet port of the valve-jet.

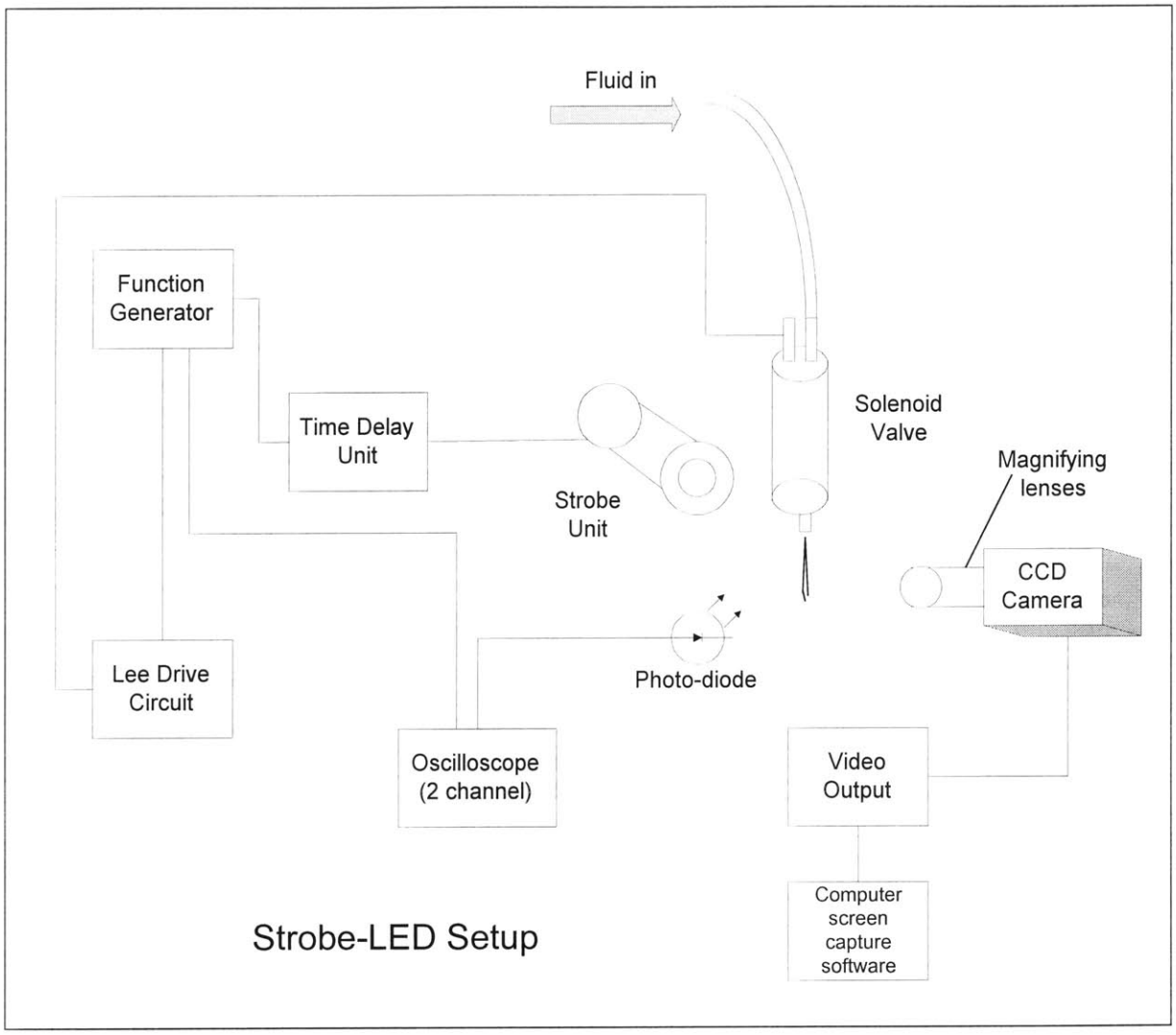

Figure 4.7: Strobe image capture and stream observation station

Figure 4.8 is the image of a single stream of water just as it is emerging from the valve-jet's orifice, taken by the strobe-light photography technique described earlier. The stream has a slight bulge at the front and a tapering shape at its tail. Its cross-sectional diameter of the stream is about 140 μm. The length of this water stream produced when the valve-jet is operating at 30 Hz (equivalent open time of 0.0167 seconds) is approximately 3.2mm long. The size of the television screen limits us to measuring only portions of the entire length of the jet-stream, hence the micrometer gauge to move the valve-jet along the vertical axis had to be adjusted to view sections of the stream at each

time and finally the total length of the jet-stream (moved on the micrometer gauge) was added up. However, we were unable to capture an image of the entire stream onto a single picture due to the limitation on the video capture equipment.

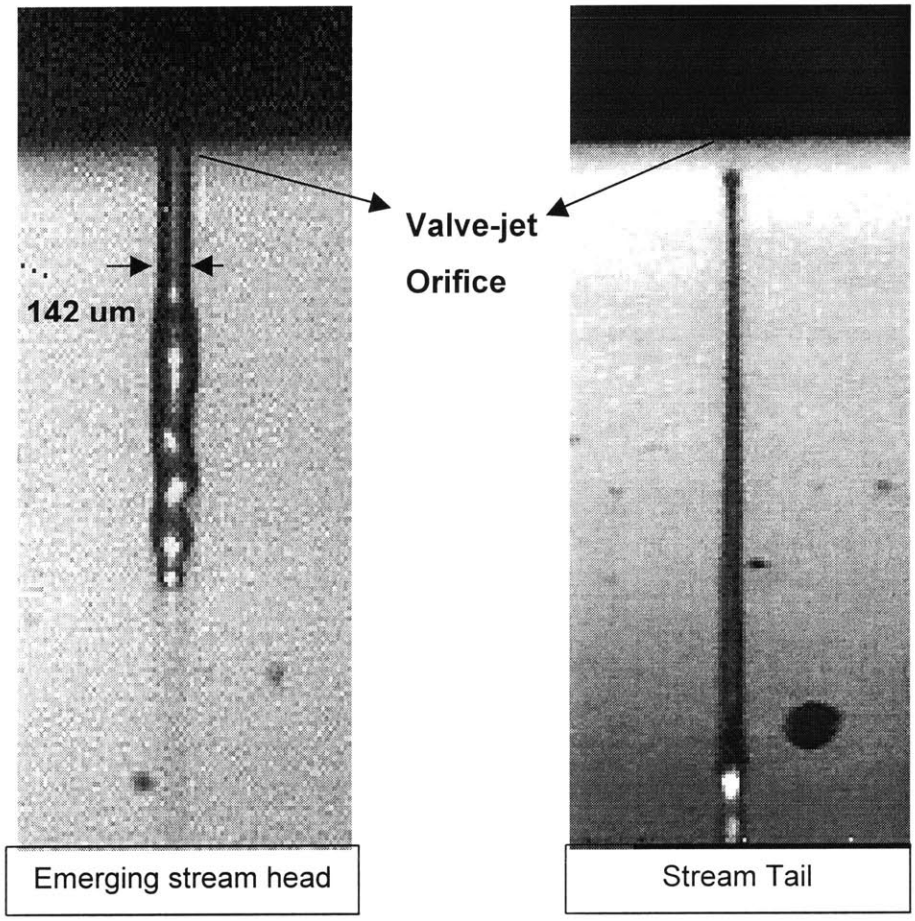

Figure 4.8: Strobe-photography image of stream head and tail
(70x magnification; 130μm diameter orifice)

This stream observation station also allows us to study the behavior of the front and back of fluid stream at various distances from the nozzle. This information is useful because it helps to determine the optimal positioning of the nozzle from the substrate during the printing operation. **Figure 4.9** and **Figure 4.10** are a series of frame images of the stream front and tail respectively taken at progressive time intervals using a pressure of 10 psi and a 30 Hz strobe frequency. Note that the number below each

picture refers to the distance of the stream front and tail respectively from the valve-jet orifice. The stream front maintains a very steady shape for large distances from the nozzle, until about 2.7 mm from the orifice where stream breakup occurs. The tail of the fluid stream however, begins to break up into satellite droplets at distances greater than only 0.5 mm from the nozzle. Therefore, to achieve the best quality printing, the valve-jet's nozzle should be positioned no more than 0.5mm away from the substrate bed. At distances greater, there is a risk of stream breakup and satellite formation at the trailing edge of the stream, which will produce less than desirable printed parts.

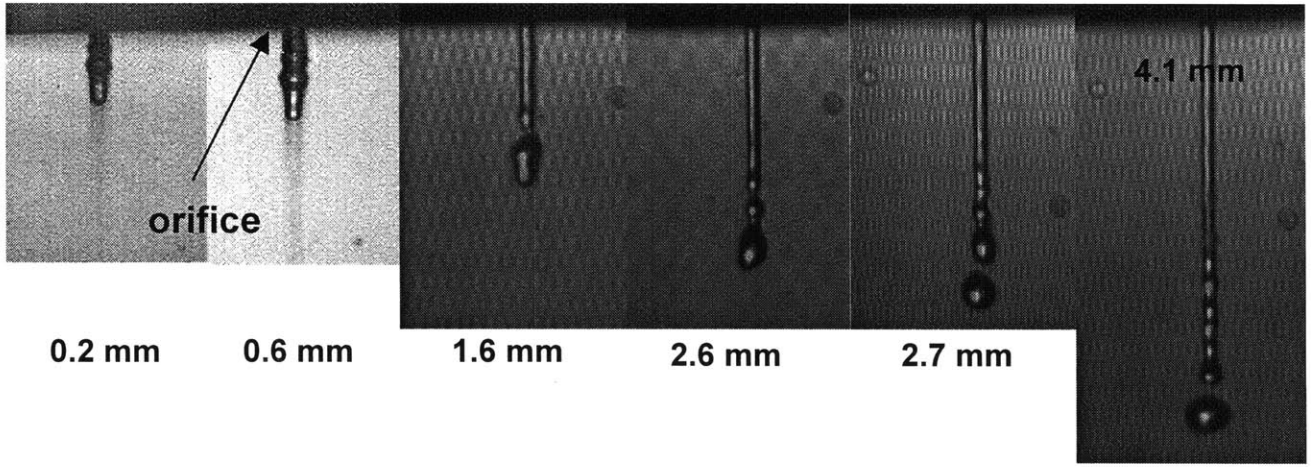

Figure 4.9: Strobe-photography images of stream front vs. distance from nozzle (Pressure =10psi; 30 Hz)

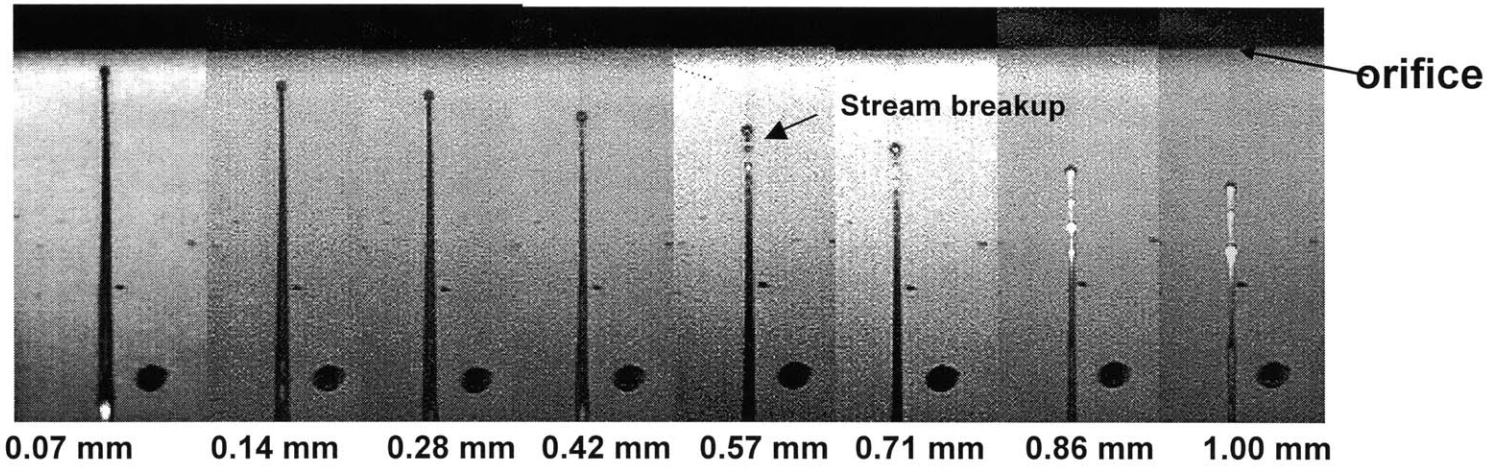

Figure 4.10: Strobe-photography images of stream tail vs. distance from nozzle (Pressure =10psi; 30 Hz)

4.4 Instantaneous jet-stream velocity

The stream observation station was used to measure the velocity at the leading and trailing edges of the jet-stream. With the valve-jet operating at 30 Hz, the initial and final position of the stream's edges were noted together with the corresponding time delays after the rising edge of the input signal. The positional and time difference was then used to calculate the leading and trailing edge velocity. This was performed at three different pressures and the leading and trailing edge velocities results together with the average velocities results obtained earlier in section 4.1.3 are summarized in **Figure 4.11**.

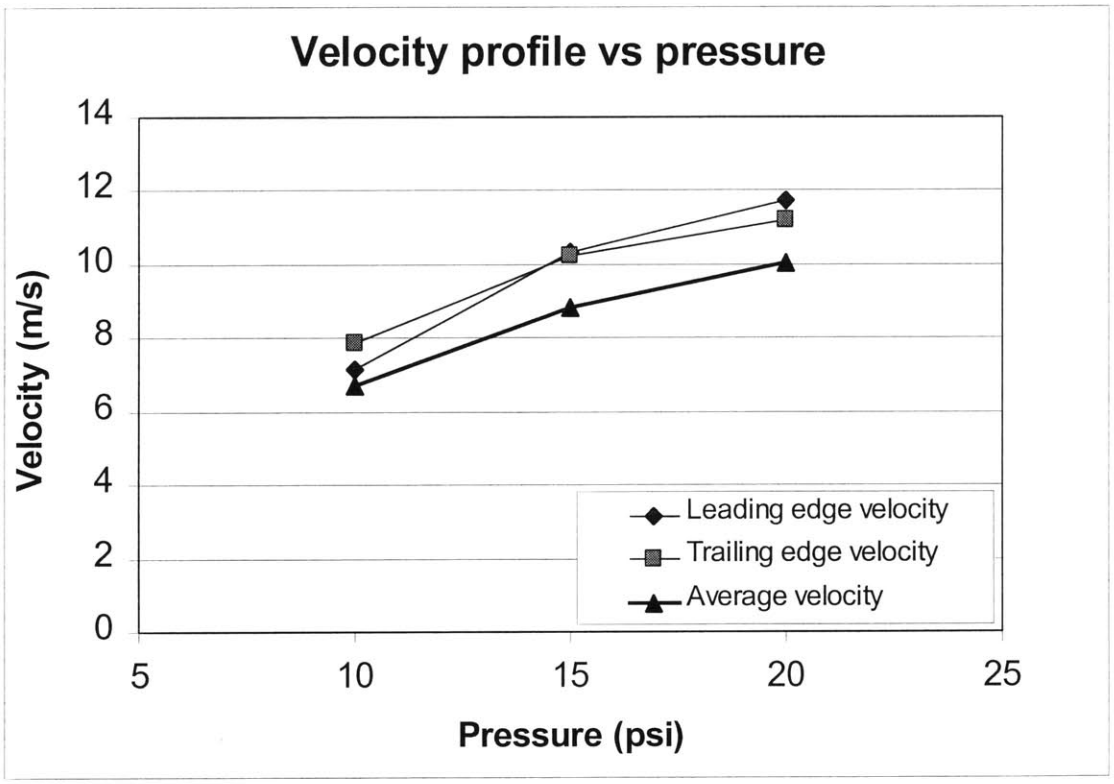

Figure 4.11: Comparison of leading edge, trailing edge and average velocities vs. pressure

We had expected an increase in both leading and trailing edge velocities with higher pressures. We will also expect the average stream velocity to lie between that of the leading and trailing edge velocities with the leading edge velocity is higher than the average stream velocity, which in turn is higher than the trailing edge velocity. The results plotted in **Figure 4.11** does not agree with the latter part of our expectations and it is difficult to conclude any meaningful relationship between the leading and trailing edge velocities and the average velocity because there is no consistent pattern in our results. There are at least two reasons why we were unable to obtain the results we had expected. Firstly, we should note that these results at best can only provide an order-of-magnitude estimation of the stream instantaneous velocities due to the large amount of estimation errors in reading the positional and time values. More sophisticated equipment needs to be used for achieving results with higher precision. Secondly, it is probably not fair to compare the average velocity with the instantaneous leading and trailing edge velocities, because we had calculated the average velocity by dividing the flow-rate with the cross-sectional area of the orifice. It is actually inaccurate to use the orifice cross-section to calculate the flow-rate because the jet-stream actually decreases in diameter when emerges from the orifice. Therefore, the actual average stream velocity should be much higher. Although the expected results was not obtained, we can provide a theory for what should be the expected results if more accurate data had been collected. The leading edge should have the highest velocity because it is pushed out under the initial pressure surge when the valve-jet opens, while the trailing edge is only getting pulled along by the main body of the jet-stream after the valve-jet closes. The tapering shape of the trailing edge we observed earlier also supports this theory that the trailing edge is moving more slowly than the body of the fluid stream. Surface tension forces generated between the fluid-stream and the thin capillary orifice tries to "attract" the back edge of the stream back into the orifice while the bulk of the jet-streams' body is being pushed outwards under pressure. This results in the trailing edge of the stream being pulled into a long tapering tail we saw under the stream observation station.

4.5 Response time

In the context of this experiment, the response time is defined as the time lag between the rising edge of the input spike-and-hold signal into the valve-jet and the time when the leading edge of the stream is first observed to be just peeking out from the orifice. The stream observation station setup with a two-channel oscilloscope in **Figure 4.7** was the experimental setup used. Channel 1 of the oscilloscope is monitoring the signal from the HP function generator while channel 2 is connected to the photo diode sensor. The time delay unit causes a delay in the strobe timing, thus we can observe the position of the stream at different controllable time delays after it emerges from the valve-jet. In trying to evaluate the response time, the time delay unit has to be adjusted so that the leading edge of the stream is observed to be just emerging from the nozzle as shown in **Figure 4.12**.

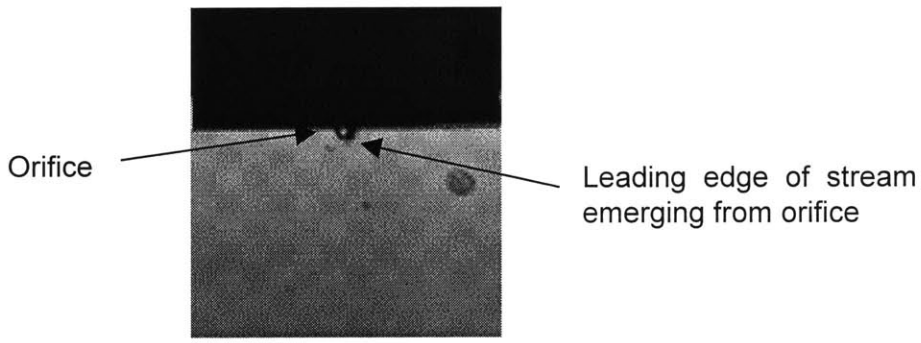

Figure 4.12: Leading edge of water stream emerging from ruby orifice
(Strobe frequency = 30 Hz; Pressure = 30 psi)

The two-channel output observed on the oscilloscope screen is shown in **Figure 4.13**. The response time for this valve-jet is approximately 0.38 milliseconds at a pressure of 10 psi using water. Note that the falling edge of the photo diode signal corresponds to the instant when the strobe light pulse is detected and the remaining portion of the signal is just the time required for the photo diode to return to its original state.

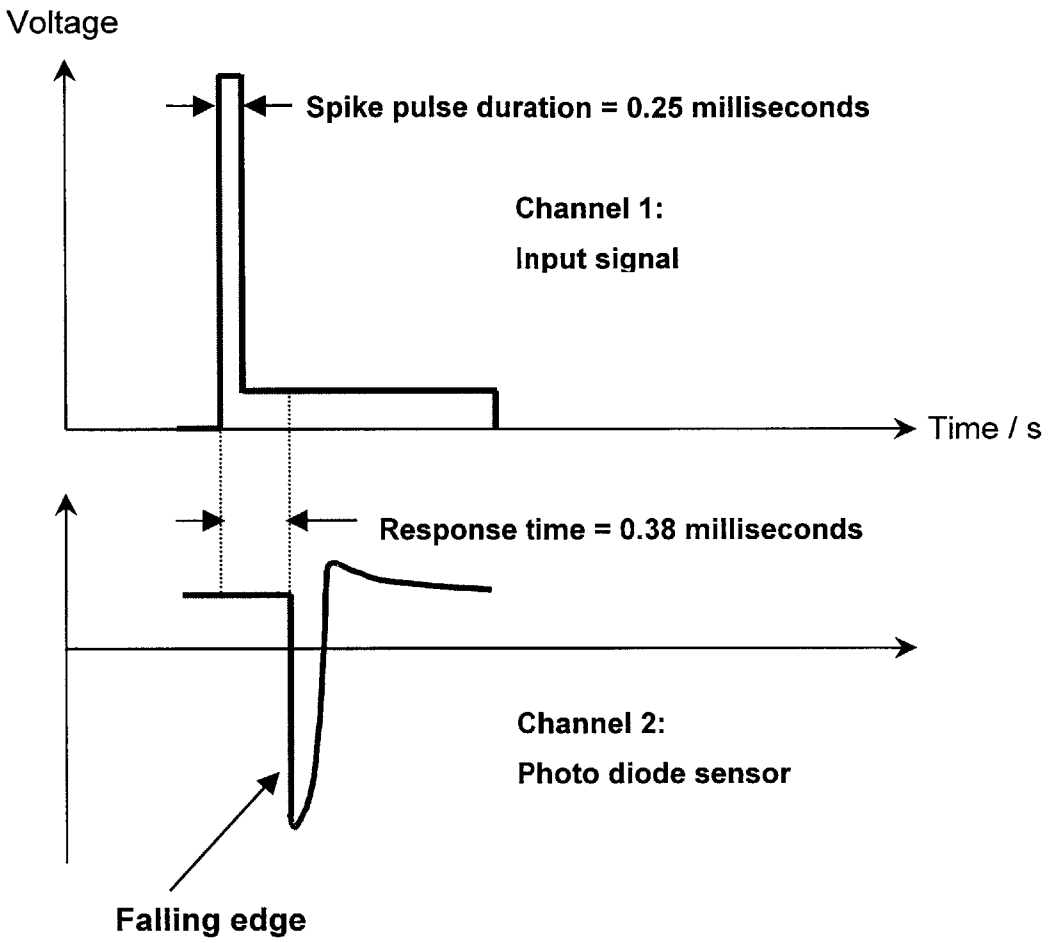

Figure 4.13: INKX0505950A valve-jet response time on two-channel oscilloscope

4.5.1 Response time as function of pressure

We can investigate the effect of pressure on response time by simply performing more iterations of the experiment at different pressures but still using the same equipment. The valve-jet's response time at different pressures is plotted in **Figure 4.14** below. As we have expected, there is an inverse relationship between response time and pressure. At higher pressures, the response time is shorter. It improves from 0.38 milliseconds at 10 psi to 0.32 milliseconds at 20 psi.

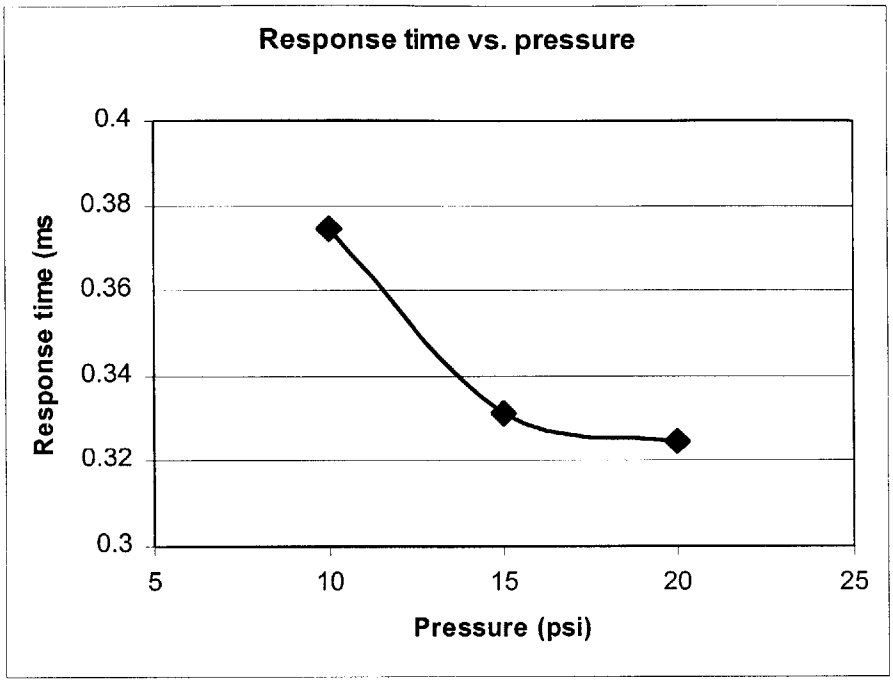

Figure 4.14: Plot of response time vs. pressure

4.6 Jet-stream variability

In section 4.3, it was experimentally determined that jet-stream breakup of the leading edge occurs approximately 2.7mm away from the valve-jet orifice while trailing edge instability and stream breakup begins at distances greater than 0.5mm from the orifice. Therefore, the valve-jet's nozzle must be positioned no more than 0.5mm from the powder-bed for good print results. Another factor influencing the valve-jet's ability to produce good print results is its repeatability or capacity to produce jet-streams that are consistently dimensionally identical and traveling at the same velocity. Inferior parts with jagged edges will be manufactured if there is a lot of variability in consecutive jet-streams produced by the valve-jet.

Using the stream observation station with the CCD camera linked to a video recorder, it is possible to record a continuous series of jet-streams that are produced by the valve-jet into a movie video format. The video player can then be used to view the

discrete jet-streams produced by the valve-jet in a frame-by-frame mode, which otherwise will be too fast for the normal eye to tell for certain if there are fluctuations in consecutive jet-streams produced by the valve-jet. The images shown in **Figure 4.15** are consecutive frames of the tail stream captured using the frame-advance mode on the video recorder. The fluctuation in the trailing edge of the stream is approximately in the range of 0.2mm. Although there are some observable fluctuations in the trailing edge, the leading edge is extremely stable with a fluctuation range of 0.02mm. The instability in the trailing edge is most probably a result of the very thin and tapering shape. Changes in fluid viscosity, presence of microscopic impurities and aerodynamic turbulence in the surrounding atmosphere are all possible causes of the tail fluctuation.

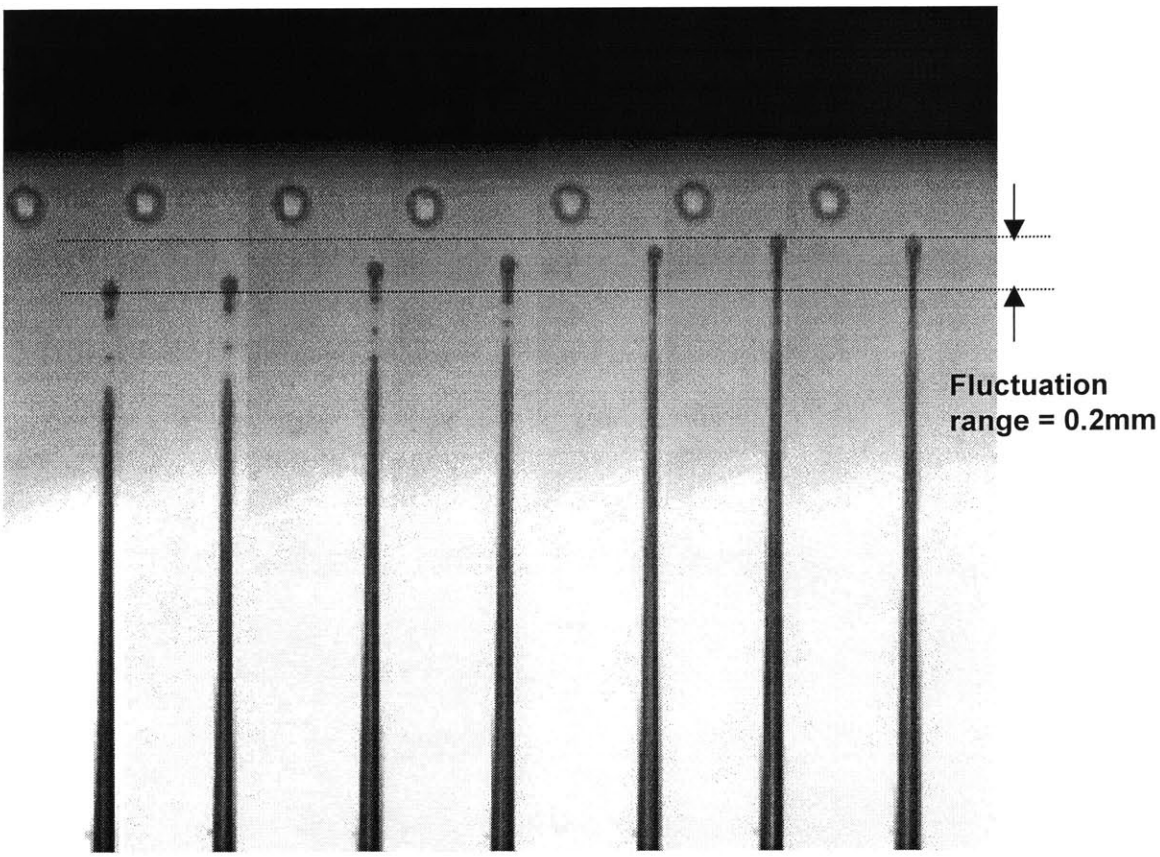

Figure 4.15: Tail fluctuation of jet-stream (video frame images)

5. 3DP™ ON A ROTARY MACHINE VIA SOLENOID VALVE-JET

5.1 Rotary-arm 3DP™ machine

To demonstrate proof of concept for 3DP™ with solenoid valve-jet, a very simple 3DP™ machine was constructed. Since the solenoid valve-jet is intended for use in high speed printing applications, the relative velocity between the substrate bed and the valve-jet must be very high. Also because the final goal is to integrate the valve-jet onto the Alpha machine to print prototype parts, the primary consideration is to have a machine capable of moving at velocities comparable to the 1.5 m/s velocity on the fast axis of the Alpha machine.

A design of a rudimentary 3DP™ machine involves moving the substrate bed in a high-speed circular motion and keeping the jet orifice stationary as shown in **Figure 5.1** below. To achieve very high velocities for the substrate bed, a very long arm is used instead of a short one. The solenoid valve-jet is mounted on a stage with a micrometer drive in the Y direction. This is so that we can control the nozzle displacement from the substrate very precisely. The substrate bed rotates under the valve-jet and arcs of varying radii can be created, by changing the distance from the center of the rotary arm to the valve-jet. A linear motor was mounted in the X direction to perform this operation.

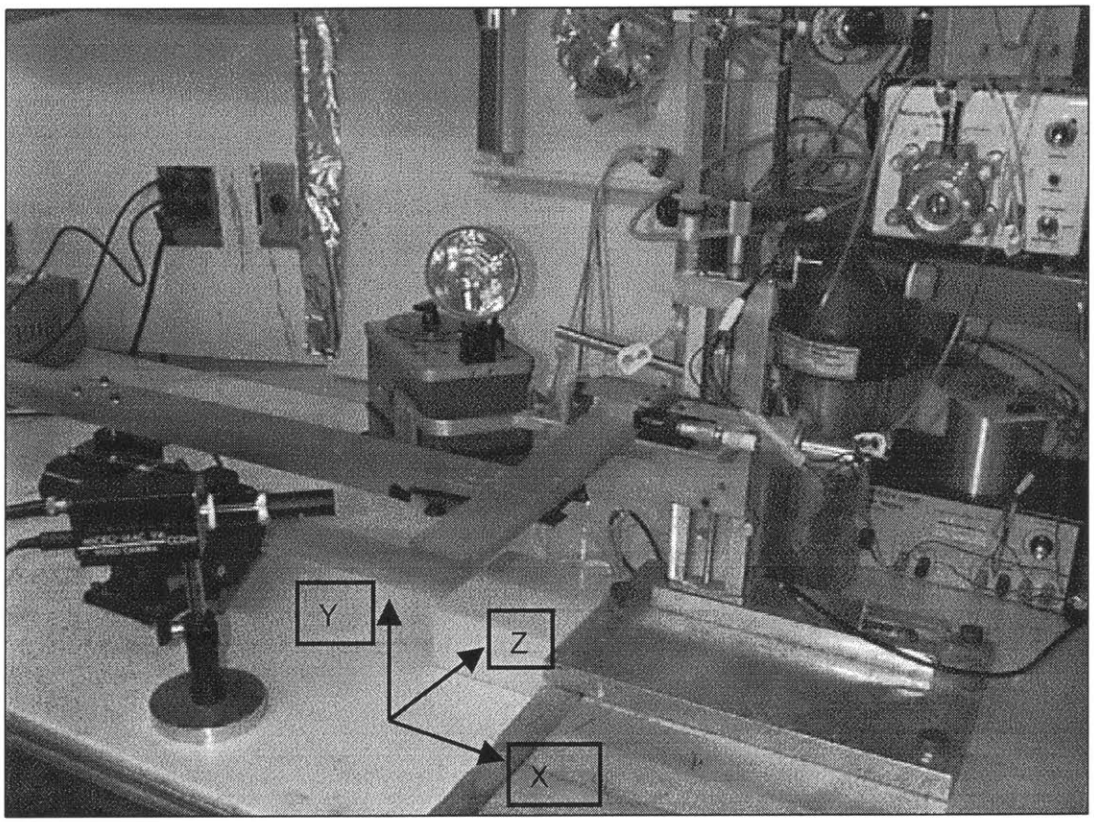

Figure 5.1: Rotary 3DP™ printing machine

5.1.1 Machine design

5.1.1.1 Repeatability

There are a few design issues to be addressed before parts can be generated using the solenoid valve-jet. Repeatability was the primary concern. Although the machine need not be as accurate as the Alpha machine, a reasonable degree of repeatability was necessary for the lines to stitch together when printing with fine metal powders. A linear motor operating at low speeds was needed to move the valve-jet at a constant velocity in a direction perpendicular to the substrate when it is rotating under the jet orifice. The motor operating the rotary arm was also calibrated to convert it angular velocity into linear velocity. The micrometer moving the valve-jet in the Y direction ensures that we are able to achieve very accurate and repeatable elevations of

the jet orifice from the substrate. Finally the attachment of the valve-jet to the moving stage was machined to have hole that can position the valve-jet in a vertical position.

5.1.1.2 Substrate material and layer generation

Two different substrate materials were experimented with: 1) ink-jet paper and 2) 2.4% volume percent mixture of 420 stainless-steel metal powder with Grade 203 PVA (polyvinyl-acrylate). For experiments with the ink-jet paper, distilled water mixed with ink was used as the fluid dispensed from the valve-jet while distilled water was used with PVA loaded stainless-steel material system. A container attachment was machined to contain the metal powder for the printing operation. Because the purpose of this machine was only for a preliminary study of the valve-jet capabilities for high speed printing operations, there was no necessity to build a piston where the powder-bed was lowered as the part was built. Instead, only single layer powder beds will be printed. Each new layer of powder was spread by hand using a roller across the top of the powder container. The printed layer was removed manually after each run.

5.1.1.3 Print control

There has to be a way to automatically turn printing on and off so that there would be some semblance of consistency at each pass of the valve-jet. This was accomplished by using a flag attached to the bottom of the substrate container to trigger an optical-interrupter which will send a signal pulse to the HP function generator to generate an input control signal into the solenoid valve-jet drive circuit. **Figure 5.2** shows the schematic of the circuit.

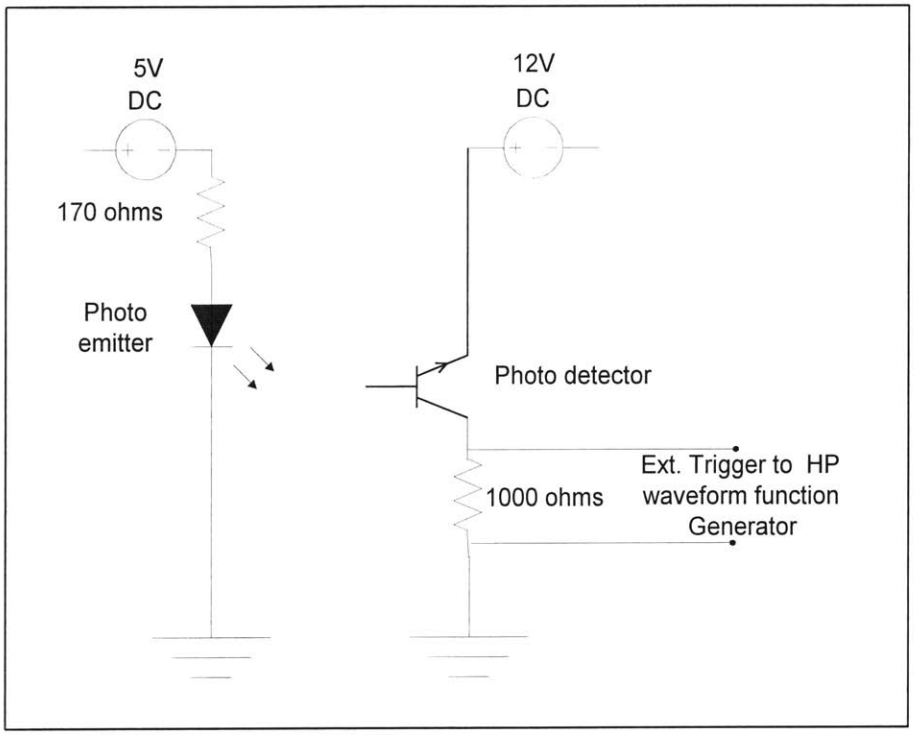

Figure 5.2: Optical interrupter circuit to automatically turn printing on and off for rotary 3DP™ machine

The circuit works as follows. The optical-interrupter is made up of two cells: 1) the photo emitter and 2) the photo detector. A very steady small current of about 20 mA flows across the gap from the photo emitter to the photo detector of the optical-interrupter. When a flag passes through the separation between them, the light is disrupted which causes the "pnp" junction on the photo detector side of the micro-switch to instantaneously stop the current flow and generate a voltage drop across the 1000 Ω resistor. This external trigger is received by the waveform generator, which releases a single pulse of the programmed waveform. The mechanical flag is attached at the bottom of the powder bed container on the rotary arm. It passes between the gap of the optical micro-switch during each revolution of the rotary arm and instantaneously triggers the waveform generator to release a stream of fluid which is printed onto either a paper or powder material substrate.

5.2 Results

5.2.1 Printing ink with paper

Ink-jet paper was the first printed substrate with the solenoid valve-jet. This is a very convenient method of looking at single layer results in the preliminary concept of proof stage. The arbitrary signal function generator with power amplifier drive circuit shown in **Figure 3.2** was used to drive the valve-jet. The substrate rests on the arm of the rotary 3DP™ machine and a mechanical flag attached to the base of the substrate triggers the optical interrupter on every revolution of the rotary arm. This in turn triggers the signal function generator to output a spike-and-hold signal to actuate the valve-jet. This setup is shown schematically in **Figure 5.3** below.

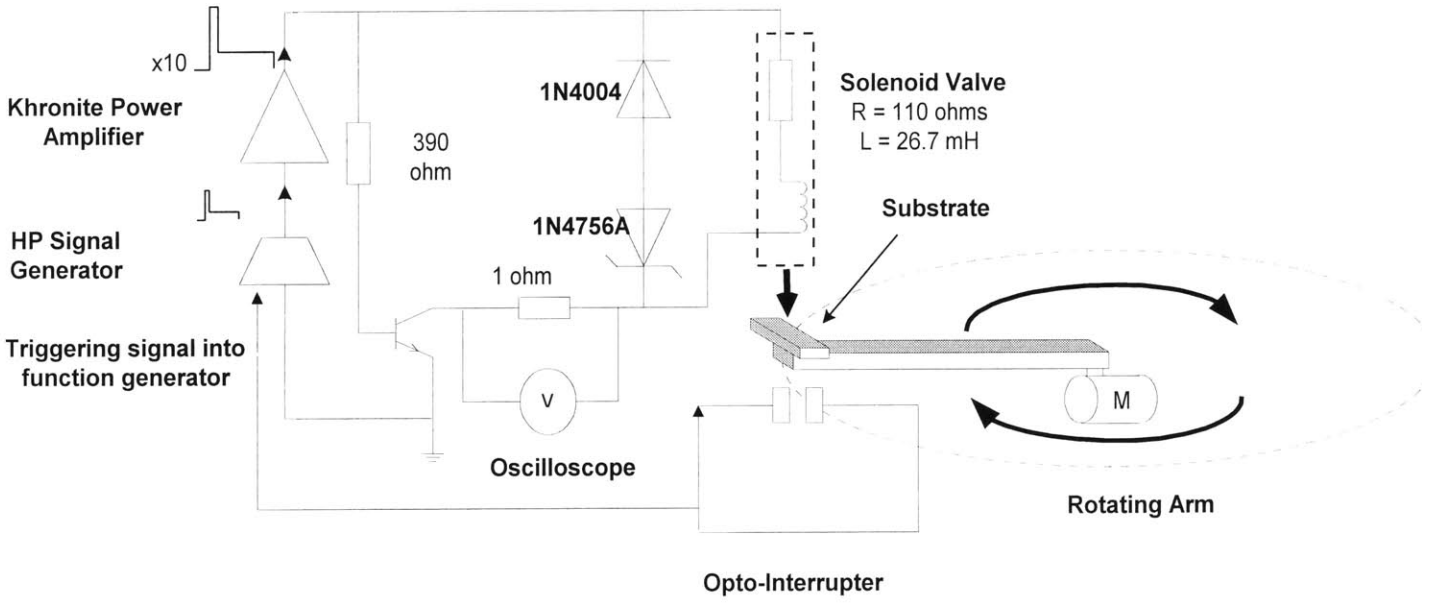

Figure 5.3: Schematic of rotary arm 3DP™ with an optical interrupter trigger

The parameters used for this preliminary print using are:

Number of valve-jets	One
Flow-rate	5 cm^3/min
Pressure	10 psi
Substrate linear velocity	1.5 m/s
Elevation of valve-jet from substrate	0.5 mm
Fluid	Water mixed with ink
Substrate	Ink-jet paper
Slow axis traverse speed	0.002 m/s

Figure 5.4 shows the series of line segments printed by the valve-jet as the optical-interrupter is triggered on each revolution of the rotary arm. The function generator is programmed to open the valve-jet for 0.02 seconds on receiving one triggering signal. Assuming that a perfectly cylindrical volume of fluid stream is produced, we should expect the printed line segment to be 3cm long when the substrate is moving at 1.5m/s. The actual printed length was 3.7cm, suggesting that the jet-stream is not a perfect cylinder and has most likely been stretched before impacting the substrate. Another interesting observation is the leading or front edge of the printed line segments seems to be better aligned together compared to the trailing edge, which is relatively uneven. Variations in the lengths as well as shape of the trailing edge of the printed line segments can be observed in **Figure 5.4**. A stray blob of ink, possibly created by a satellite droplet, can almost be seen at the trailing edge. A slow axis traverse speed of 0.002 m/s was found to be sufficiently fast to prevent consecutive lines from overlapping, so that we can see each printed line segment clearly.

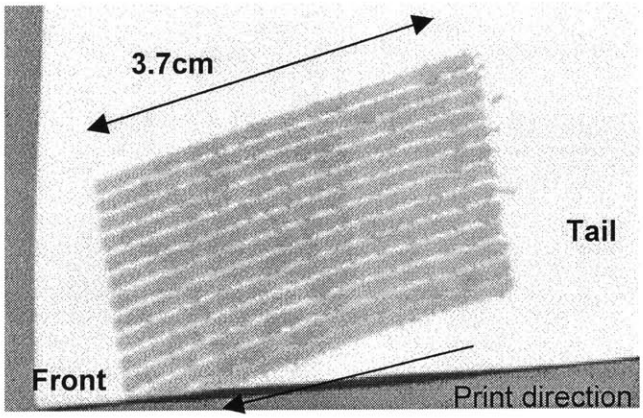

Figure 5.4: Line segments printed with ink on ink-jet paper

The difference in the leading and trailing edge variability can be observed more clearly by printing shorter sections at a higher frequency. **Figure 5.5 and 5.6** shows four printed sections with a valve open time of 0.00264 seconds. The expected line length of 3.96mm is again shorter than the actual length of 6.0mm. The prints in **Figures 5.5 and 5.6** were obtained using methods of triggering the optical interrupter. **Figure 5.5** was printed using one mechanical trigger (i.e. flag passes through the optical interrupter) to trigger the valve-jet to open four times, each of during 0.00264 seconds, while **Figure 5.6** was printed using four mechanical triggers. Each mechanical flag passing through the gap of the optical interrupter triggers the signal generator to release one signal, which opens the valve-jet for 0.00264 seconds. Close observation reveals that there is some difference in the quality of the leading edges of the 3rd and 4th sections of the two prints. The leading edge was slightly crooked for the print with one mechanical trigger, but was nearly a straight line for the prints with four mechanical triggers. This is completely unexpected because we are sending the same electrical signals to the valve-jet, with the difference that in one case trigger was performed once mechanically and the four programmed signals is automatically generated by the function. In the other case, the signal is only sent when the mechanical flag passes through the optical interrupter, and this was done four times. It was unexpected that the same electrical signal sent to the same valve-jet, but using different triggering sources should produce printouts with

different leading edge quality. It was later narrowed down later that the fault lied in the inconsistent angular velocity of the motor driving the long rotary arm. In the case of one mechanical trigger, the time gap between each of the subsequent trigger is fixed regardless of the velocity of the rotary arm, while in the four mechanical trigger case, each signal is triggered only when the flag passes through the optical interrupter, and hence even though the velocity of the arm may change, the leading edge will still be triggered at the same place. Our conclusion from this test was that the valve-jet was capable of producing very good quality prints at the leading edge with little variation, while the trailing edge's quality was comparatively inferior with a slightly fuzzy and jagged appearance and a larger variation in the lengths that can be printed. The initial print test results using paper and ink was satisfactory which prompted us to move on to the next step, which is to print with fine metal powders and determine if we are able to get the same results.

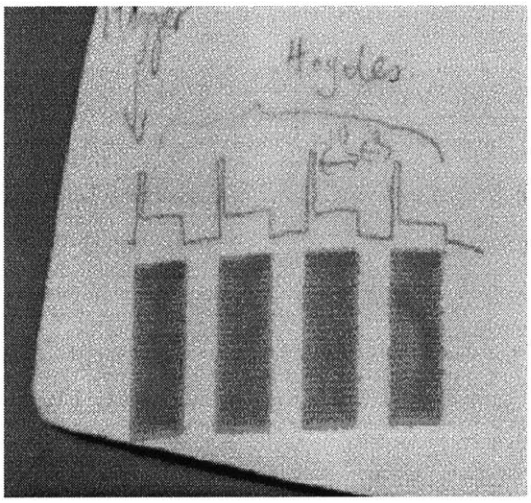

Figure 5.5: Line segments printed using ink on paper

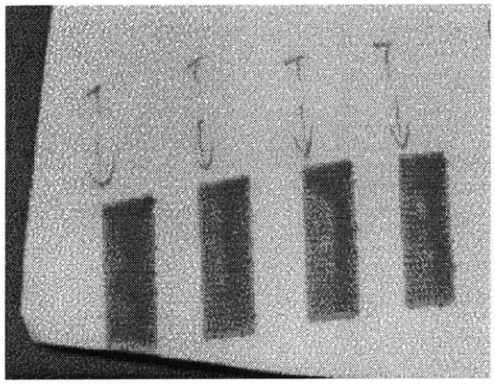

Figure 5.6: Line segments printed using ink on paper

5.2.2 Printing single layer PVA loaded stainless steel powder and PVA

All the "parts" printed on the rotary machine were rectangle shaped single layer of 420 stainless steel powder approximately 0.4mm thick. The rotary arm was turning at 200 rpm to produce a linear velocity of 1.5 m/s on the substrate bed, which is placed 45cm away from the center of rotation. The frequency of the spike and hold signal used was 200Hz, meaning that the valve-jet was open for 0.005 seconds every time the mechanical flag triggers the optical micro-switch on each revolution of the rotary arm (assuming the plunger opens instantaneously when it receives the signal, i.e. valve-jet response time = 0 seconds). The line spacing used was determined by a trail and error method to print a single layer that did not have deep ridges between consecutive lines and provided sufficiently good stitching. A line spacing of 300μm was chosen. Since the rotary arm makes a revolution in 0.3 seconds, the X-axis linear motor was set to move at 0.001m/s in order to produce the required 300μm line spacing. A 400Watts projector lamp with a reflector was directed at the powder-bed for 30 seconds after each layer is printed to dry the layer and reduce the amount of bleeding.

Figure 5.4 shows the single layer of stainless steel printed using one solenoid valve-jet on the rotary machine. The printing direction is counter-clockwise. Using the velocity and frequency parameters used in the printing, we can expect to produce a single layer, which is 7.5mm in length along the fast axis of printing. The actual printed

layer is approximately 9mm in length, agreeing quite closely with our theoretical expectation. The difference may be caused by transient times during opening and closing of the valve-jet and the changes in stream shape (especially the tapering shape at the trailing edge) and velocities due caused by aerodynamic conditions. An important observation from our results is that the leading edge of the printed layer is considerably smoother than the trailing edge. The jaggedness at the trailing edge of the printed layer is due to two reasons:

1) Fluctuations at trailing edge of jet-stream observed earlier. The fluctuation of 0.2mm at the trailing edge of the stream shown in **Figure 4.15** can be translated to a time fluctuation of the jet-stream of 0.03 milliseconds using the fact that the trailing edge velocity is approximately 7m/s. Assuming that the rotary arm holding the substrate moves at a linear velocity of 1.5m/s, we should expect a difference of 0.045mm in the trailing edge of the shortest and longest line segment. The actual length difference measured from the trailing edges of the printed layer in **Figure 5.4** was approximately 0.07mm.
2) Tapering shape of the jet-stream produced by the valve-jet. The stitching between consecutive lines is close enough in the front and middle section of the printed layer, but is poor at the trailing due to the thinner diameter of the stream caused by the tapering shape. This results in unfilled "gaps" and a saw-tooth appearance at the trailing edge.

The goal of the rotary arm machine was to show that it was possible to manufacture 3-D parts using the solenoid valve-jet on fine metal powders. The results achieved were very promising and therefore justified moving to the next step in the development of the valve-jet for high-speed print applications, which was to adapt the solenoid valve-jet printing of metal powders to the Alpha machine to create complete geometrical 3-D parts.

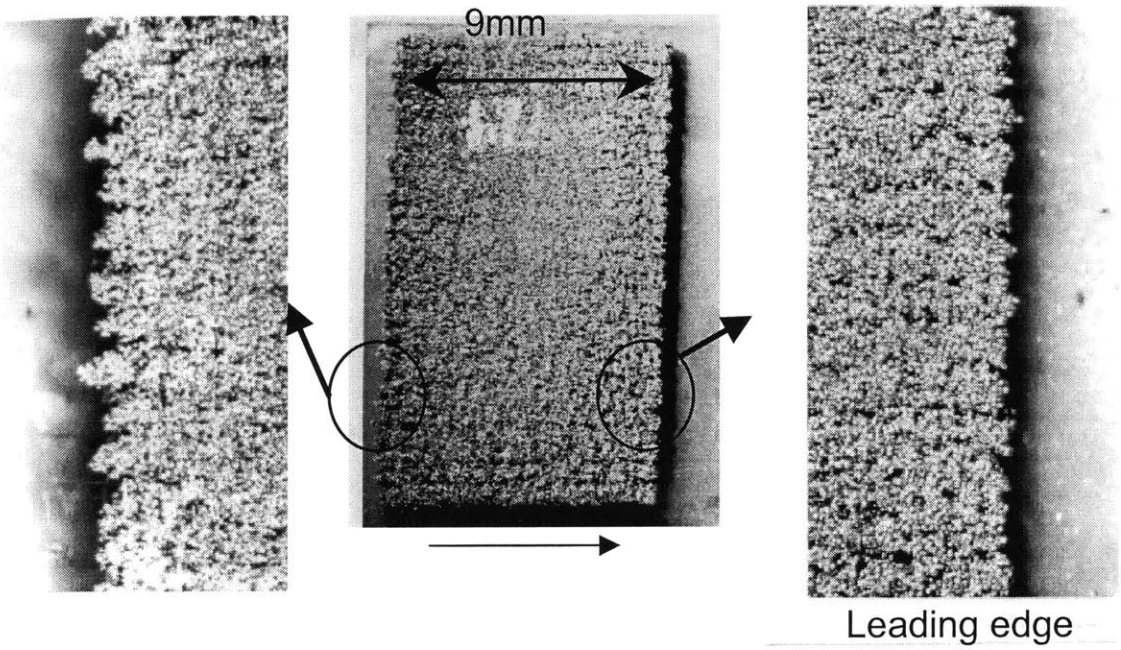

Figure 5.4: Top view of single layer

6. 3DP™ WITH SOLENOID VALVE-JET ON ALPHA MACHINE

This chapter presents the modifications required to integrate the solenoid valve-jet drive circuit onto the Alpha 3DP™ machine to 3D print prototype parts. With the electrical interface and structural support appropriately set up, primitive lines and droplets were then printed, followed by complete geometrical parts.

6.1 Electronics interfacing from Alpha 3DP™ machine to Lee drive circuitry

The Alpha 3DP™ machine at MIT outputs a square wave signal of either 0 or –12 V_{DC}, where 0 V_{DC} represents a catch (i.e. no-print) and –12 V_{DC} is a print. If a 0 V_{DC} signal is received, the droplet is deflected into the catcher and therefore not printed onto the powder-bed, while a –12 V_{DC} signal will not deflect the droplet, allowing it to impact the powder substrate. However, the Lee drive circuit accepts an input control signal between 0 to +5 V_{DC}, where a 0 V_{DC} signal closes the valve-jet, while a +5 V_{DC} will kick the valve-jet into its open position. A LM 311 comparator chip is used to perform this conversion shown in **Figure 6.1** below.

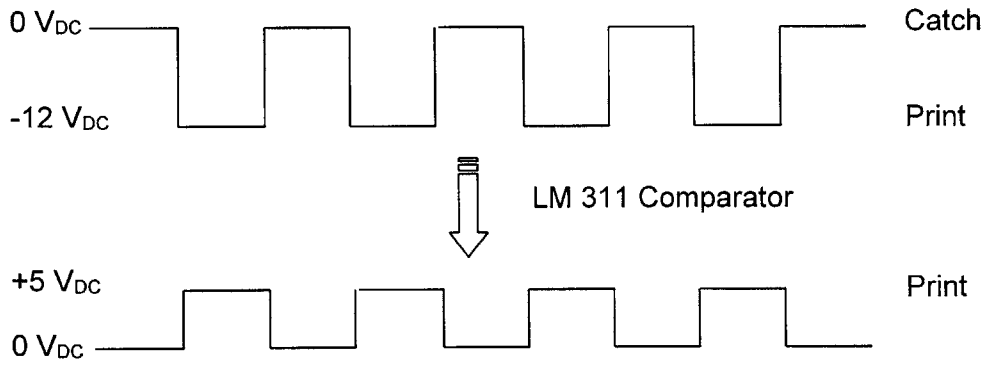

Figure 6.1: Signal conversion from Alpha machine output to Lee drive circuit input

Figure 6.2 is the circuit diagram illustrating the wiring of the interfacing electronics. The LM311 is used as a comparator while the LF 411 op-amp is set up as a follower circuit. The pair of 2 Kohm resistors between pins 1 and 4 of the LM 311 comparator was selected so as to set the reference voltage (for the voltage to flip over between "catch" and "print") at –6 V_{DC}. The LF 411 operational amplifier was also added in series with the comparator in a follower circuit setup to act as a buffer to isolate the drive circuit from the comparator output.

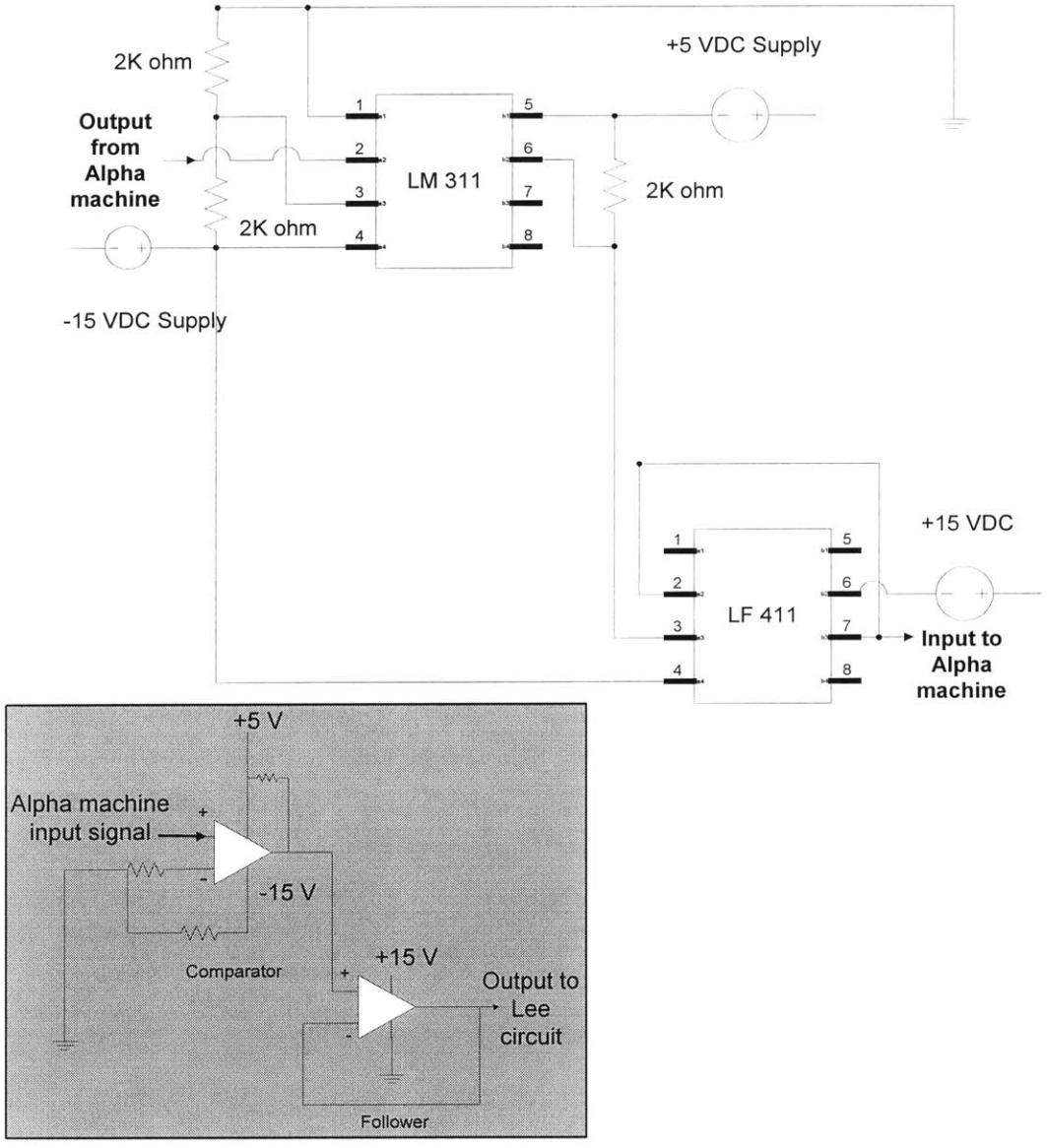

Figure 6.2: Interfacing electronics from Alpha 3DP^{TM} machine to Lee drive circuitry

6.2 3DP^{TM} file preparation

The process for preparing the .3dp file is summarized in **Figure 6.3**. The prototype part is first drawn up in a CAD solid-modeler such as SolidWorks or ProEngineer. This creates a part file (.prt), which can be loaded onto a rapid-prototyping slicing software such as the Materialise software from Materialise Corporation, which allows the user to visualize the part placement onto a rapid prototyping machine. Rotational, translation and scaling commands can be performed to get the desired part location in the substrate bed. A (.cli) file is automatically created after slicing the solid model file. The next step of the file preparation process involves encoding the (.cli) file using a 3DP file encoder developed at MIT. This program allows the user to select various print parameters such as: row and layer spacing, number of jets used in printing and uni-directional or bi-directional printing. A (.slc) file is created after this encoding step. The last step simply involves converting the (.slc) file into a (.3dp) file, which can then be downloaded onto the Alpha machine controller for actual printing. The (.3dp) file contains all the essential part geometry, jet velocity, row and layer spacing information required to print the desired prototype part. Further information on using the software is obtainable from the 3DP^{TM} laboratory at MIT.

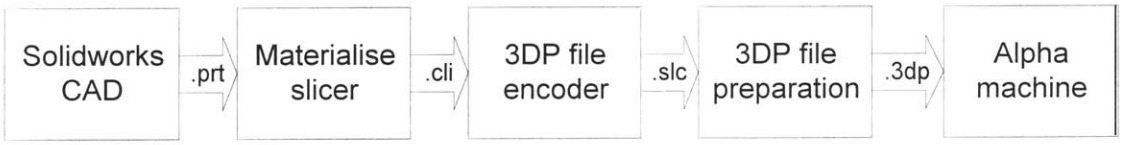

Figure 6.3: Flowchart for .3dp file preparation

6.3 Printing primitive lines and droplets

Figure 6.3a shows a single strand of 3D printed line created by a single stream of water impacting into 2.4% PVA (polyvinyl-acrylate) loaded stainless steel powder substrate on the Alpha machine. The ballistic impact of the fluid has displaced the surrounding powder and both ends of the line segment appear to be slightly sticking

above the plane of the powder-bed, upwards out of the page. This phenomenon could be caused either by warping of the line segment during the drying process with the effect most clearly seen at both ends or that there is some momentum transfer occurring between the stream and the powder-bed during impact. This printing test was performed at a rapid traverse speed of 1.5 m/s with a fluid pressure of 10 psi. The ruby orifice was maintained at a distance of 0.5mm above the substrate to avoid any stream-tail breakup which was shown earlier in section 4.3 to occur at distances greater than 0.5mm from the jet orifice. The signal duration sent to create this line was about 3.3 milliseconds. Assuming that there are no response time delays, aerodynamic interferences and that fast axis arm is moving at 1.5 m/s, we should theoretically expect a line segment of 5mm. Instead the line produced is 5.98mm in length, but still close to our expectation.

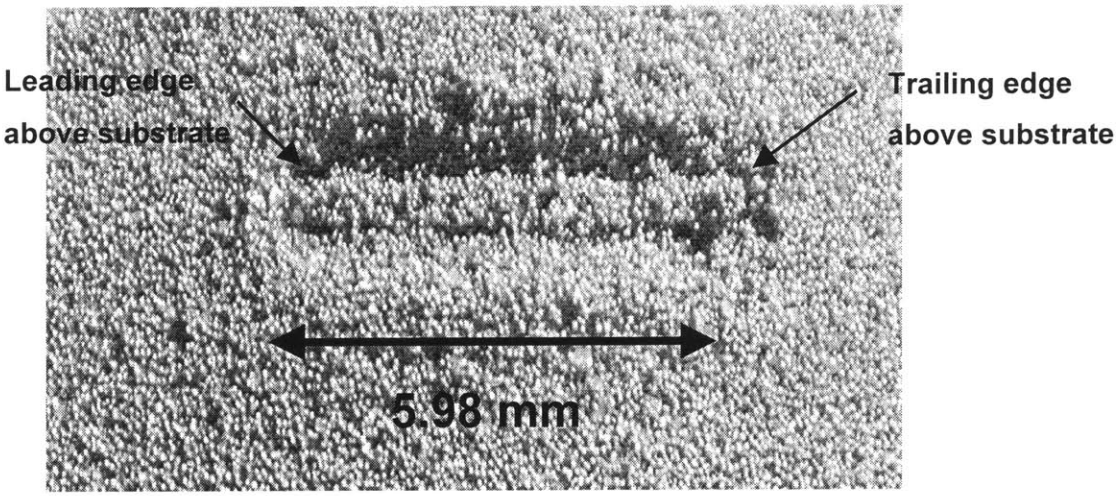

Figure 6.3a: Single 3DP line created by valve-jet fluid stream after impact in 420 SS powder substrate

Figures 6.4a and 6.4b shows the physical dimensions of the single strand of printed stainless steel powder removed from the substrate bed (in **Figure 6.3a**). A primitive strand of PVA loaded stainless steel printed with water using a 130 μm orifice has an approximate width of 0.484 mm and a thickness of 0.397 mm. Noteworthy also is the characteristic tapered tail, which corresponds closely with the tapering stream shape emerging from the valve-jet discussed earlier in section 4.3. The characteristic tapering trailing edge is once again very noticeable in the top view of the line in **Figure 6.4a**. The

side-view of the line strand in **Figure 6.4b** shows clearly that the leading and trailing edges are pointed upwards, sitting slightly above the powder bed than the main body of the printed line.

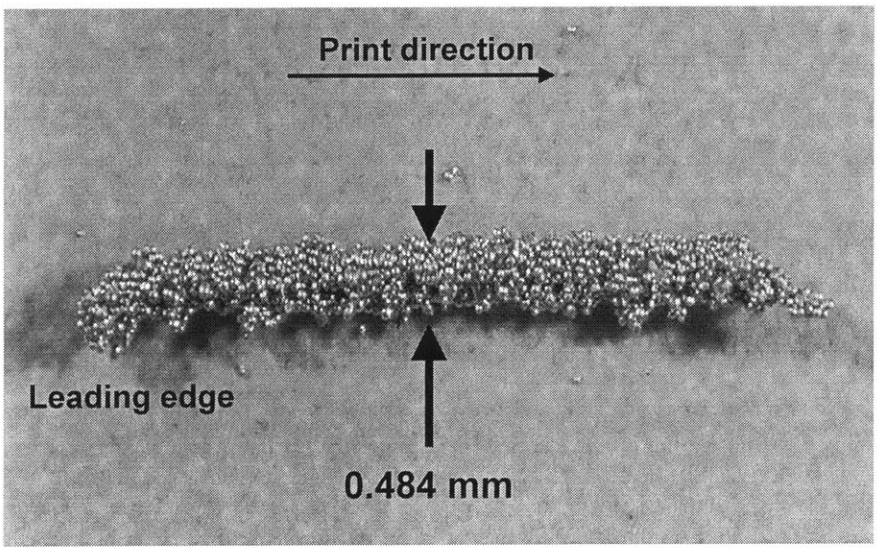

Figure 6.4a: Single line printed; 420 SS powder (Top-view)
Strand width = 0.484 mm

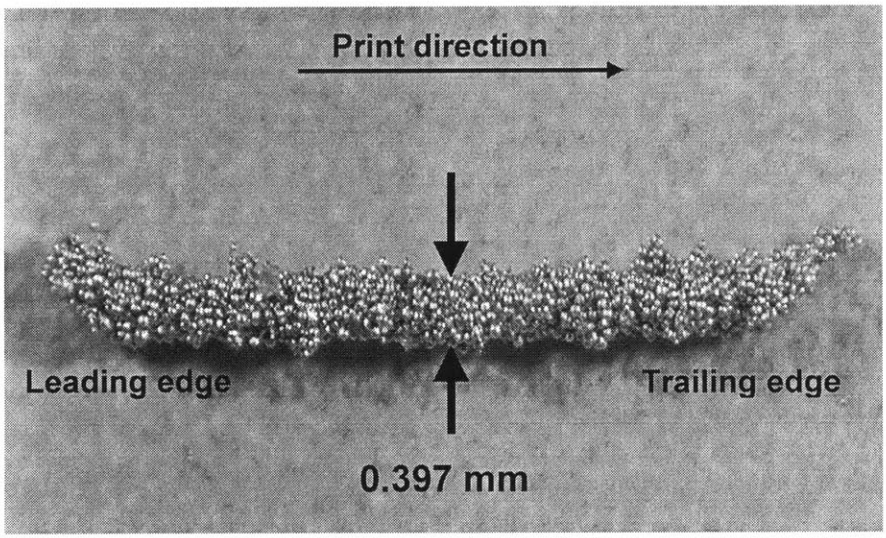

Figure 6.4b: Single line; 420 SS powder (Side-view)
Strand thickness = 0.397 mm

Figures 6.5a and 6.5b are pictures of the smallest droplet of printable stainless steel powder; it is also the smallest feature producible with the INKX0505950A solenoid valve-jet using the Lee drive circuit at a pressure of 10 psi. It has a length of 1.27mm along the fast axis of printing, with a width of 0.46mm and thickness of 0.386mm through its mid-section. Although it is not very clear, we can still see a semblance of a tapering tail at the trailing edge of the droplet in the side-view of **Figure 6.5b** as well as a bent shape in the droplet caused possibly due to warping during drying. The duration of the signal pulse for generating the droplet is about 0.3 milliseconds which leads us to expect a printed length of 0.45mm with a fast axis speed of 1.5m/s. The actual droplet length of 1.27mm is considerably larger than our expectations. A large portion of this length is attributed to the tapering tail, which is produced by complex aerodynamic and surface tension interactions between the orifice, the atmosphere and the fluid surface beyond the scope of this study.

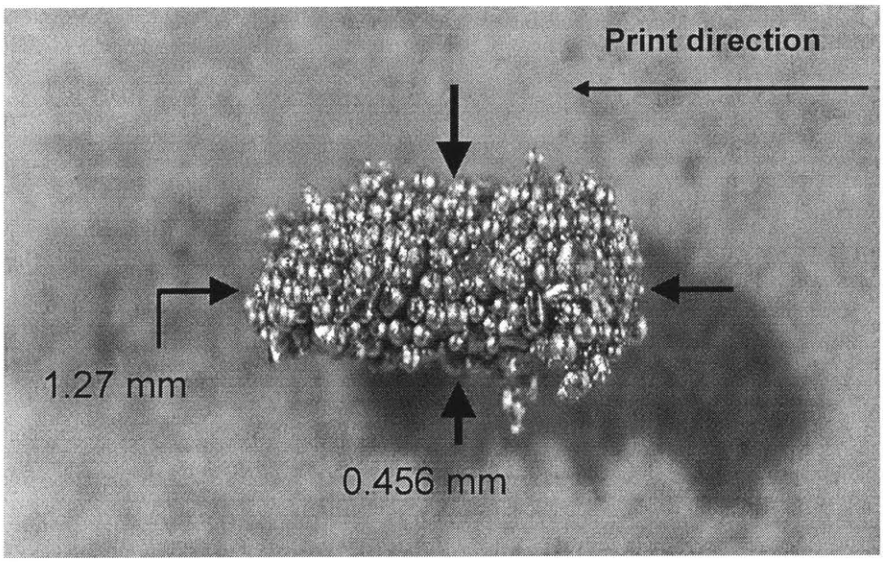

Figure 6.5a: Smallest printable droplet; 420 SS powder (Top-view)
Length =1.27mm; Width = 0.456 mm

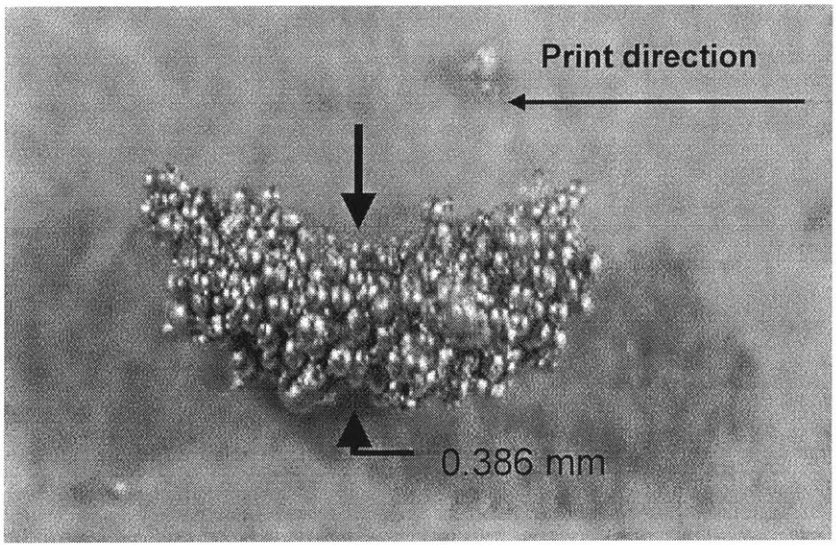

Figure 6.5b: Smallest printable droplet; 420 SS powder (Side-view)
Thickness = 0.386 mm

6.4 Printing geometrical parts

6.4.1 Part geometry

Several different part geometries were printed on the Alpha machine using the solenoid valve-jet. These first parts printed were meant to show: 1) Part appearance and surface texture 2) dimensional accuracy 3) strength and integrity of green part and 4) the total time taken to print a volume of powder material on the Alpha machine with the solenoid valve-jet. Four geometries were selected: 1) rectangle brick 2) a donut geometry 3) a double cylinder with center hole 4) trapezoid with step intervals and internal holes to evaluate the criteria listed earlier. The four geometries (with duplicates) put together into a single .3DP file for printing represented a total built volume of 150x300x30 mm. Orthographic and 3D views of the four geometries are shown in Appendix B.

6.4.2 Part printing

Our first attempt at 3DP™ using the INKX0505950A solenoid valve-jet was performed under the following conditions:

Number of valve-jets	One
Print direction	Uni-directional
Fast axis speed	1.5m/s
Pressure	10psi
Flow-rate	5.05 cm^3/min
Row spacing	400 μm
Layer thickness	350 μm
Jet elevation	0.5mm from powder bed
Saturation level	99%
Material system	2.4% volume PVA with 420 stainless steel powder
Drying time per layer	70 sec. (initial 20 layers) 50 sec. (remaining layers)

6.4.2.1 Line spacing

A saturation calculation was performed, varying layer thickness and row spacing while keeping the powder packing density constant. The calculation assumes that the binder printed with the layer only infiltrates the top layer. This assumption should be true since the PVA is pre-mixed into the stainless steel powder, and thus the addition of the water-jet will immediately dissolve the PVA binder, forming polymeric bonds between the powder particles with little migration. The saturation calculation assumes that all the remaining liquid (water) from the powder-bed is completed evaporated after each drying process. Also, the solid binder left behind after all the liquid has evaporated does not close off any porosity in the powder-bed.

Different line spacings were experimented with and a row spacing of 400 μm with layer thickness of 350 μm was found to be ideal. The saturation level of approximately 90% was calculated using the computer algorithm on the Alpha machine with this line and layer thickness parameters with flow-rate of 5cm^3/min, rapid traverse speed of 1.5m/s and a powder bed packing density of 60%. It will allow for sufficient overlapping between consecutive rows since the width of a single printed line was determined to be about 480 μm.

6.4.2.2 Drying issues

Drying time of 70 seconds was used in between layers to vaporize the excess water (from the large flow-rate) to avoid smudging during the subsequent powder spreading process. This was subsequently reduced to 50 seconds per layer after the 20th layer after the bed has "warmed up" sufficiently. Excessive drying beyond these amounts has the effect of causing the layers to curl in the powder-bed due to the drying stresses. This drying time requirement is very much longer compared with the typical 20 seconds in CJ printheads; however this is unavoidable due to the much higher flow-rates used. High flow-rates is desirable, however, there is always need to optimize flow-rate with drying time requirements. Long drying will dramatically reduce the built rate of the part.

6.4.3 Results

6.4.3.1 Part appearance and surface texture

Good parts were produced for each of the four geometries categories described. Pictures of the 3DP™ parts and close-ups of the surface textures for each of them are included in **Figures 6.6, 6.7, 6.8** and **6.9** below. The rectangle and trapezoid extrusions in **Figures 6.6** and **6.7** showed that the solenoid valve-jet is capable of printing geometries with sharp transitions. The faces at both the leading and trailing edges are very clean. It is very difficult to distinguish between the entrance and exit face without a microscope. The exit face has the characteristic tapering tail shape we saw previously in single line strands. A cross-section view reveals that the line-segments are lined up in a neat and orderly array. The surface quality of the internal holes in Figure 6.7 was also of an acceptable quality. No signs of disintegration or weakness were seen.

Curved and circular geometries were also evaluated using the donut and cylinder extrusions in **Figures 6.8** and **6.9**. The "steps" from one layer to the next is evident in curved geometries. This also accounts for the relatively rough appearance of the donut and double cylinder geometries printed. A possible way to improve surface quality may

be to use a smaller diameter orifice or to create a slicing algorithm, which decreases the step sizes between layers.

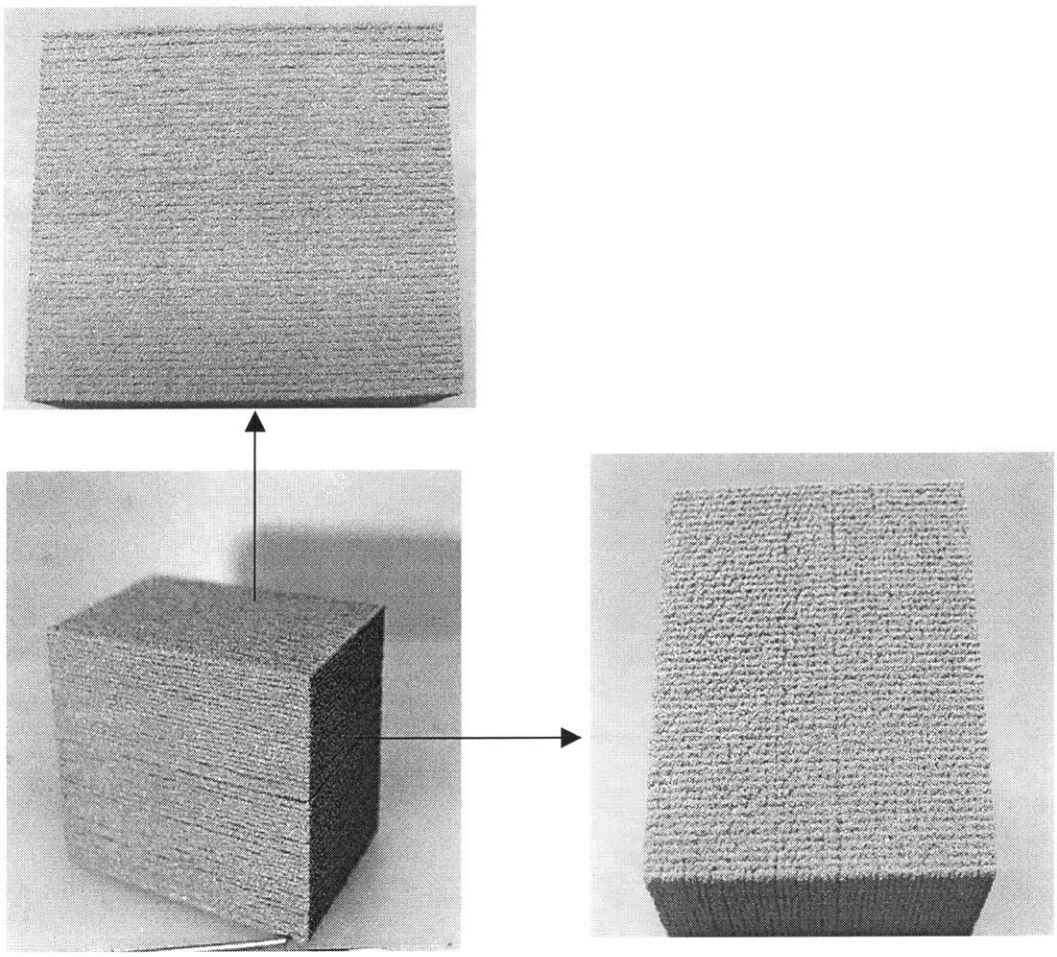

Figure 6.6: Rectangle block extrusion

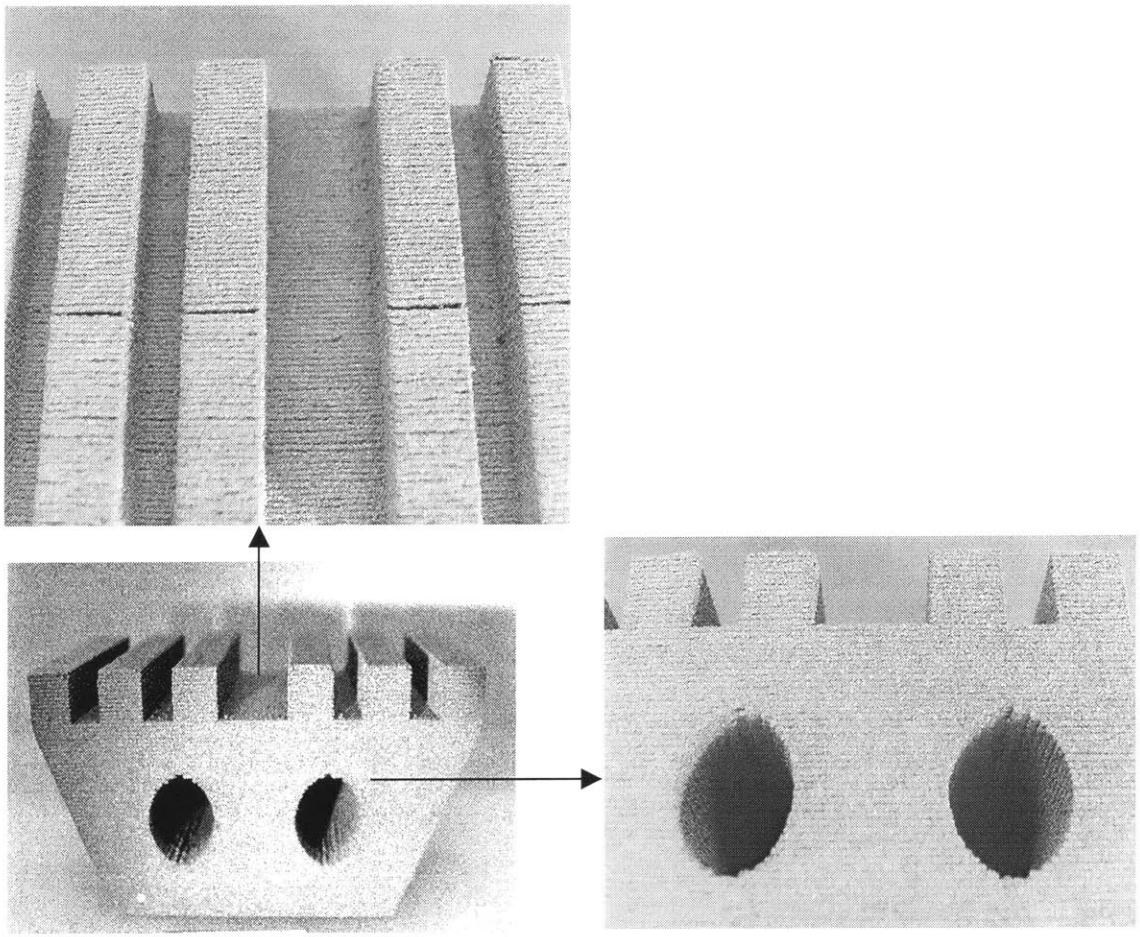

Figure 6.7: Trapezoid extrusion

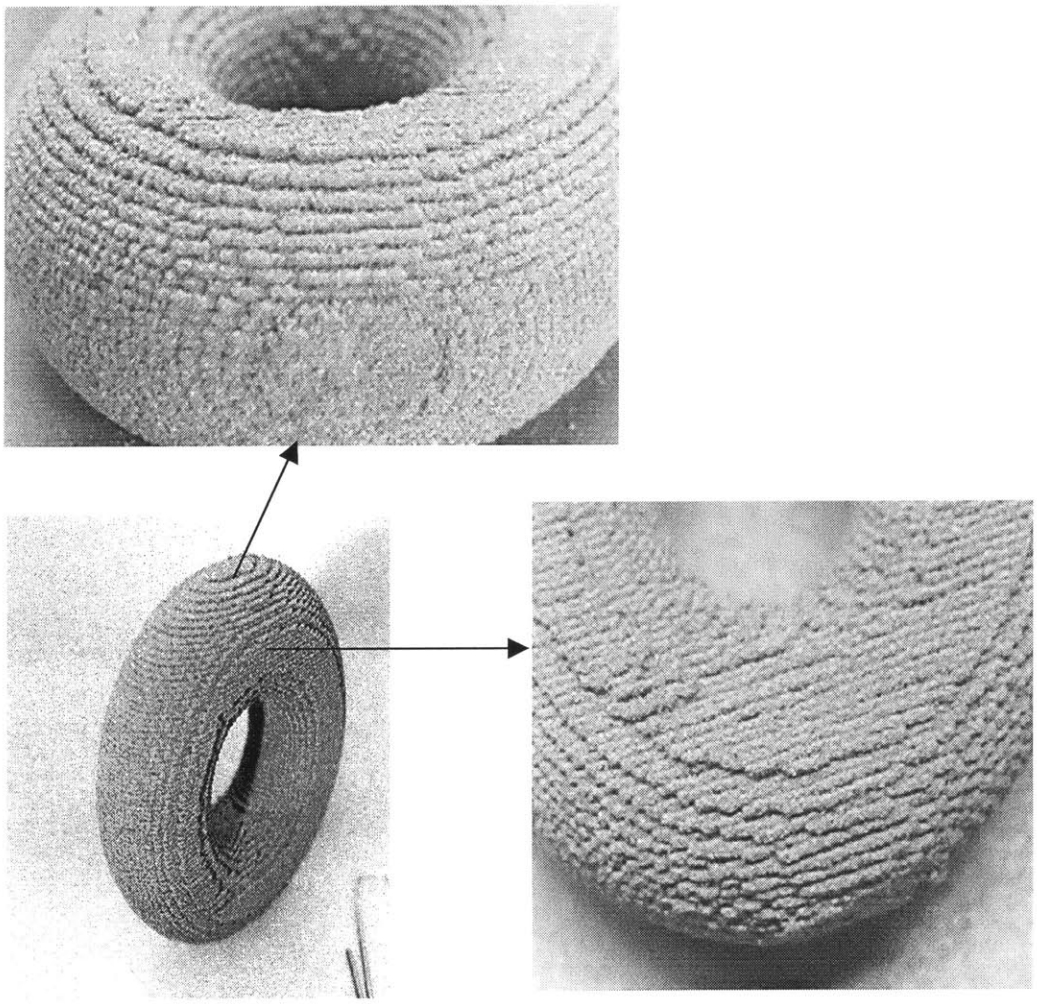

Figure 6.8: Donut extrusion

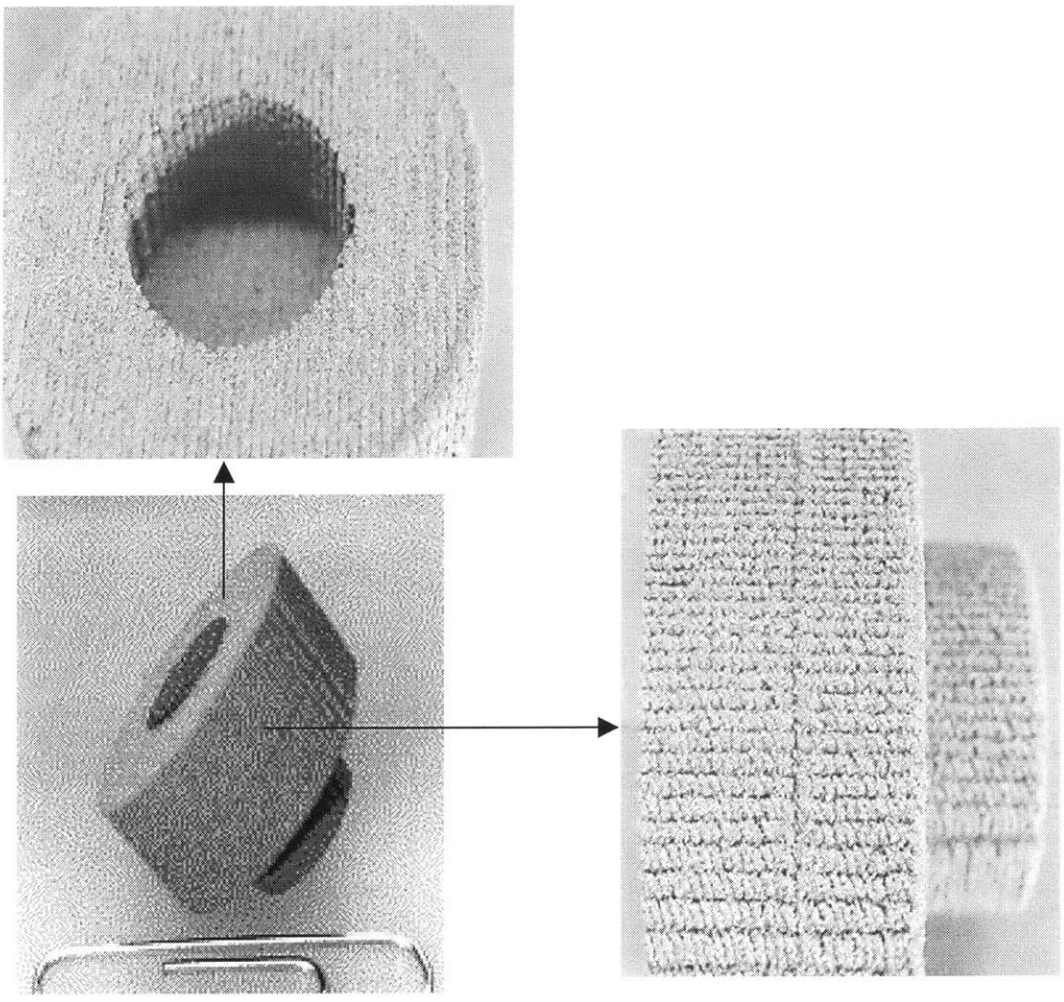

Figure 6.9: Double cylinder

6.4.3.2 Dimensional accuracy

In actual print applications, we want the dimensions of printed parts to match as closely as possible to the CAD model specifications. If they are different from the required values, then some correction factor has to be applied to correct for this.

The measured dimensions of the four printed geometries are included in parenthesis next to the actual dimensions in Appendix B. Results indicate that the valve-

jet is capable of creating both straight edged and curved parts, which closely matches the CAD model. However, there are two important observations that should be noted and possibly be improved upon for even better dimensional accuracy. Firstly, the actual printed distance is always about 1mm larger than the intended distance. The reason for this is discussed in section 7.1. However, this also tells us that we will have to apply a compensating factor during printing, either designing the CAD part smaller or altering the signal duration, in order to get better parts. Secondly, internal dimensions are always smaller than the intended dimensions, as seen in the internal circles of the trapezoid and donut geometries. Again this is cause by the dimensions on one side of the internal feature being larger than required.

6.4.3.3 Strength and porosity of green part

By weighing a part and measuring its dimensions, it is possible to obtain an estimate of the green part density. This is easiest performed with the rectangle block geometry.

	Length (fast axis)	Width (slow axis)	Height (piston)
Nominal (intended)	30mm	20mm	20mm
Measured (actual)	31mm	20.6mm	20.1mm

Table 6.1: Nominal and printed dimensions for rectangle brick extrusion

It is noted that the fast axis is larger than the intended dimension. We believe this is due to the presence of the tail at the trailing edge of the stream; this is further discussed in section 7.1. The mass of the part is 50.1 g, and the density of stainless steel is 7.8 g/cm^3. The green part density is calculated with the following equation:

$$\rho_{Green\ part} = \frac{mass_{printed\ part}}{L * W * H * \rho_{steel}} \qquad (6.1)$$

where L = length, W = width and H = height of rectangle block. This formula ignores the mass of the binder PVA in the green part. Therefore the calculated green density will be larger than the actual value. The green density for the rectangle brick extrusion was calculated to be 50%. This is lower than the tap density of 60% for 420 stainless steel. A higher green density may be obtained if the powder was tapped to increase the packing density. But since we are only looking for an approximation number, this value is sufficient.

6.4.3.4 Total build time

The total built volume of the four geometries, with a duplicate of each, was 150x300x30mm. A total of 86 layers were laid. The build time was approximately 4.0 hours, decomposed as such:

Spreading:	8	seconds
Printing:	90	seconds
Drying:	50	seconds
Total:	148	seconds

Printing and drying processes remain the major components of the total build time. It appears that the valve-jet is capable of handling much higher velocities beyond 1.5 m/s producible on the pendulum arm of the Alpha machine. However, this may only be achieved with a new mechanical design of a new Beta machine with an entirely different architecture in order to achieve fast axis speeds of a higher order of magnitude. The drying time is more difficult to reduce, as we have to allow time for evaporation to occur. A possible modification that can be made to increase evaporation rate is to add a fan blowing air gently over the powder surface without disturbing the material, simultaneously during the drying process. This will reduce drying time by increasing air circulation in the air vicinity above the powder bed.

6.4.4 General printing observations

Although the first printing with the solenoid valve-jet went successfully, there were a few minor problems encountered and observations made along the way.

One problem was that there was a tendency for powder to collect on the bottom plate of the valve-jet surrounding the orifice. If the powder accumulation becomes severe, the jet-stream will tend to flood around the orifice forming a sphere droplet, disrupting the printing operation. It is unclear why this happens because it appears to be a random occurrence. Two possible causes are: 1) small powder particle can easily get thrown up from the substrate and sticks onto the base as the valve-jet traverses at high speeds at only 0.5mm separation from the powder-bed. 2) The magnetic field created in the valve-jet is sufficiently strong to attract small bits of powder to accumulate at the base of the valve-jet. The solution to rectify this was simply to add a brush station at the ends of the print carriage's traverse such that the valve-jet has to brush lightly against them at the end of each pass. This idea was implemented and the powder accumulation problem was resolved.

An interesting observation during the printing process was that minute specks of printed powder gets displaced and is deposited at the trailing edges of each pass. These specks are possibly produced by powder getting displaced from the powder bed due to the ballistic impact of the jet-stream against the substrate. Another explanation may be that the stream tail breaks off and form satellites just before impact with the powder bed. And these specks of printed powder are the satellite droplets. Finally, we also observed that the first line segment printed seems to be embedded deeper in the substrate than the subsequent lines. The first line printed helps to reduce the momentum during impact in subsequent printed lines. Thus, they do not lie as deep into the substrate as the first line.

7. MORE TESTS WITH VALVE-JET

Having established that a single solenoid valve-jet is capable of printing parts with good dimensional accuracy and surface texture, further tests were conducted to investigate more detailed performance capabilities and limitations of the valve-jet. This chapter discusses the results of the minimum printable feature test, bi-directional printing, long-term continuous runs results, degree of operational variability between different valve-jets and finally, multiple-jet printing operation.

7.1 Minimum feature size

There are 2 objectives for the minimum resolution test: 1) To determine the smallest printable feature using the INKX0505950A valve-jet, and 2) Test intended CAD dimension versus actual print dimensions. A "cooling-fin" geometry with regularly decreasing step size was specially designed for the minimum feature size test. As shown in the 3D and orthographic views in **Figure 7.1**, each step is in decreasing sizes from 5mm to a minimum of 0.1mm, to be aligned in a direction perpendicular to the fast axis during printing.

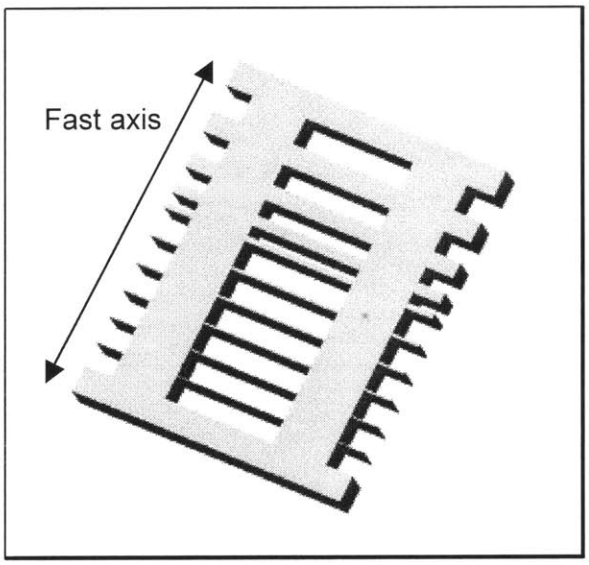

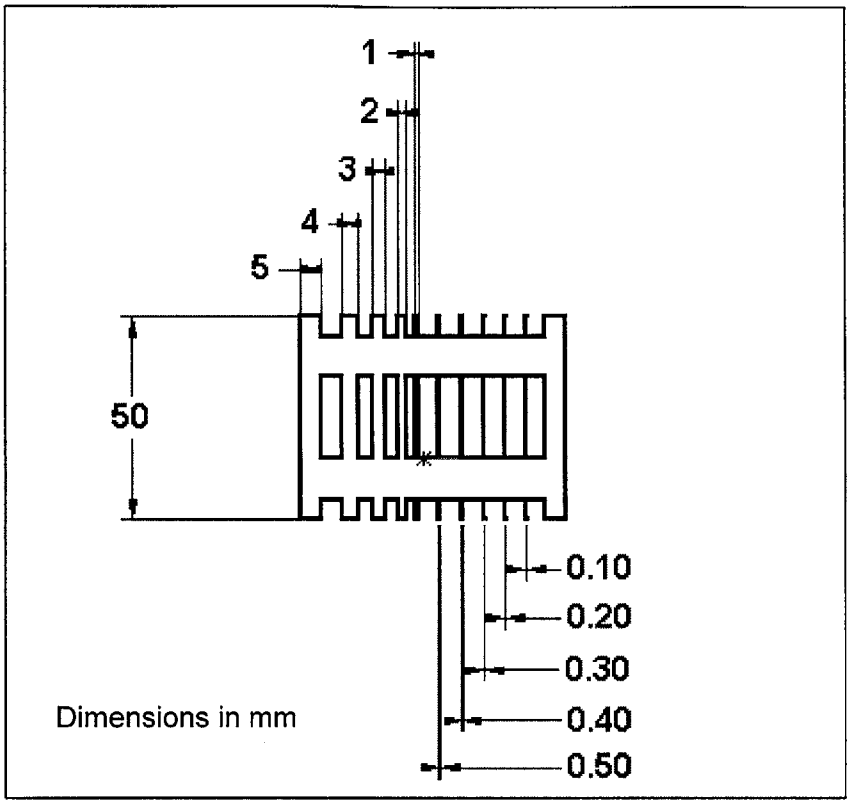

Figure 7.1: 3D and top-view of fin geometry for testing minimum feature size

It is hoped that with the decreasing step size, we will be able to identify the transition from the smallest printable feature to the first non-printable feature. It should be emphasized that the minimum feature size obtainable may vary from one valve-jet to another caused by manufacturing tolerances. The topic of variability between valve-jets is discussed in section 7.4 and eventually manifests itself during multiple-jet printing operations in section 7.5. However, we will restrict ourselves to single valve-jet operations for now.

Figure 7.2 shows the 3D printed fin geometry using the Alpha machine. The parameters used to produce this part were:

- Single valve-jet
- Uni-directional
- Water at pressure = 10 psi; flow-rate = 5.05 cm^3/min

- Row spacing = 400 μm
- Layer thickness = 350 μm
- 2.4% volume PVA binder with 420 stainless steel powder
- Drying time per layer = 70 seconds (initial 20 layers);
  50 seconds (remaining layers)

Results of this test run reveals that the 0.1mm and 0.2mm fin sections in the original CAD solid-model were not producible, while sections equal to or larger than 0.3mm were obtainable. Based on 0.25 milliseconds duration of the "spike" voltage (discussed in section 3.2) use to "kick" the valve-jet open and a fast-axis traverse speed of 1.5 m/s, we can deduce that the smallest printable feature (in the CAD solid model) must be larger than 375 μm, assuming the stream produced takes the shape of a perfect cylinder. Therefore, the experimental results agree closely with our theoretical expectation.

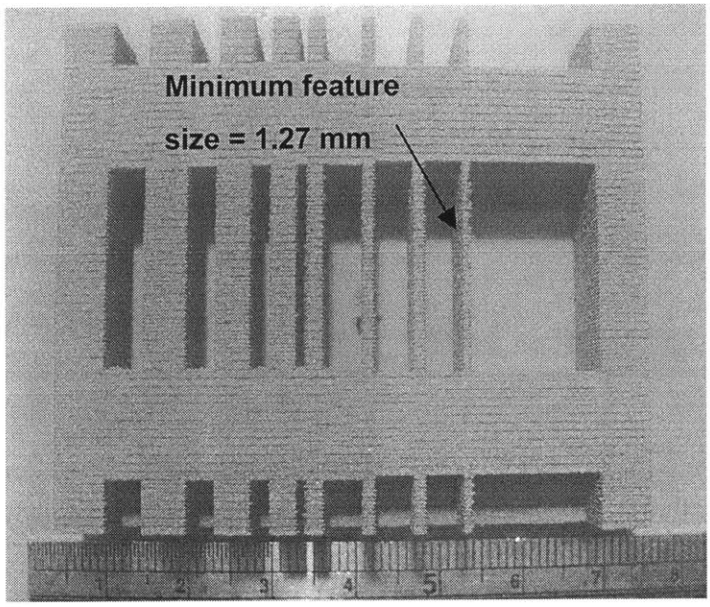

Figure 7.2: 3DP™ fin geometry (single valve-jet; unidirectional)

These results can be explained by observing the duration of the current passing through the solenoid. A plot similar to that in **Figure 7.3** is observed on the oscilloscope during a single pass of the fast axis. **Table 7.1** summarizes the step sizes and

corresponding signal durations. The signal durations corresponding to the 0.1mm and 0.2mm dimensions, created by the slicing algorithm are shorter than the rise time of the spike voltage to a level (24V) sufficiently large to actuate the plunger into the open position. It usually takes 0.25 milliseconds for the voltage to rise to the 24V level to open the valve-jet. Thus, the voltage levels reached for durations of 0.067 and 0.133 milliseconds may only be (for example) 10V and 15V respectively, which is not sufficiently large to actuate the valve-jet. At the transition zone, a signal of 0.2 milliseconds duration is created for the step size of 0.3mm. We should not expect the valve-jet to be actuated because this is lesser than the 0.25 milliseconds, however, it is very likely that the 0.2 milliseconds was just sufficient for the valve-jet to hit the minimum spike voltage of 21V (section 3.4), and hence actuate the valve-jet.

Step size (mm)	Signal duration (ms)	Print / No Print ?
0.1	0.067	No Print
0.2	0.133	No Print
0.3	0.200	Print
0.4	0.267	Print
0.5	0.333	Print
1	0.667	Print
2	1.333	Print
3	2.000	Print
4	2.667	Print
5	3.333	Print

Table 7.1: Step size vs. signal duration/printability

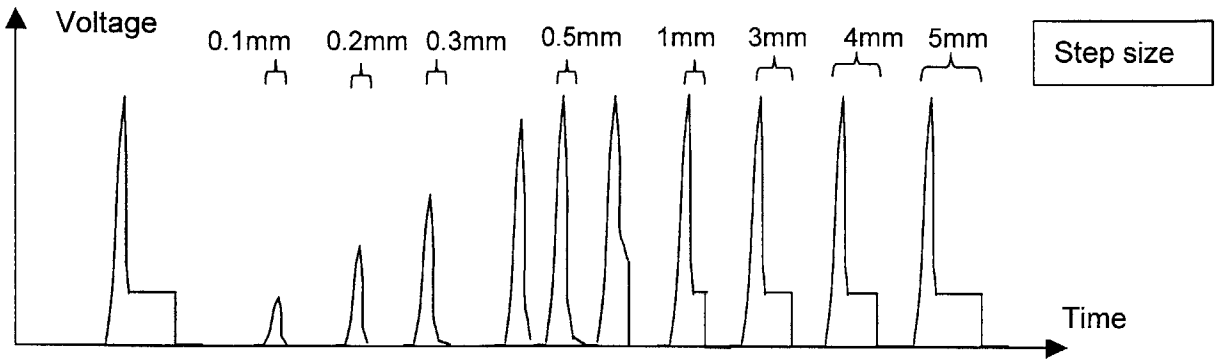

Figure 7.3: Current waveform corresponding to step size in fin geometry

It is not possible to achieve printed geometries with exact dimension to the CAD model because conditions are less than ideal. Effects of surface tension, aerodynamic turbulence and gravity all act to distort the shape of the droplet or stream produced. **Figure 7.4** is a plot of the intended distance against the actual print distance. It shows a curve-fitted line with a slope of approximately 1 (45° slope) intercepting the Y-axis at 1.12mm. In perfect printing process, where a jet-stream takes the shape of a perfect cylinder and a droplet is a perfect sphere, we should expect this 45° line to pass exactly through the graph origin. The intercept at 1mm may be attributed to the presence of a tapering "tail" at the trailing edges of a droplet or stream. The length of this tail in both the case of a droplet or jet-stream is 1mm.

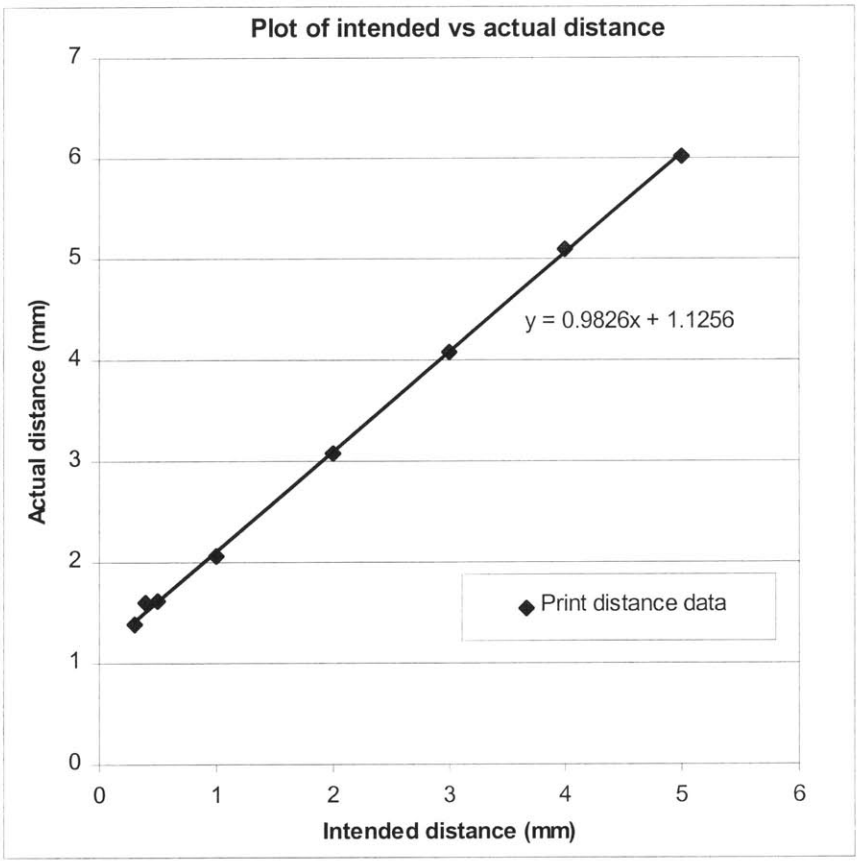

Figure 7.4: Intended vs. actual print distance

7.2 Bi-directional printing with single jet

7.2.1 Time of Flight

Earlier we observed that the trailing edge of the jet-stream breaks up into satellite droplets at distances more than 0.5mm from the orifice. For the best print results, the nozzle should be positioned at an elevation no more than 0.5mm from the powder-bed.

Using the stream observation station, it is possible to determine the time of flight (TOF) for both the leading and trailing edges to arrive at the position 0.5mm away from the nozzle. The leading edge time of flight is defined as the elapsed time between when the rising edge of the input signal and when the stream front reaches a position 0.5 mm from the valve nozzle. This is effectively the time between when the input signal to open the valve is applied to when the head of the stream impacts the powder-bed (assuming it is 0.5mm from the orifice). The trailing edge TOF is similarly defined as the elapsed time between when the falling edge of the input signal and when the stream tail reaches a position 0.5 mm from the valve nozzle. This is effectively the time between when the input signal to close the valve is applied to when the tail of the stream impacts the powder-bed. We found that for a jet-stream 3.2mm in length, the TOF of the leading edge is 0.49 milliseconds, while the TOF of the trailing edge is 0.89 milliseconds. A reason that the TOF of the trailing edge is longer than the leading edge is because the valve-jet is not able to close as quickly as it is to open despite the inclusion of the diode clamp. As a consequence of the TOFs difference, we should expect a printed line segment to be longer than if the TOFs were identical, where the difference in length is given by the difference in TOF multiplied by the printhead velocity. This idea is illustrated in **Figure 7.5**.

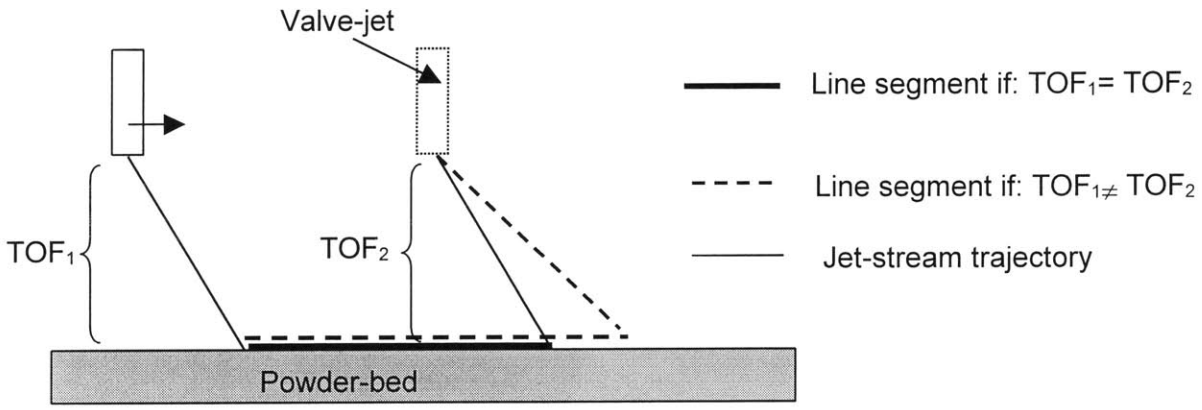

Figure 7.5: Dimensional errors caused by TOF difference

7.2.2 Time of flight correction for bi-directional printing

A single pass on the fast axis of the Alpha machine takes approximately 1 second. Hence, the total printing time can be reduced by a factor of 2 if two-way printing is implemented. Before we can print bi-directionally with the solenoid valve-jet, a time of flight correction has to be used to align the front and back edges of consecutive line segments so that they will all perfectly lined-up without jaggedness or stepped appearance. The stepped edges produced by bi-directional printing without TOF correction is shown in **Figure 7.6**. On the Alpha machine, the TOF is related to the amount of physical shift and linear velocity of the printhead by the following relationship:

$$\text{Shift} = \text{TOF} \times \text{Linear velocity} \times \text{fudge factor} \tag{7.1}$$

The fudge factor is used for the purposes of "fine tuning" after the shift is approximately in the required range. Note that the actual shift on each edge is only half the amount calculated in equation 7.1, because we are simultaneously moving both consecutive lines.

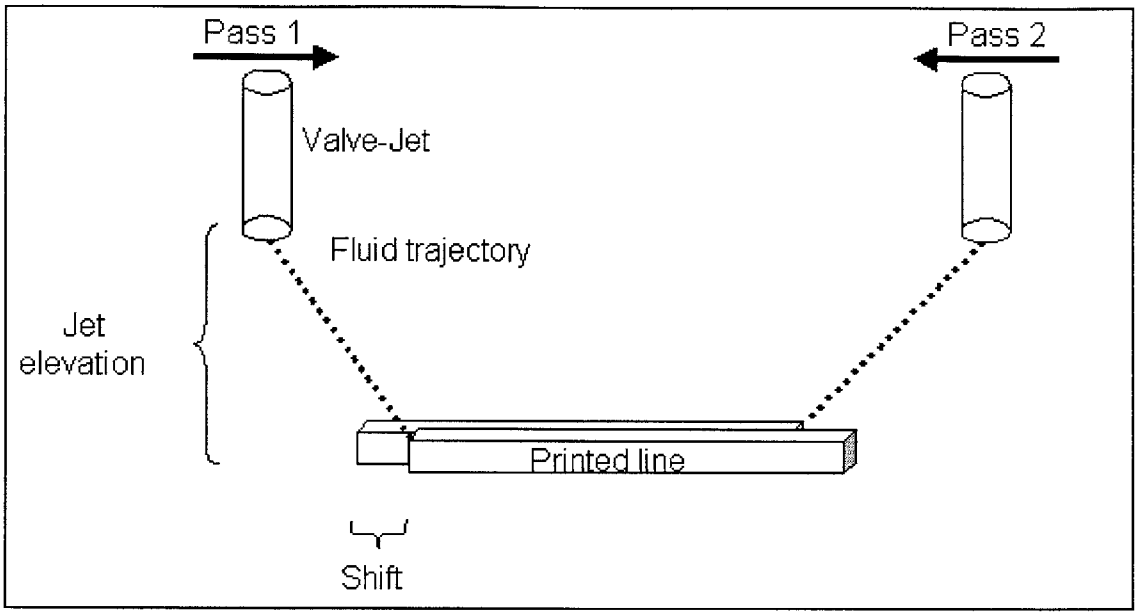

Figure 7.6: Shifted edges from bi-directional printing

The TOF correction required for edge-alignment is determined by trial and error. A single layer is printed and the edges are viewed under a microscope. This procedure is repeated until the best quality edge is determined. The results are shown in **Figure 7.7** with the corresponding amount of TOF correction (in milliseconds) below each photo. Note that these images were all taken for the same edge. The other edge shows exactly the similar interlocking pattern, just a mirror image of this. At an elevation of 0.5mm from the powder-bed, a TOF correction of 0.8 milliseconds gives the best edge straightness results. Hence, this value will be used in all subsequent bi-directional prints. If the nozzle elevation or fast axis velocity is changed, then the TOF correction will have to be determined again using a similar procedure.

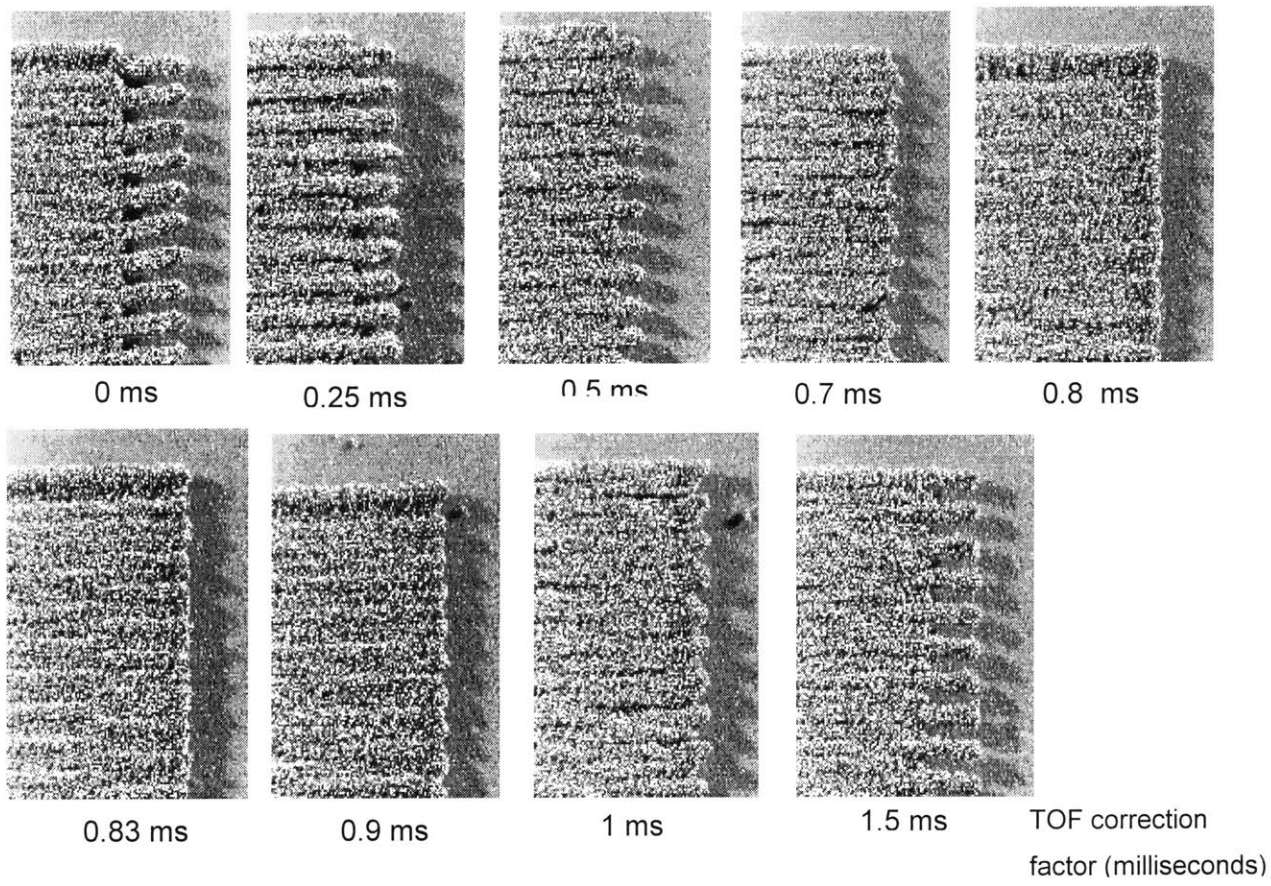

Figure 7.7: Effects of TOF correction (single layer)

7.2.3 Geometrical parts with bi-directional single valve-jet printing

Figure 7.7a shows the bi-directionally printed fin geometry using one single valve-jet. The parameters used to produce this part were:

Number of valve-jets	One
Print direction	Bi-directional

Fast axis speed	1.5m/s
Pressure	10psi
Flow-rate	5.0 cm^3/min
Row spacing	400 μm
Layer thickness	350 μm
Jet elevation	0.5mm from powder bed
TOF correction	0.8
Material system	2.4% volume PVA with 420 stainless steel powder
Drying time per layer	70 sec. (initial 20 layers) 50 sec. (remaining layers)

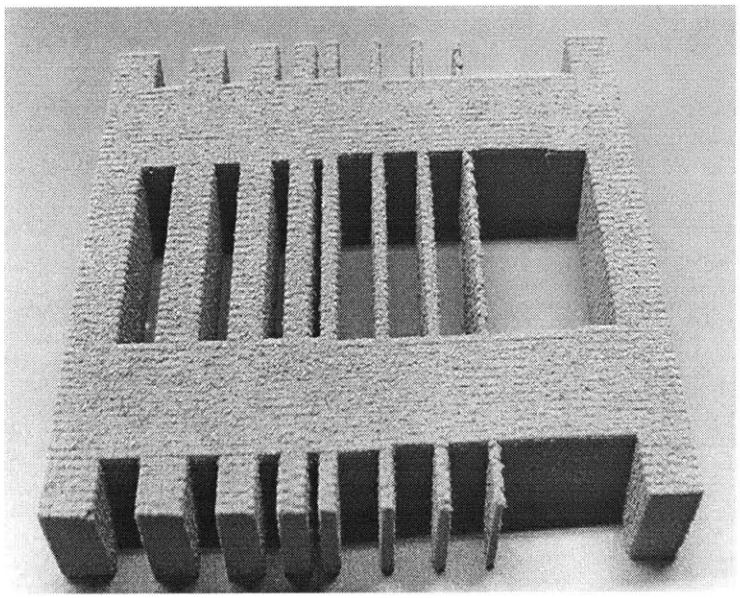

Figure 7.7a: 3DP™ fin geometry (single valve-jet; bi-directional)

The fin geometry printed with a single valve-jet operating bi-directionally was identical to that printed with a single valve-jet operating uni-directionally. In fact, the parts are almost indistinguishable from each other. The 0.1mm and 0.2mm fin sections in the original CAD solid-model were not producible, while sections equal to or larger than 0.3mm were obtainable. The edges on the fin sections were sharp and the surface texture was of a high quality. The printed lengths of each of the fin section was

measured and the results were very also very close to that of the uni-directional print in Figure 7.4 and so is not repeated here. There is no difference in valve-jet performance and part quality between uni-directional and bi-directional printing if an appropriate TOF correction is chosen.

7.3 Long-term continuous duration run

One of the most important considerations for deciding if the solenoid valve-jet can be used in a scaled-up machine is its durability and robustness for stable and consistent performance when subjected to long periods of operation. A long-term duration test was designed to evaluate this aspect of the valve-jet. Two valve-jets were tested, each operating at 30 Hz and a pressure of 10 psi over a continuous period of 5 days. The HP function generator with the Lee circuit was used to provide the 30 Hz signal over the test period while the recycling clam-shell fluid system provided a continuous supply of fluid to the valve-jet. Three parameters were measured at daily intervals: flow-rate, time of flight for the head and tail to travel a distance of 0.5mm from the nozzle.

Figure 7.8 summarizes the two valve-jet's flow-rate over the five days period. The flow-rate variation for valve-jet 2 was over a range $\pm$ 0.2cm^3/min between the two highest and lowest extreme values while that for valve-jet 5 was $\pm$ 0.06cm^3/min. These results indicate that there is no significant deterioration in performance over long periods of continuous operations. Although we did not observe a declining pattern in flow-rate, there were some flow-rate fluctuations especially for valve 2 between days 1 and 3. Note that these flow-rate measurements were taken for 1 minute at the steady state condition.

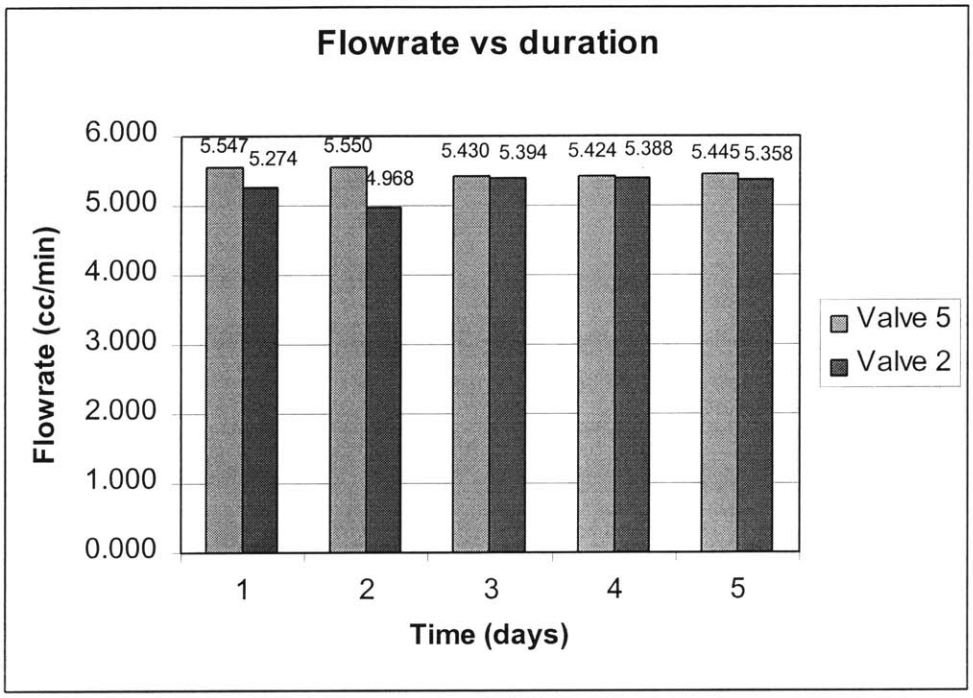

Figure 7.8: Flow-rate over five days

Results of the leading and trailing edge time-of-flight (TOF) to reach a distance of 0.5mm (stream tail breakup distance) from the orifice provides even stronger evidence that a single valve-jet's performance does not change significantly over continued periods of operation. In **Figure 7.9**, the TOF of the leading edge of a jet-stream produced from valve 2 is very constant at about 0.465 milliseconds, while that of valve 5 is approximately at 0.49 milliseconds throughout the five day duration. Although the performance of one valve-jet is very producible, there is a noticeable difference between discrete valve-jets. Variability between valve-jets is discussed in the next section.

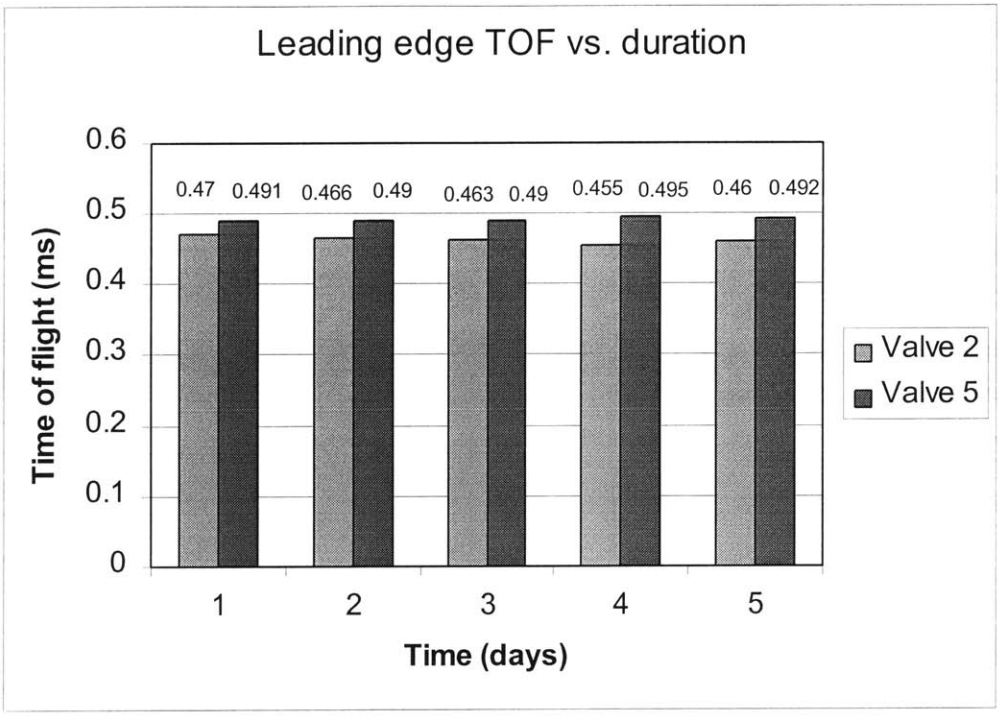

Figure 7.9: Leading edge TOF over five days

Results for the trailing edge are very similar to those of the leading edge TOF. As shown in **Figure 7.10**, there is very little variation in the trailing edge TOF of a single valve-jet over the five days period, however there is a noticeable difference in the TOF of two discrete valve-jets. Interestingly, valve-jet 2 which takes a lesser amount of time to reach the 0.5mm position on the leading edge also takes less time on the trailing edge to reach the 0.5mm mark, compared to valve-jet 5 which is slower on both edges. Since all other conditions were controlled in this experiment, it tells us that the difference in TOF performance most likely stems from a difference in the internal construction of the valve-jet inherited from manufacturing tolerances. This can possibly be physical differences in the diameter of orifice, spring constants etc., or differences in electrical properties of the valve-jets.

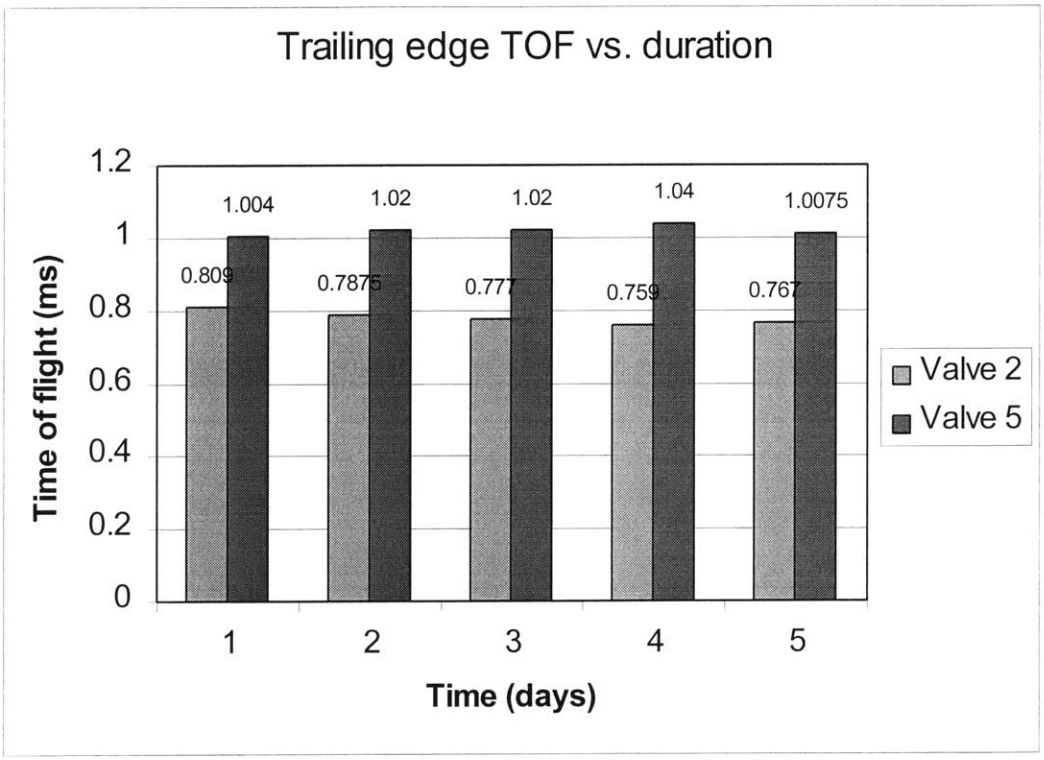

Figure 7.10: Trailing edge TOF over five days

7.4 Variability between different valve-jets

It is expected that there will be performance difference between valve-jets. No two valve-jet can be made perfectly identical due to the limitations on manufacturing tolerances. Previously, a large proportion of the Lee valve-jets were made manually; however, by increasingly automating the manufacturing process, the Lee Co. hopes that the amount of variability will decrease.

The objective of this effort is to arrange an array of these valve-jets into a single printhead with a single jet printing a portion of the entire geometry and then stepping over. If there is a great deal of variability between valve-jets, then parts with stepped or jagged edges will be printed. Variability between valve-jets is to be expected; we have

to determine what this amount of variation is and if we can modify any of the print parameters to compensate for this deficiency.

A variability test was designed to determine the amount of variation between one valve-jet to the next. A sample size of five valve-jets was tested for three parameters: 1) Flow-rate variation 2) Response time variation and 3) Time of flight variation.

7.4.1 Flow-rate variation

The same experimental setup consisting of a waveform function generator with the Lee circuit and the recycling clam-shell fluid system was used. The valve-jets were numbered one through five this experiment. Water at 10 psi was collected at steady state condition for 1 minute. **Figure 7.11** summarizes the flow-rate results of the five valve-jets tested. The variation between the valve-jet with the highest and lowest flow-rate is 0.205 cm^3 /min. This is only a very small percentage of the 5 cm^3 /min flow-rate being used. Thus, the amount of flow-rate variation between the five valve-jets is not significant.

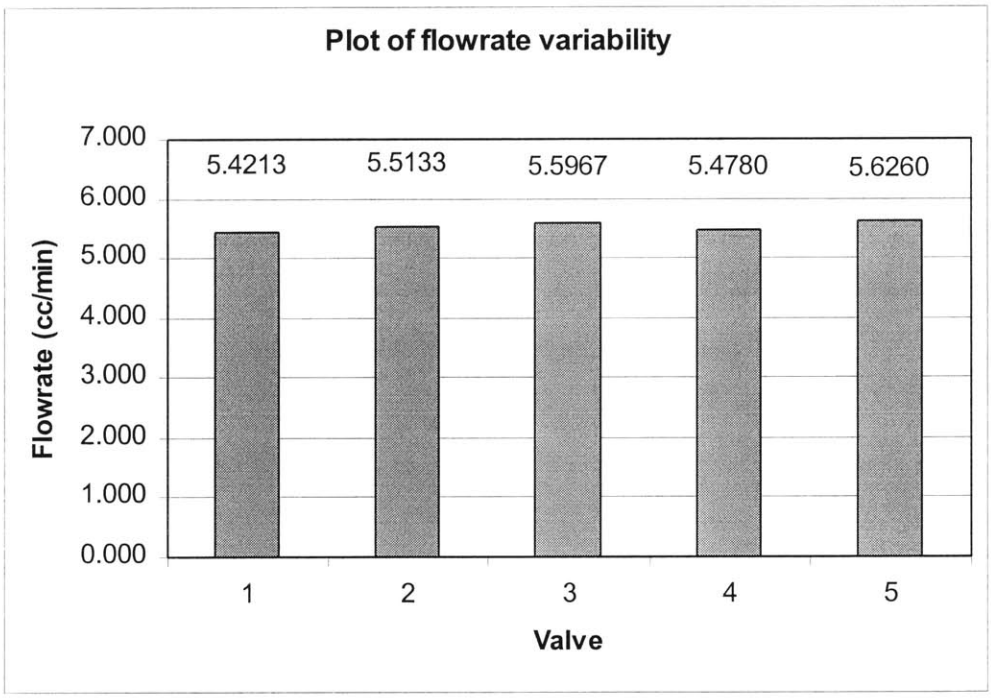

Figure 7.11: Flow-rate variability

7.4.2 Response time variation

Recall that the response time of a valve-jet was defined as the time between the rising edge of the spike and hold signal and when the stream is first observed to emerge from the orifice. **Figure 7.12** shows that the "fastest" valve had a response time of 0.396 milliseconds and the "slowest" valve-jet took 0.423 milliseconds. The range of 0.027 milliseconds is considerably small. Assuming that the fluid is immediately printed onto the substrate when it emerges from the orifice, this response time variation translates only into a physical difference of 0.0405 mm in the line segment printed by a printhead moving at 1.5m/s. This difference is sufficiently small to be considerable negligible and therefore the response time variation is acceptable.

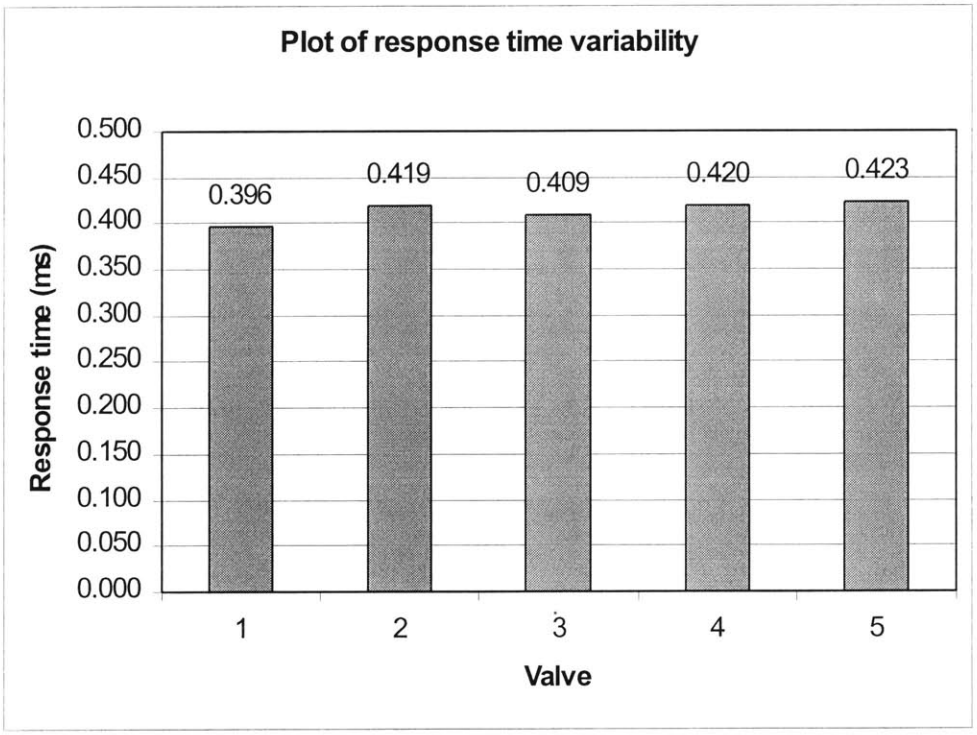

Figure 7.12: Response time variability

7.4.3 Time of flight variation

Figure 7.13 shows the time of flight for the leading edge of the stream to reach a position 0.5 mm from the orifice. The variation between the fastest and slowest valve-jet

is 0.027 milliseconds. Assuming that a fast axis traverse speed of 1.5 m/s is used, we should expect a maximum difference of 0.0405 mm on the leading edge between lines printed by the fastest and slowest valve-jets during a single pass. Thus, the length difference resulting from the leading edge TOF variation is so small that it will hardly be noticeable for practical printing applications, especially when the intended use of this valve-jet is for printing large geometrical parts.

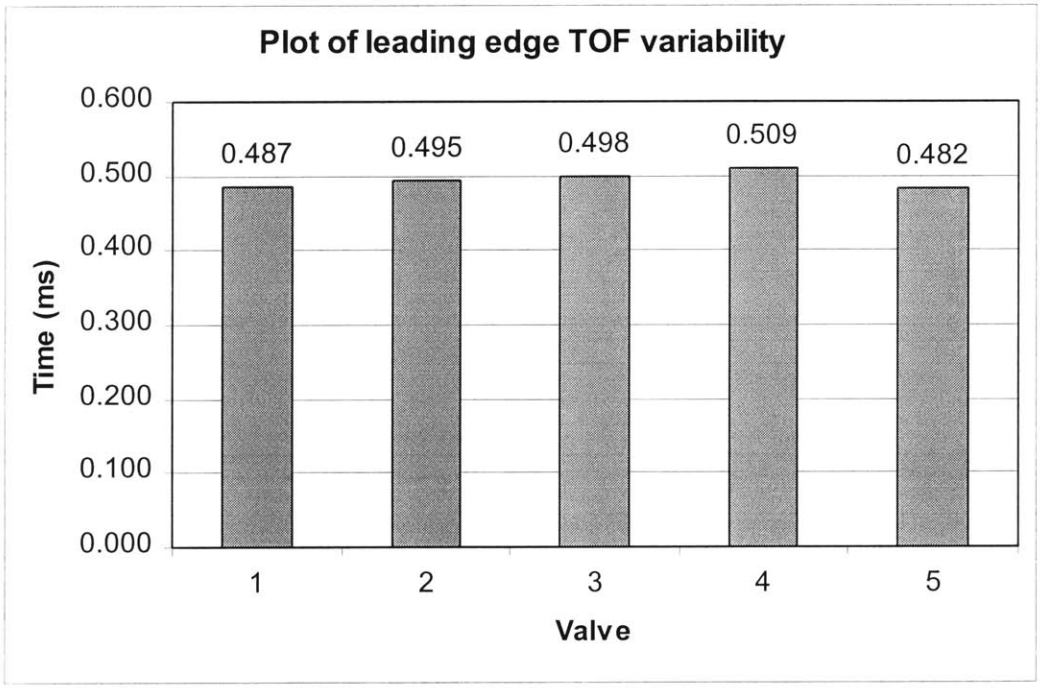

Figure 7.13: Leading edge TOF variability

Similarly, **Figure 7.14** shows the times of flight values of the trailing edge to travel a distance of 0.5 mm from the orifice. The range of time variation from among the valve-jet is 0.353 milliseconds. This translates to a maximum difference of 0.53 mm between lines produced by valve-jets on the trailing edge of a single pass when the fast axis moves at 1.5 m/s.

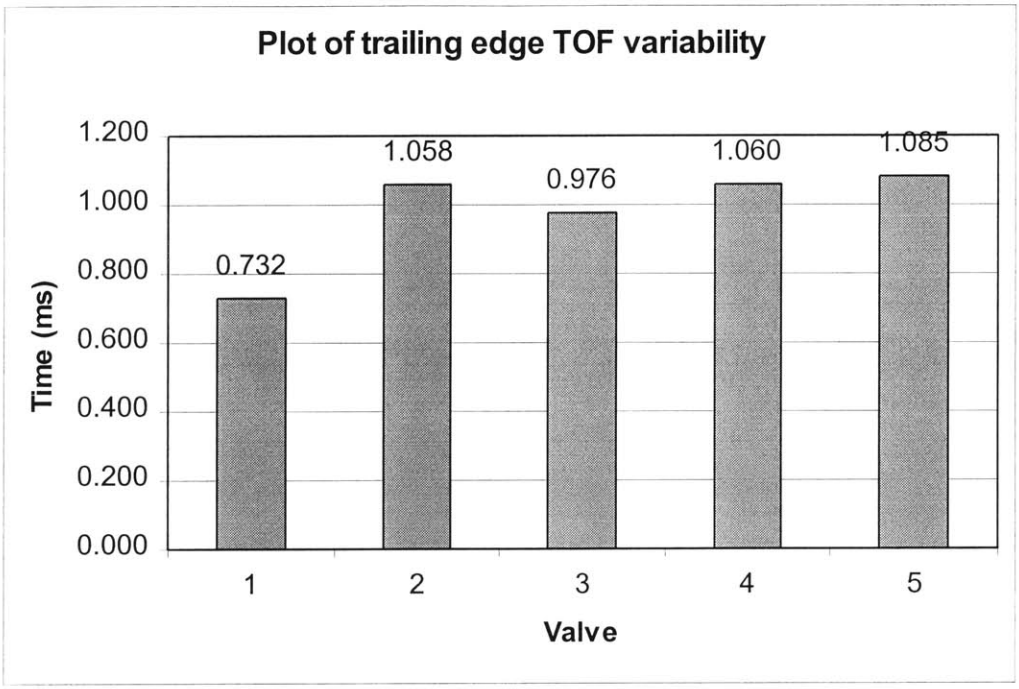

Figure 7.14: Trailing edge TOF variability

7.5 Multiple valve-jets operation

There are two methods of to evaluate printing with two valve-jets:

Scenario 1: Slice one geometrical part to print with a single valve-jet using the 3DP™ file preparation software. The same signal can be tapped out in parallel from the same channel on the Alpha machine controller to two separate drive circuits linked to two different valve-jets. Result is both valve-jets will independently be printing two separate parts. This is as though they are two single valve-jets, simultaneously printing on the same substrate. Attachment brackets will have to be machined to hold the valve-jet sufficiently apart such that the printed parts' footprints do not overlap.

Scenario 2: Slice one geometrical part to be printed by two valve-jets. Two different signals will be tapped from two different channels on the Alpha machine controller to two separate drive circuits linked to two different valve-jets. Both valve-jets will simultaneously be printing different sections of the same geometry. We will have independent control of the line segments printable by each valve-jet. Attachment

brackets will have to be machined to space both valve-jets an appropriate integer spacing apart, as defined by the slicing algorithm.

There is nothing to be learnt from printing in Scenario 1 because it essentially is just printing with a single valve-jet; with the difference that we now have two valve-jets doing duplicate tasks simultaneously. The objective of printing with two valve-jets is to study the interaction between them as they perform the operation of printing one single common geometrical part. Scenario 2 helps us achieve this. From the results, we will learn if the variability between valve-jets (as determined in section 7.4) manifests itself in the printed prototypes. And if the variability is indeed observable, we want to know where are the dimension boundaries where it becomes less severe, and the printed part can start to appear as though it were produced using one single valve-jet. The two scenarios are illustrated in **Figure 7.15** below.

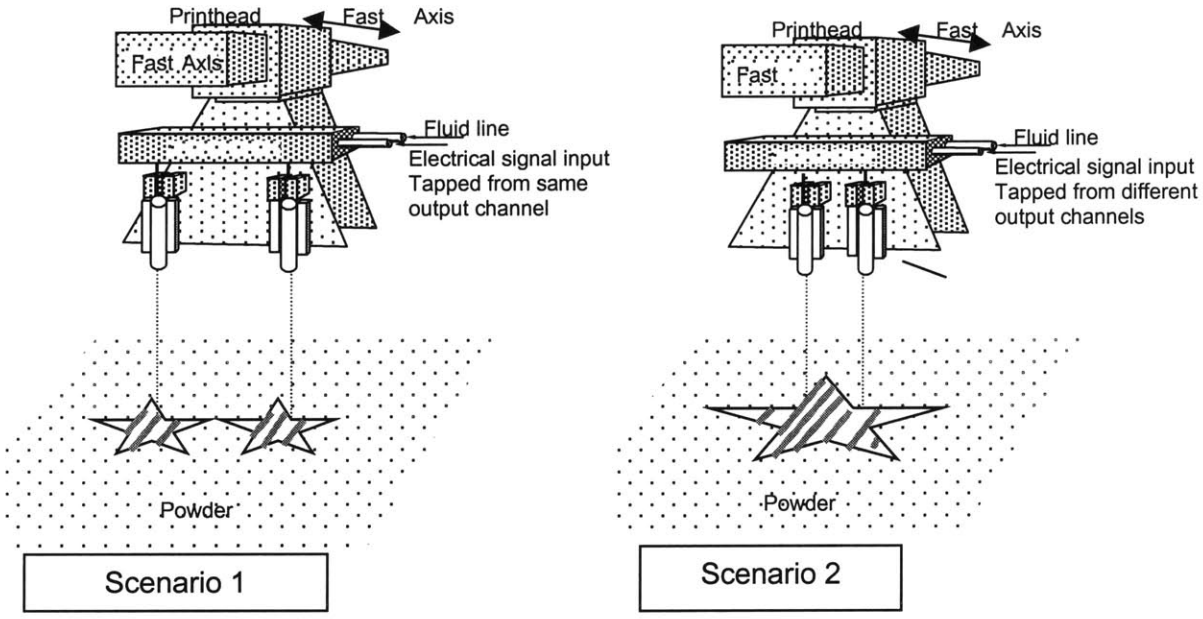

Figure 7.15: Possible methods of two-jet printing

Because the valve-jets will be using the Alpha machine controller electronics and slicing algorithm, we need to machine the attachment brackets not just to hold the valve-jets,

but also to place them an appropriate offset distance apart so the first and last line segments printed by two different jets will stitch together seamlessly. The Alpha machine controller software requires consecutive nozzle on the printhead to be positioned an exact distance of $^{1}/_{6}$ " (0.4233mm) apart. Unfortunately, the center-to-center distance between the solenoid valve-jets is larger than this value, and therefore it is impossible to position two jets along a straight line. A staggering of valve-jets will have to be done. The staggering distance of 4.36mm will be compensated for, by adjusting the "crooked jet correction" parameter in the Alpha machine controller software. The correction factor essentially tries to correct for the staggering distance by releasing the jet-stream earlier from one of the valve-jets than if no correction was used. This bracket and the dimensions of the machined holes to accommodate the valve-jets' required jet spacing and crooked jet correction is shown schematically in **Figure 7.16**.

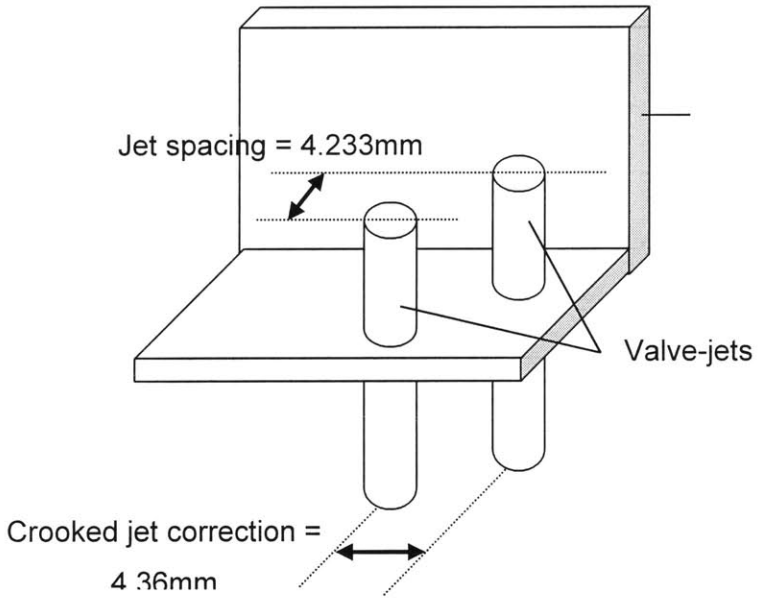

Figure 7.16: Jet spacing and crooked jet correction

7.5.1 Uni-directional print

7.5.1.1 Experimental parameters

The parameters used in the uni-directional test with two valve-jets were:

Number of valve-jets	Two
Print direction	Uni-directional
Fast axis speed	1.5m/s
Pressure	10psi
Flow-rate	5.10 cm^3/min
Row spacing	360 μm
Layer thickness	350 μm
Jet elevation	0.5mm from powder bed
TOF correction	0
Material system	2.4% volume PVA with 420 stainless steel powder
Drying time per layer	70 sec. (initial 20 layers) 50 sec. (remaining layers)

A few experimental layers were printed to evaluate the quality of printed parts. A row spacing of 400 μm was found to produce poor stitching results between lines printed by the last pass of the first jet and the first pass of the second jet before the stepping motion. The row spacing was thus reduced to 360 μm for printing with two valve-jets as this was found to produce parts, which were less vulnerable to breaking up.

7.5.1.2 Results

7.5.1.2.1 Rectangle brick

Figure 7.17 shows the 3DP™ rectangle brick geometry. The entrance edge of the printed part is straight and the lines segments were very well aligned and almost indistinguishable from each other, even under the light microscope. It also shows that the staggering of valve-jets and the crooked jet correction was performed successfully. However, the exit edge has a stepped appearance between lines printed by one valve-jet and the other. This is illustrated in the schematic drawing in **Figure 7.17**. We believe the stepped edge appearance is caused by the variation in closing times (TOF variation) between valve-jets as discussed in section 7.4.3. Valve-jets 3 and 5 from section 7.4 were used for this printing experiment. The difference in the trailing edge TOF between

these two valve-jets (from the plot in **Figure 7.14**) is 0.109 milliseconds. Assuming that the printhead was traversing at 1.5m/s, we should expect to see a difference of 0.164mm in the printed line segments. The actual difference in lengths between line segments printed by the two valve-jets was 0.2mm. Thus, results from this and the earlier TOF experiments agree well with each other.

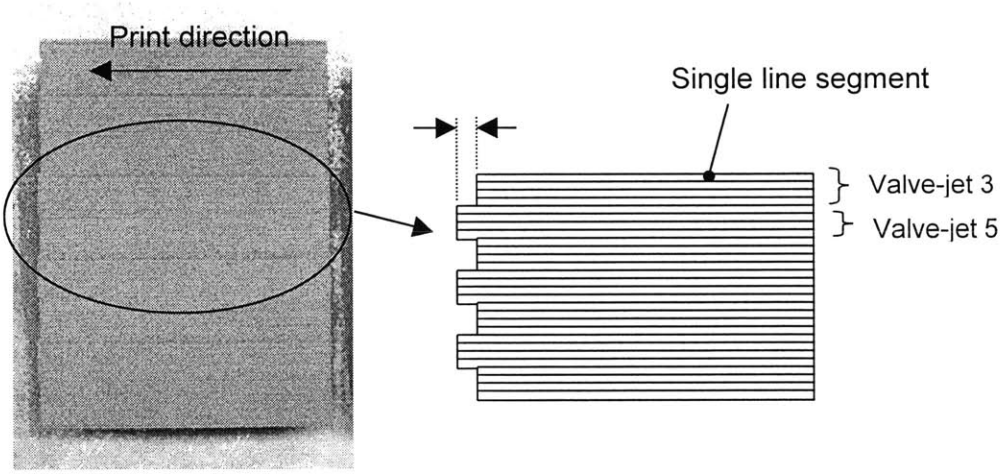

Figure 7.17: Rectangle block (two-jets; uni-directional)

7.5.1.2.2 Fin geometry

Figure 7.18 shows the 3DP™ fin geometry printed uni-directionally with two valve-jets. Identical to printing with a single valve-jet in section 7.1, the intended 0.1mm and 0.2mm sections were not printable. Furthermore, the 0.3mm section, although printable using two valve-jets, was broken off during the part removal process from the Alpha machine because part of the 0.3mm section printed by one of the valve-jet was too thin and hence too weak to withstand the forces generated as the surrounding unprinted powder was being removed.

Focusing on the fin geometry successfully retrieved from the substrate, the leading edges of each fin section, including the smallest section (0.4mm) turns out well. The line segments printed by the two different valve-jets were almost indistinguishable on the final geometry. However, a similar stepped pattern in the line segments was

evident on the trailing edge, as shown in the magnified image taken under a light microscope in **Figure 7.18**. The difference in length shows up most clearly in the short fin sections, but became less obvious for longer sections above 4mm. The results are summarized in **Table 7.2**.

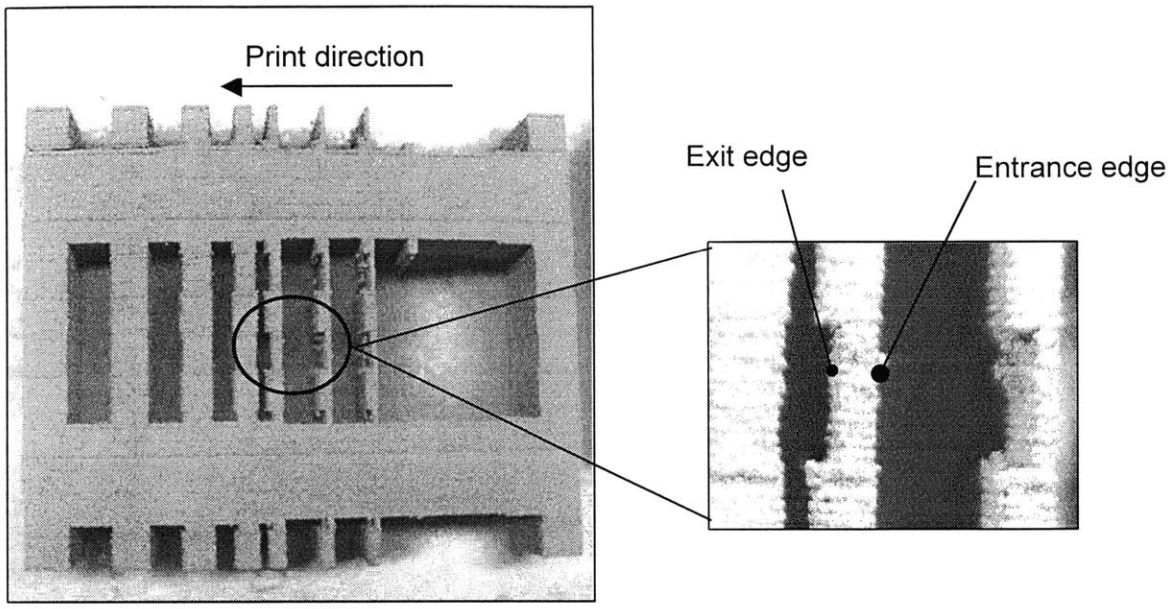

Figure 7.18: Fin geometry (two-jets; uni-directional)

Expected length /mm	Actual length /mm (Valve-jet 3)	Actual length /mm (Valve-jet 5)
0.1	No print	No print
0.2	No print	No print
0.3	Print but broken off	Print but broken off
0.4	0.62	1.42
0.5	0.65	1.52
1	1.12	1.91
2	2.12	2.68
3	3.14	3.54
4	4.09	4.10
5	5.05	5.10

Table 7.2: Intended distance vs. actual distance for two-jets, uni-directional printing

Finally, we looked at the lengths of fluid streams produced by both valve-jets under the jet-stream observation station to ascertain that the dimensional difference in the printed parts were indeed caused by differences in the lengths of the jet-stream produced by the valve-jets. Both valve-jets were operated with an input signal of the same duration, and the lengths of the streams produced were noted. The results are summarized in **Table 7.3** below. These results agree with the stepped appearance we see in the printed fin geometry. For line segments that have an expected length of shorter than 0.4-0.5mm, there is a big difference in the lengths of stream lengths that can potentially be produced by different valve-jets. When the printed line segment becomes larger, the difference in the length of jet-streams progressively becomes smaller. Thus it appears that there is a "danger" zone, which must not be breached during multiple-jet operation. The design and manufacturing tolerance on the Lee valves seems to limit us to printing CAD geometries no smaller than 1mm for multiple-jet operations if good quality parts are desired.

Expected length/mm	Signal duration / ms	Stream length /mm (Valve-jet 3)	Stream length /mm (Valve-jet 5)
0.1	0.00667	No fluid	No fluid
0.2	0.133	No fluid	No fluid
0.3	0.200	1.65	2.30
0.4	0.267	1.75	2.70
0.5	0.333	2.75	3.15
1	0.667	5.00	5.20
2	1.333	8.70	8.60
3	2.000		
4	2.667		
5	3.333		

Table 7.3: Lengths of jet-stream from different valve-jets subjected to input signal of same duration.

Two important conclusions can be made from these results:

1) A single valve-jet acting alone is capable of producing repeatable print results. The evidence supporting this claim is the regularly stepped pattern of the fin sections.
2) There is a degree of variation in the line segments lengths printed by these two valve-jets for small dimensions, but this difference decreases and converges at larger dimensions (approximately 4mm). It appears there will be a lower limit on the minimum feature size for multiple jet operation. This limit should not be breached if good quality parts are to be printed.

7.5.2 Bi-directional print

7.5.2.1 Experimental parameters

The parameters used in the bi-directional printing test with two valve-jets were:

Number of valve-jets	Two
Print direction	Bi-directional
Fast axis speed	1.5m/s
Pressure	10psi
Flow-rate	5.10 cm^3/min
Row spacing	360 μm
Layer thickness	350 μm
Jet elevation	0.5mm from powder bed
TOF correction	0.8
Material system	2.4% volume PVA with 420 stainless steel powder
Drying time per layer	70 sec. (initial 20 layers) 50 sec. (remaining layers)

7.5.2.2 Results

7.5.1.2.1 Rectangle brick

Figure 7.19 shows the 3DP™ rectangle brick geometry using bi-directional, two-jets printing. The line segments printed have a fuzzy overall appearance at both the entrance and exit edges. The edge quality is inferior compared to the earlier parts printed bi-directionally using one single valve-jet. The stepped edges seen previously in uni-directional printing with two valve-jets were less obvious here using bi-directional printing due to the overlapping effect of line segments in both directions. But this overlapping effect, although masking the steps seen previously, has also reduced the edge quality of these parts. The TOF correction is the most important parameter that has to be adjusted by trial and error until the front and back edges of the line segments printed in both directions line up correctly (discussed earlier in section 7.2.2). Although we have determined previously that a TOF correction of 0.8milliseconds produced the best edge quality for a single valve-jet (at elevation of 0.5mm from the substrate), this value may not be the best to use in the case of printing with two valve-jets. We notice that the portion printed by one valve-jet seems to be very well aligned at both edges, but the edges printed by the other valve-jet were not as seen in **Figure 7.19**. The fuzzy appearance is mainly caused by the one valve-jet that did not have the correct TOF. It appears that two different TOF corrections values have to be used for different valve-jets due to the slight variations in their opening and closing times. Using the same TOF correction for two different valve-jets will only lead inferior parts being printed.

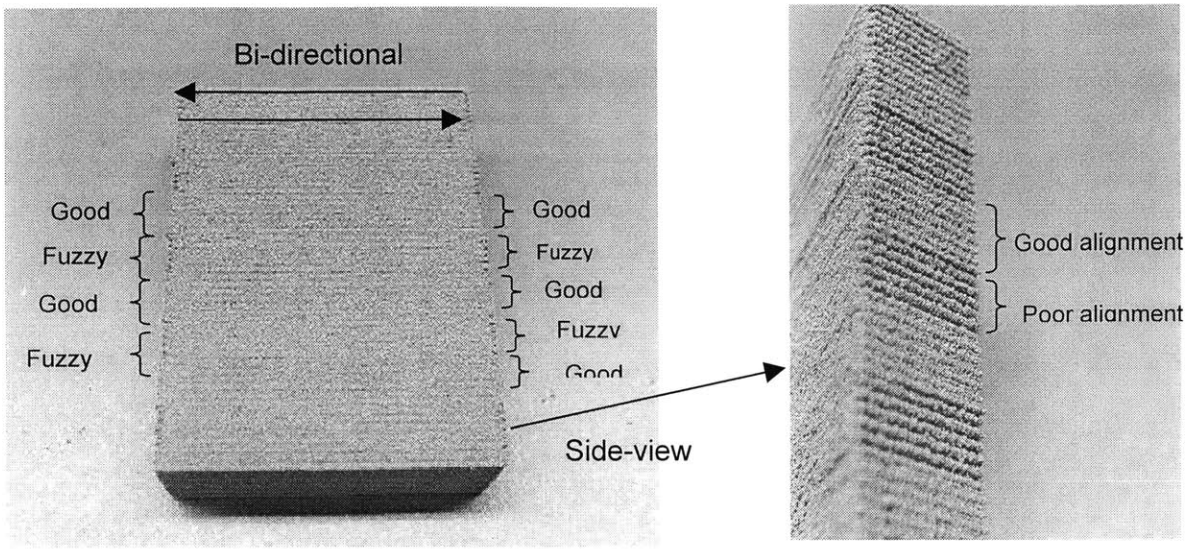

Figure 7.19: Rectangle block (two-jets; bi-directional)

7.5.1.2.2 Fin geometry

Figure 7.20 shows the 3DP™ fin geometry printed bi-directionally with two valve-jets. As in the printing with a single valve-jet, the intended sections 0.1mm and 0.2mm sections were not printable. Furthermore, although the 0.3, 0.4 and 0.5mm sections could be printed using two valve-jets, they broke off during the part removal process from the Alpha machine because the portions printed by one of the two valve-jets was too thin and hence too weak to withstand the forces generated as the unprinted powder was being removed. Weak sections are produced due to insufficient stitching between subsequent passes especially for the 0.3, 0.4 and 0.5mm sections. The poor stitching may be caused by either less than ideal TOF adjustment or simply that the dimensions were too short.

Focusing on the printed fin geometry successfully retrieved from the substrate, the edges on the fin sections have a non-distinct, fuzzy appearance similar to the rectangle block geometry earlier although the effect is more seen more pronouncedly due to the thinner sections. Again, the edge quality is inferior compared to the uni-directional print with two jets, although the stepped appearance was not observable in

the 1mm section (compare with the uni-directional print earlier). Although not as obvious as the rectangle geometry earlier, certain portions of the geometry printed by one valve-jet appears to be better than those printed by the other. The problem is most likely due to an inappropriate TOF being used for one of the valve-jets. The bottom-line is that the correct TOF appropriate to each valve-jet must be programmed into the Alpha machine controller software. But the software only allows one TOF correction for all the valve-jets and thus it may not be possible to find a single TOF that can be used to suit both valve-jets perfectly.

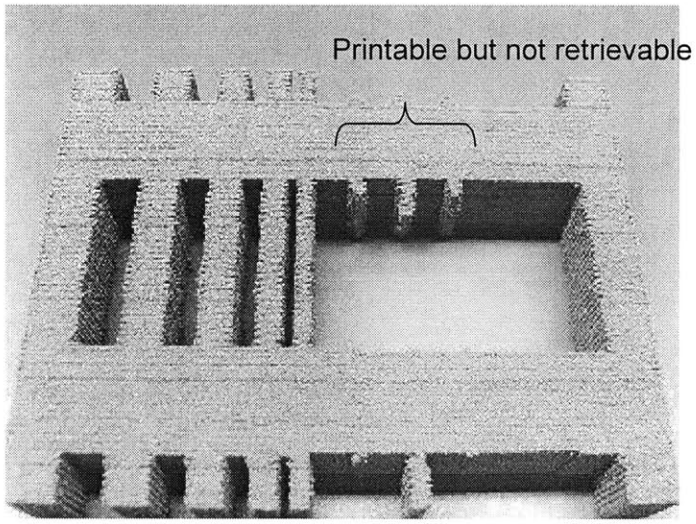

Figure 7.20: Fin geometry (two-jets; bi-directional)

8. CONCLUSIONS AND OUTLOOK

8.1 The key issues for 3DP™ with solenoid valve-jet

The two most important parameters for 3DP™ with the solenoid valve-jet are signal pulse duration and fluid pressure. Signal pulse duration determines the length of line segment printed. Fluid pressure determines the flow-rate of the valve-jet, which indirectly affects the built rate in 3DP™.

A single valve-jet is capable of printing lines segments with a variation in length of ±0.015mm on the leading edge and ±0.15mm on the trailing edge with a rapid traverse speed of 1.5m/s. Overall, parts printed with a single valve-jet printing both uni-directionally and bi-directionally display good surface texture and have a green density typically of 50%. Multiple jet operation appears more difficult to execute cleanly compared to single jet operations. The part exit edges produced a stepped appearance during uni-directional printing with multiple-jets. It is now known that variability among different valve-jets, especially between closing times, is the cause of the stepped edges. The range of time variation from among the sample of valve-jets evaluated is 0.353 milliseconds. This translates to a maximum difference of 0.53 mm between lines produced by valve-jets on the trailing edge of a single pass when the fast axis moves at 1.5 m/s. Although there is very little variation in performance of a single valve-jet, considerably significant differences may exist between two different valve-jets, and this presents the most severe obstacle to successful multiple-jet operation. The issue is to realize that such variations between different valve-jets exist and some form of compensation has to be done. This can be in the form of sorting out valve-jets with similar performance characteristics together to put onto the same printhead, or programming an equivalent amount of offset in the machine controller that makes up for this difference.

Overall, the solenoid valve-jet is an attractive candidate for use in a scaled-up 3DP™ machine because it is extremely robust and durable, requires low maintenance and can be easily assembled into a complete printhead operated by a simple electrical

drive circuit. Its robustness and durability has been demonstrated by results of long-term experimental runs where little evidence of performance deterioration was observed. The flow-rate variance of $\pm 0.2 cm^3/min$ was observed over entire five days test duration. It is important to recognize that the resolution obtainable with the valve-jet is inferior to that from current CJ technology. Large-scale, high-speed operations requiring low-resolution parts will be the best area to apply this technology.

8.2 Future work

8.2.1 Machine design

The next step in the development of the solenoid valve-jet would be construct an automated observation station where the solenoid valve-jets can be tested and calibrated for operational characteristics such as response time, time of flights and flow-rates quickly and reliably. This is essential because putting together an array of valve-jets, each with widely varying operating capabilities will only produce poor quality parts with inaccurate dimensions and bad surface texture. Depending on the part resolution required, the range of variability in the valve-jets selected for the printhead can be changed accordingly.

The current observation setup requires manual adjustment of strobe lighting, time delay and axis movement. A lot of time and effort is wasted in getting these conditions precisely for the best observation results. Building a permanent automated station will helps to eliminate all these current problems and many more valve-jets can be tested and calibrated, quickly and effectively.

The acid test for the solenoid valve-jet would be with a truly large-scale machine capable of a build volume of 2000x1000x2000mm, to build the mold pattern for a car engine block. The printhead may have an array of 96 valve-jet each spaced 10mm apart. The fast axis arm would probably require a new mechanical design capable of moving faster than current speed and still able to carry the weight of 96 valve-jets with minimum deflections. Finally, it was noted that the drying process is a major component of total build time. Hence, a better drying method may need to be used which can dry the bed

faster without warping the green part. The inclusion of an air re-circulation system may offer a partial solution to this problem.

8.2.2 Printhead development

The concept of dispensing fluid using a plunger mechanism, which opens and closes against an orifice is simple and elegant. Unfortunately, performance variability stemming from manufacturing tolerance in mass production seems to have reduced the potential applications of these solenoid valve-jets to only large prototypes requiring relatively low resolutions. Changing the design of the internal architecture of the valve-jet while still retaining the basic on-off plunger concept may increase the capability and potential applications of valve-jets to an equivalent of the CJ printhead. A possible new design is to use a core and plunger made of permanent magnets. A permanent repulsive force can be used to maintain the two components apart in the normal position. The application of a current may then create a magnetic field that goes against this repulsive force, simultaneously opening the orifice for fluid-flow. The repulsive force of the permanent magnets replaces the function of the spring with the major advantage that there is no physical contact between the parts, and the forces can be controlled much more precisely than that of the spring constant. In our conversation with the Lee Co., their solenoid valve-jets all uses the same induced magnetic force and spring design. Thus, a decision to pursue possibilities in this direction would require a new printhead research effort.

The INKX0505950A solenoid valve-jet investigated has the advantage that it comes with an integrated ruby orifice. But this also limits us to an orifice size of 130 μm. The INKX0503850A model of valve-jet will allows us to flexibly change nozzle sizes. Since smaller nozzle sizes help to increase resolution of printed parts, another possibility for future work is to use the INKX0503850A valve-jet and experiment with varying size orifices to print finer parts. Finally, we may also want to expand the range of binder materials, which can be used on the valve-jets beyond just water.

9. APPENDICES

Appendix A: Solenoid valve-jet specification drawings

A.1) INKX0505950A valve-jet

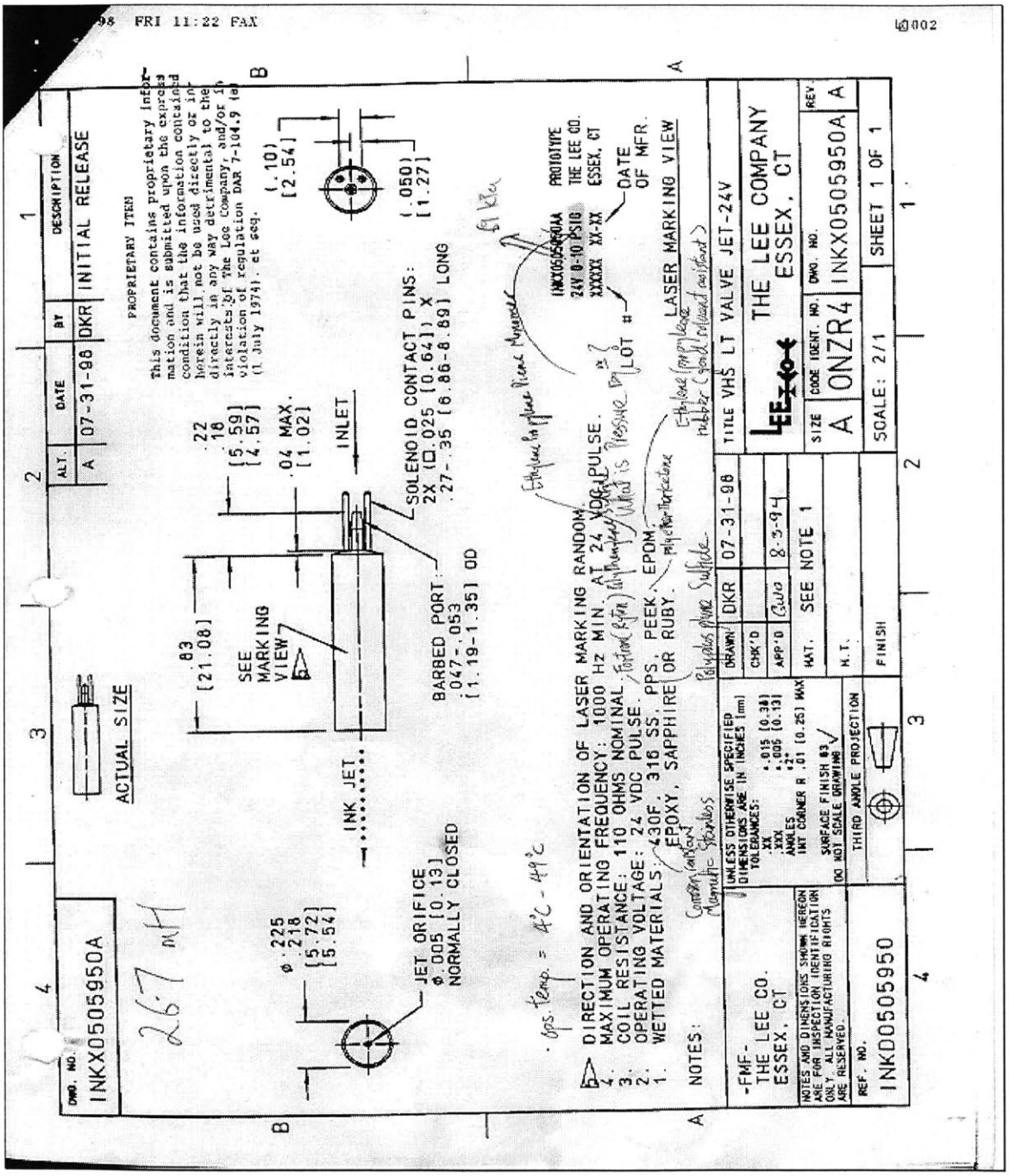

A.2) INKA2457210H valve-jet

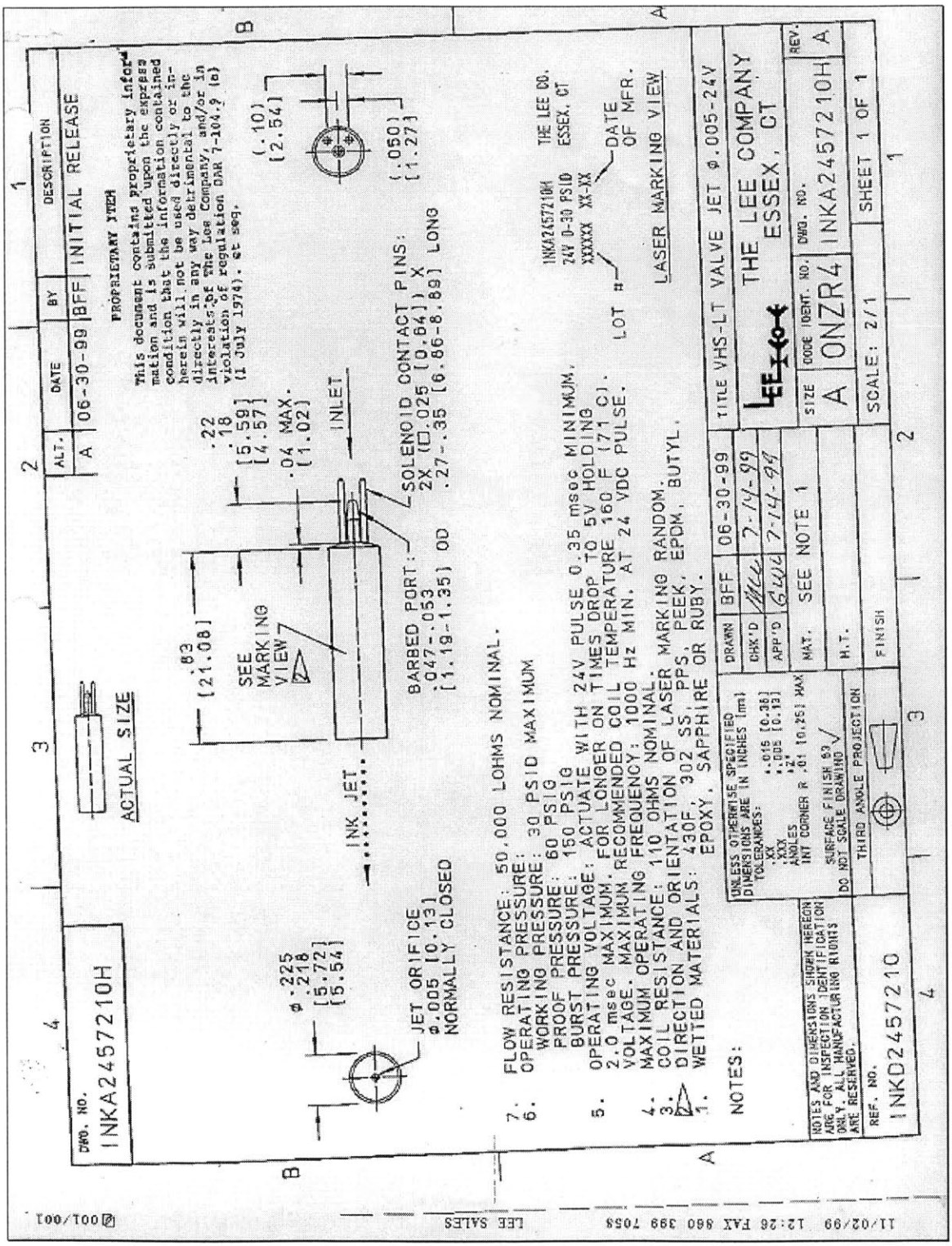

A.3) INKX0503850A valve-jet

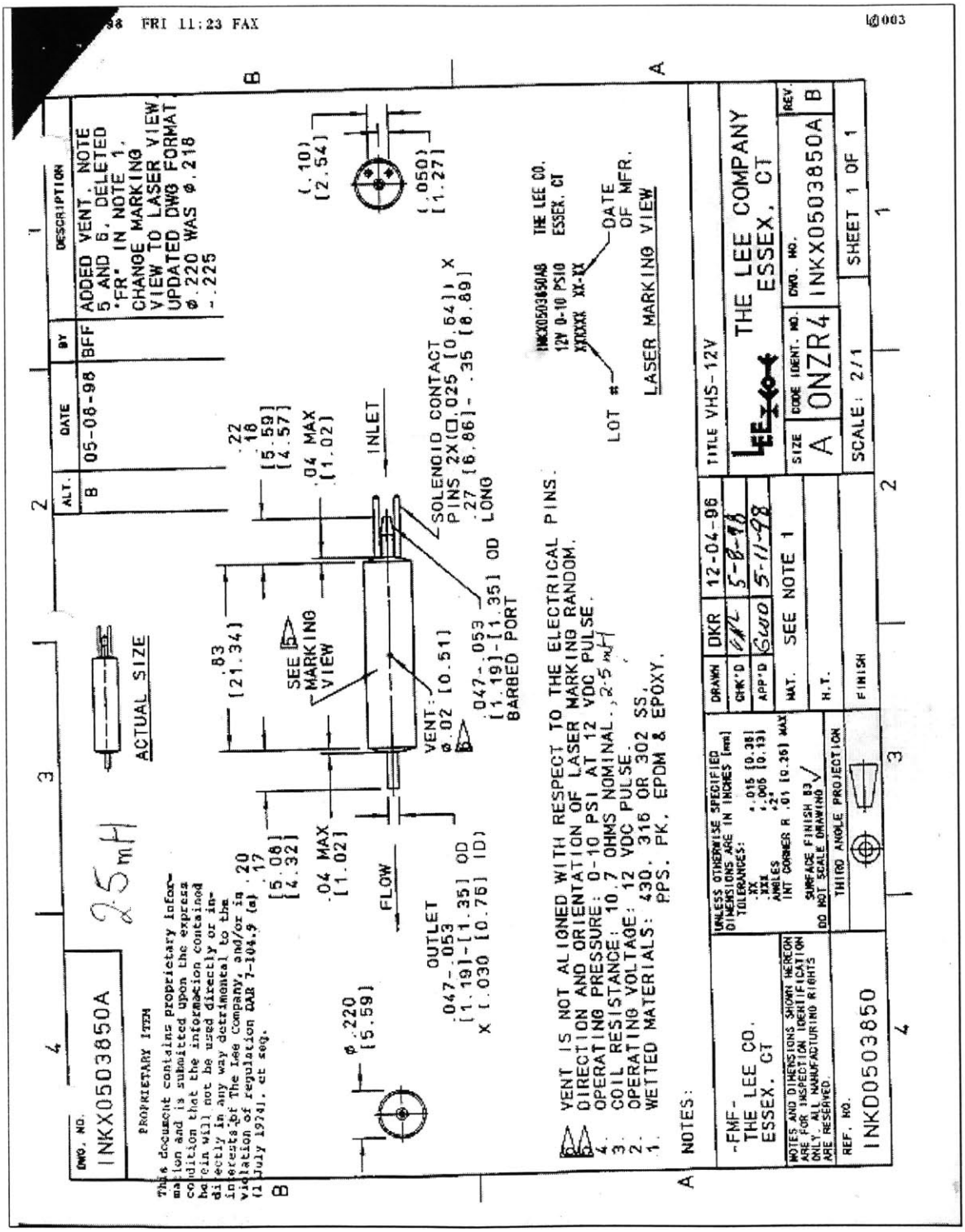

Appendix B: Printed part geometries

1) Double cylinder geometry

Solid-Model and orthographic views

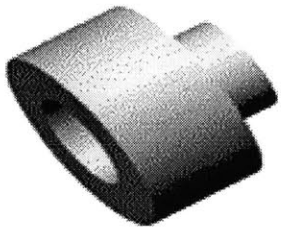

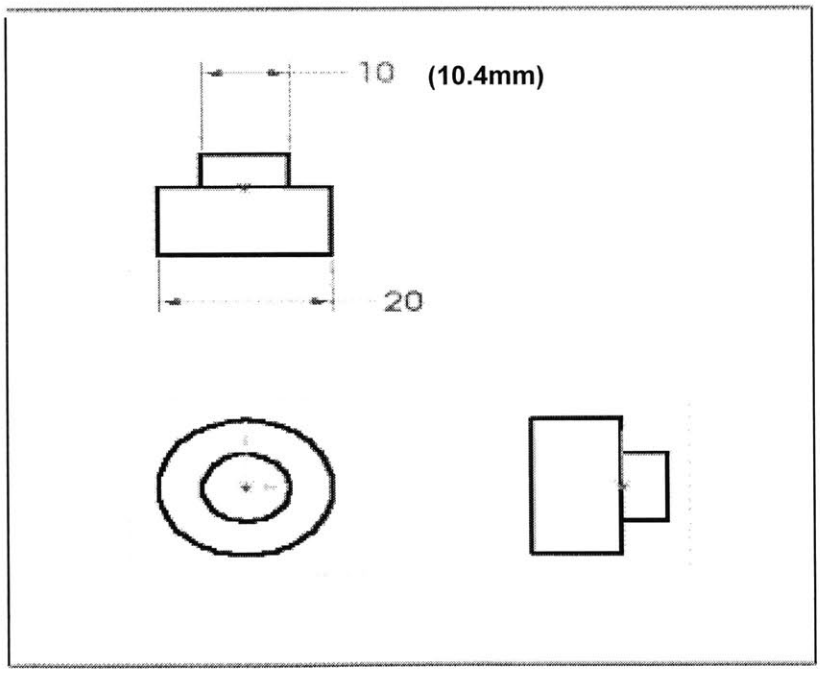

2) Trapezoid geometry

Solid-Model and orthographic views

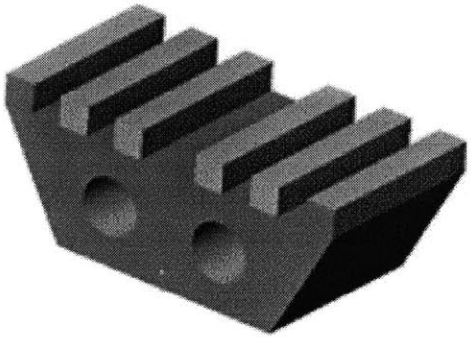

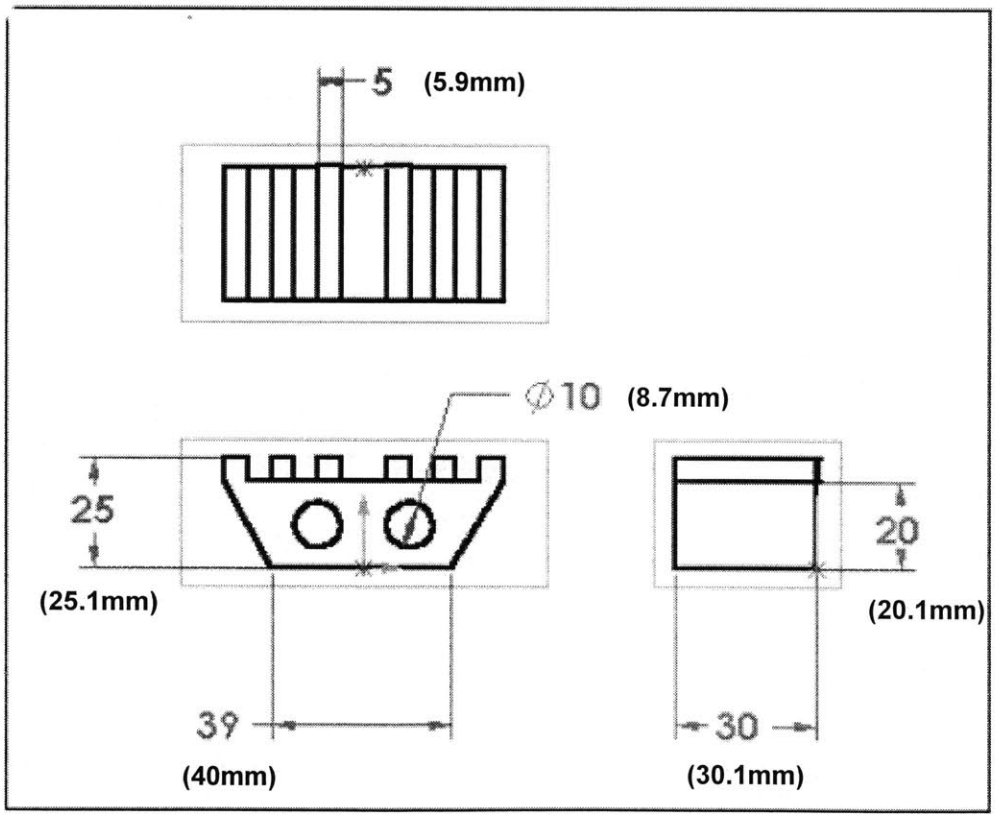

3) Donut geometry

Solid-Model and orthographic views

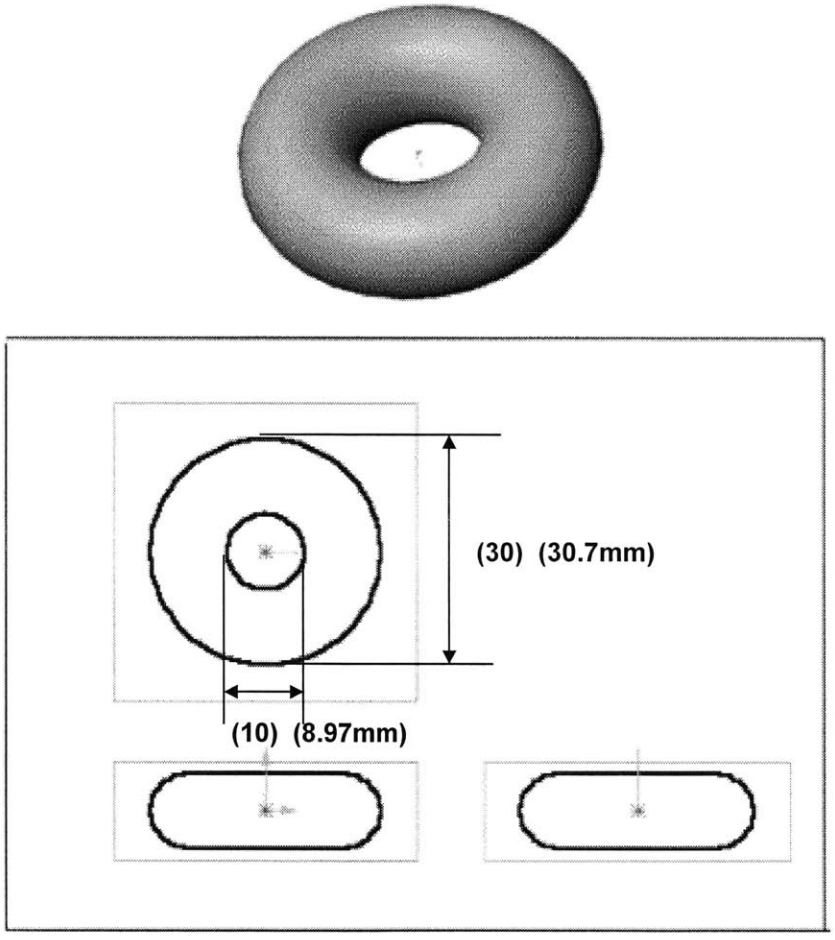

4) Rectangle brick geometry

Solid-Model and orthographic views

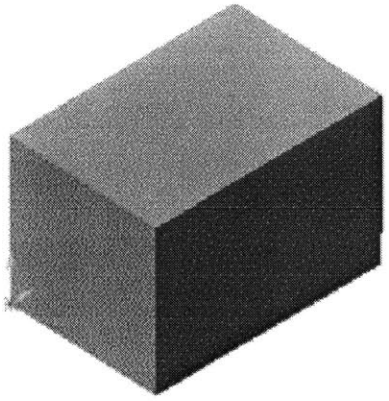

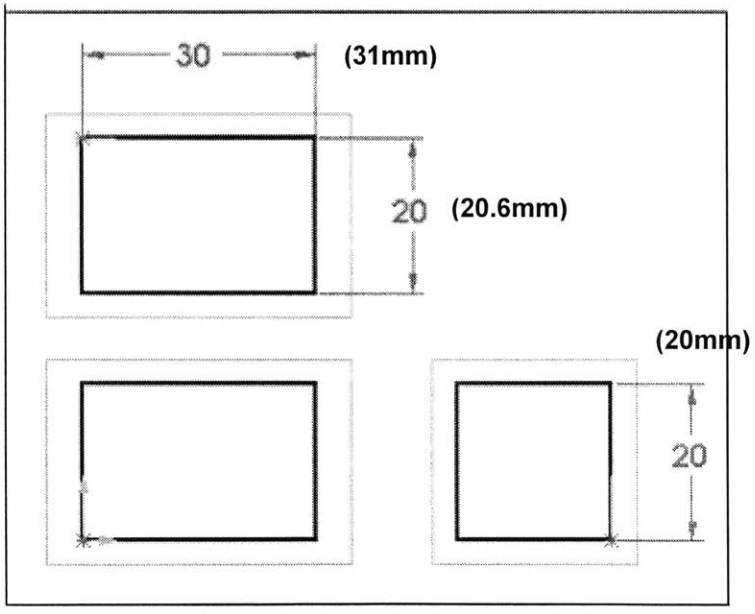

REFERENCES

[1] Sachs, E. Cima, M. Williams, P. Brancazio, D. Cornie, J. "Three Dimensional Printing: Rapid Tooling and Prototypes Directly from a CAD Model", Journal of Engineering for Industry, Vol. 114, No. 4, November 1992, p. 481-488

[2] Sachs, E. Haggerty, J. Williams, P. Cima, M. U.S. Patent, 5204055, 1993

[3] Sachs, E. "Development of the Three Dimensional Printing Process for Direct Fabrication of Automotive Tooling for Lost Foam Casting", ATP Program, Massachusetts Institute of Technology, Cambridge, 1997

[4] Baker, P. "Three Dimensional Printing with Fine Metal Powders", MS thesis Massachusetts Institute of Technology, Cambridge, 1997

[5] Williams, P. "Three Dimensional Printing: A New Process to Fabricate Prototypes Directly from CAD Models", MS thesis Massachusetts Institute of Technology, Cambridge, 1997

[6] Holowitz, P. Hill, W. "The Art of Electronics", Second edition, Cambridge University Press, 1989

[7] "HP33120A Function Generator / Arbitrary Waveform Generator User Guide" Hewlett Packard, 1989

[8] "Electro-fluidic systems technical handbook" 6th edition, The Lee Co., 1994